AN INVESTIGATION INTO THE PARAMETERS AFFECTING THE PERFORMANCE OF TUBE MILLS:

The behaviour of a single particle on a corrugated liner inside a rotating cylinder

K. von Bentheim

April 1991

Submitted to the University of Cape Town in partial fulfilment of the requirements for the degree of Master of Science in Engineering.

I, Karl-Heinz von Bentheim, submit this thesis in partial fulfilment of the requirements for the degree of Master of Science in Engineering. I declare that all the work in this thesis is essentially my own and has not been submitted in this or any other form for a degree at any University.

ACKNOWLEDGEMENTS

Thanks are due to ESKOM, whose support of this project is much appreciated, in particular Mr. A. Robinson of the Milling Division.

The assistance and suggestions as well as morale support from the project supervisor Assoc. Prof. G.N. Nurick are acknowledged with much gratitude.

The assistance and suggestions of Prof. B.D. Reddy are also acknowledged with much gratitude.

Thanks are also due to the technical staff of the Department of Mechanical Engineering for their assistance during the experimental phase of the project.

I would like to thank my parents and family for their continual support and encouragement throughout the duration of this thesis.

SYNOPSIS

This thesis is the second stage of a project to investigate the parameters affecting the performance of tube mills. The main topics that the project will cover is the motion of the mill charge and the wear characteristics of the mill charge and mill liners. Nates[1], in his thesis, performed a literature survey that highlighted the need for an investigation into the motion of a particle with emphasis on the response to changes in the coefficient of friction between the particle and the liner. Nates developed theoretical models for a particle moving on the inside of a rotating liner. The models developed were for a block and sphere moving on a flat liner. Although a better understanding of the motion of a particle was achieved the models did not take all the variables into account. One of the assumptions made by Nates was that the particle was moving on a flat liner. This thesis concentrates on the motion of a particle on a corrugated liner in a rotating cylinder.

Two formulations are presented that model the motion of a particle. The first model assumes that the particle being modelled is a block. The modelling of the particle as a block ensures that the particle does not roll. There are two possibilities as to the type of motion which the block can experience. The first possibility is where the block moves at the same velocity as the rotating liner whilst the second possibility is where the block can slide relative to the rotating liner. Three different liner configurations were used in the investigation of the motion of a block.

The second model assumes that the particle can move with pure rolling as well as with a combination of rolling and sliding. For pure rolling it is assumed that at the point of contact between the sphere and liner that there is no skidding or sliding.

The governing equations for the model of a block on a corrugated liner are solved numerically using a Fourth-Order Runge-Kutta Method. The theoretical predictions of the motion of a block on a corrugated liner are presented and discussed. The model for a sphere on a corrugated liner was derived but no

attempt was made to solve it numerically. It is envisaged that the numerical solution of the model for a sphere will be included in the next stage of the project.

An experimental investigation was done to validate the theoretical model for a block on a corrugated liner. Only two of the three liners used in the numerical investigation were tested. There was good correlation between the experimental results and the theoretical predictions. All the experimental results are presented and comparisons made between the theoretical predictions and the experimental results.

The thesis is concluded with a discussion of trends and observations made during the investigation into the motion of a block on a corrugated liner, and it is shown that the model for a block on a corrugated liner does satisfactorily predict the response of the block to varying initial conditions. Suggestions are also made as to possible ways to improve and expand on the current models used to describe the motion of a mill charge.

TABLE OF CONTENTS

LIST OF FIGURES

LIST OF TABLES

NOMENCLATURE

a	=	Ball Radius	(m)
$\underset{\sim}{e}_1, \underset{\sim}{e}_2$	=	Cartesian Unit Vectors	
$\underset{\sim}{e}_r, \underset{\sim}{e}_\phi$	=	Radial and Angular Unit Vectors	
$f(\beta)$	=	Corrugated Liner Function	(m)
$f'(\beta)$	=	First Derivative of the Liner Function	
$f''(\beta)$	=	Second Derivative of the Liner Function	
g	=	Acceleration due to Gravity ($9.81 ms^{-2}$)	(ms^{-2})
h	=	Time Increment for 4th Order Runge-Kutta Method (δt)	(seconds)
k_n	=	Constants used in the Runge-Kutta Solving Method	
m	=	Mass	(kg)
$\underset{\sim}{n}$	=	Unit Normal Vector to Liner Surface	
$\underset{\sim}{t}$	=	Unit Tangent Vector to Liner Surface	
$\underset{\sim}{r}(\beta)$	=	Vectorial Position of a Particle	(rad)
$\dot{\underset{\sim}{r}}(\beta)$	=	Vectorial Velocity of a Particle	($rads^{-1}$)
$\ddot{\underset{\sim}{r}}(\beta)$	=	Vectorial Acceleration of a Particle	($rads^{-2}$)
t	=	Time	(seconds)
v_x	=	Velocity of Block in the x direction at POD	(ms^{-1})
v_y	=	Velocity of Block in the y direction at POD	(ms^{-1})
x,y	=	Coordinates of the centre of a particle	(m)
B,C D,E	=	Letters used to represent terms in the Governing Equation of Motion	
I	=	Second Moment of Inertia of a particle	(kgm^2)
J	=	Percentage Fill of a Mill	(%)
N_c	=	Davis Critical Velocity	(rpm)
N_r	=	Normal Reaction Force of the Liner on a Particle	(N)

N_t	=	Tangential Friction Force between the Liner and a Particle	(N)
$\underset{\sim}{R}$	=	Normal Reaction Force Vector	(N)
$\underset{\sim}{T}$	=	Tangential Friction Force Vector	(N)
$\underset{\sim}{W}$	=	Weight Vector	(N)
α	=	$\dfrac{1}{\sqrt{f(\beta)^2 + f'(\beta)^2}}$	(m^{-1})
β	=	Angular Position of the Block Relative to its Starting Point on the Liner	(rad)
ϕ	=	Angular Position of a Particle on a Liner	(rad)
$\dot{\phi}$	=	Angular Velocity of a Particle on a Liner	($rads^{-1}$)
$\ddot{\phi}$	=	Angular Acceleration of a Particle about the Mill Centre	($rads^{-2}$)
μ	=	General Coefficient of Friction	
ρ	=	Mean radius of Liner	(m)
ρ_1	=	Radial Position of Block at the Point of Sliding	(m)
θ	=	Angular Position of a Particle on a Liner	(rad)
$\dot{\theta}$	=	Angular Velocity of a Particle on a Liner	($rads^{-1}$)
$\ddot{\theta}$	=	Angular Acceleration of a Particle about the Mill Centre	($rads^{-2}$)
Ω_m	=	Mill Velocity	($rads^{-1}$)
ω	=	Angular Velocity of the ball about its own centre	($rads^{-1}$)
$\dot{\omega}$	=	Angular Acceleration of the ball about its own centre	($rads^{-2}$)
ξ	=	Starting Point of Block	(rad)
ζ	=	No. of Corrugations per 360°	

GLOSSARY

AOD	: Angle of Departure of a Particle from the Liner.
Cascading	: Term used to describe a particle that is rolling down the face on the 'en masse' region.
Cataracting	: Term used to describe a particle that is in flight above the body of the charge.
Critical Velocity	: The mill velocity at which a particle becomes centrifuged to the liner.
POD	: Point of Departure of a particle from the liner.
POI or POD	: Point of Return or Point of Impact of the particle onto the liner.
N_c	: The Davis Critical Velocity of the mill for centrifuging to occur.
Keyed in	: The term used to describe the charge that is moving at the same speed as the liner.
Shoulder of Charge	: The upper most section of the bulk charge, from which the charge is then projected into flight, or tumbles down the liner.
Toe of Charge	: The lowest part of the charge, onto which the cataracting balls impact.
C3	: A Liner which is Cosine in shape and has a Corrugation Amplitude of 0.003m.
C8	: A Liner which is Cosine in shape and has a Corrugation Amplitude of 0.008m.

SK	:	The liner configuration found by Skorupa, in industrial tests, to be the most wear resistant.
BSP	:	Large Block with Steel-PVC Liner Interface.
SSP	:	Small Block with Steel-PVC Liner Interface.
BCP	:	Large Block with Cloth-PVC Liner Interface.
SCP	:	Small Block with Cloth-PVC Liner Interface.
Trough	:	Is the section of liner between two peaks or crests of a liner.

Chapter 1

INTRODUCTION

South Africa has one of the largest coal reserves in the world. This reserve is a mixture of low and high grade ores. South Africa pursues a policy of making the best use of its energy reserves and therefore relies on the use of progressively lower grades of coal in its new power stations. By pulverising the low grade ore the energy content of the coal is fully utilised. ESKOM decided that to utilise the lower grade coal milling plants would be used to crush the coal. The milling plants consist of tube mills approximately 5m in diameter and 8m in length.

The power station receives the coal ore in 30 mm sized pieces. This ore is then fed into the tube mills. The crushed ore exits the tube mill in the form of a fine powder. The average particle size of the pulverised coal is approximately 75 μm. The tube mills are charged with steel balls and the rotary action of the mill causes the steel balls to grind the ore to the required particle size. During the grinding process the balls and replaceable liners are worn away. The percentage fill of the mill has to be kept at an optimum and this is done by replacing the worn balls. This is done at a cost of approximately R1000 per mill per week. On average the new power stations have six boiler units and five mills per boiler. The sacrificial liners have an average lifetime of 35 - 40 thousand hours. The cost of replacing one set of liners is approximately R120 000 per mill. The cost of replacing the balls and liners in the early 1990's was estimated to be approximately R10 million per annum[1].

This prompted ESKOM to investigate ways of cutting the costs associated with tube mills. An investigation was initiated to determine the charge motion and wear characteristics of the balls and tube mill liners. The main objective of this research project is to develop a better understanding of the parameters that affect the motion of the mill charge. Once the charge motion of the mill is understood then a study of the nature of the wear of the balls and liners can be undertaken.

The research project was started by Nates[1] who conducted a literature review into milling with special regard to the charge behaviour within operating mills. The aim of the literature review was to identify areas of lesser expertise so as to provide a logical starting point for the project. It was decided that a viable starting point for this project would be to develop a formulation that included the effects of friction on a particle's behaviour.

Nates' thesis forms the initial stages of the entire project. The initial stage of the project was limited, firstly, to the behaviour of a single particle. The reason for this is that a full understanding of the behaviour of a single particle is needed before a study can be undertaken into the behaviour of multiple particle systems. Secondly, the particle was modelled in a mill devoid of lifter-bars or liners. This was done to simplify the initial model. Finally, the effect of the interaction between the coal and the grinding media is ignored. The inclusion of the effect of the coal would transform the system into a multi-particle system and would not be a suitable starting point.

The aim of this thesis is to develop and test a model that incorporates the effects of friction and a corrugated liner on the behaviour of a single particle inside a rotating cylinder. Only a single particle will be investigated and the effects of the interaction between the coal and the balls will be ignored.

To achieve these objectives, the thesis develops formulations for some of the possible behaviour patterns of a single particle on a corrugated surface. The governing equations are derived using vector analysis. These governing equations are then solved numerically using a modified version of the program developed by Nates[1]. Experiments were conducted in an attempt to verify the derived model. Conclusions are drawn regarding the results obtained from the theoretical and experimental investigations. Finally recommendations have been made for possible areas of further research.

Chapter 2 contains a literature review of recently published dissertations. The authors reviewed were Nates[1], Powell[11] and Skorupa[19]. Nates investigated the behaviour of a single particle on the inside of a smooth rotating cylinder. Powell performed a theoretical and experimental

investigation into the effect of liner design on the charge motion in a rotary mill. Skorupa investigated the wear of tube mill liners for the South African power industry.

In Chapter 3 the equations of motion for the behaviour of a block on a corrugated liner are derived. Two distinct types of motion can occur, namely the sliding of the block relative to the liner and the sticking of the block to the liner. The governing equations are solved using numerical methods.

In Chapter 4 a model is derived for the pure rolling of a sphere on a corrugated liner. A model is also derived for a sphere moving on a corrugated liner with a combination of rolling and sliding. The governing equations derived are not solved numerically.

Chapter 5 presents the results obtained from the numerical solution of the governing equations for a block on a corrugated liner. The effects of the mill speed, coefficient of friction and the liner configuration on the angle of departure is investigated.

Chapter 6 explains the experimental investigation. In Chapter 7 a comparison between the experimental and theoretical results was performed and the findings are presented.

Chapter 8 discusses the findings and observations made concerning the theoretical and experimental work performed.

1.1 General Milling Terminology.

Tube mills are used mainly in the mining and power industries to crush coal (power industry) and mineral bearing ore (mining) for further processing.

A cross section of a tube mill is shown in Figure 1.1. A mill charge consists of both coal ore and grinding media. The grinding media can consist of balls, rods or pebbles. The amount of charge in the mill is referred to as the Percentage Fill (J). The mill charge is divided into two distinct regions.

These regions are divided by the line AB. The region of the mill charge that falls below this line is known as the 'en Masse' region. The 'Angle of Repose' is the angle of line AB to the horizontal.

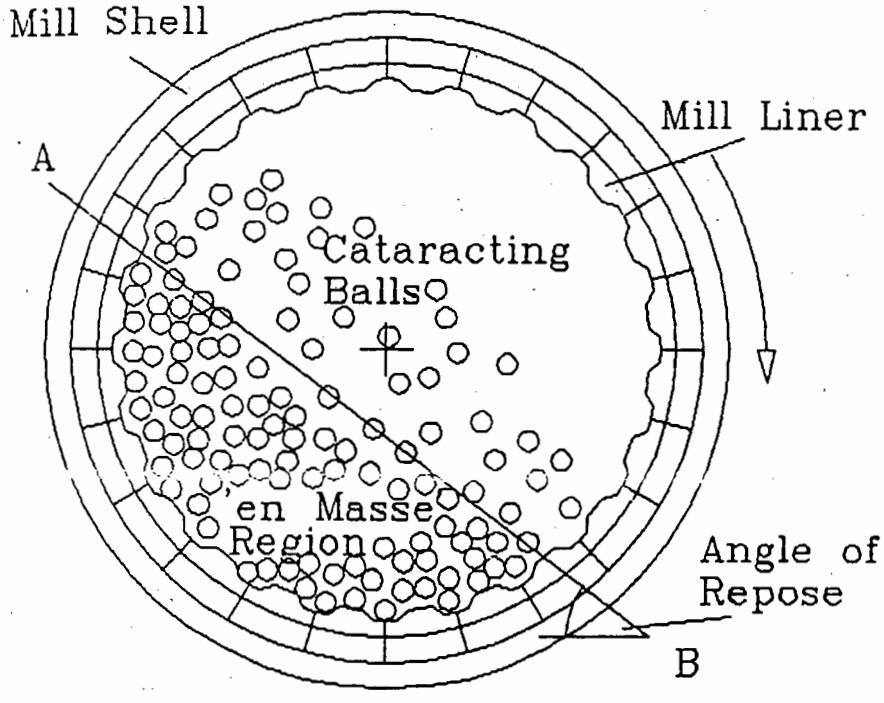

Figure 1.1: Cross-section through a tube mill[1].

The motion of the balls can be defined by using one of two terms, cataracting or cascading. A ball is defined as cataracting if it detached from the main body of the charge. If the ball does not leave the body of the charge but rolls down the charge face it is defined as cascading.

The point where the balls leave the charge is defined as the **Point of Departure** (POD). The angle of this point, above the horizontal through the mill centre, is known as the **Angle of Departure** (AOD). If the mill speed is increased then the AOD will also increase. The AOD will increase to a point (90°) where the charge no longer leaves the liner. This condition is known as centrifuging. The theoretical velocity at which this occurs was defined by Davis[4] as being the Mill Critical Velocity (N_c).

In tube mills coal ore is ground by a combination of abrasion, attrition and impact. The large portions of coal that are fed into the mill are initially broken up by the cataracting action of the larger balls impacting on the coal at the toe of the charge. The mill speed is controlled so that the cataracting balls impact on the toe of the charge. If the mill speed is too high then the balls impact on the exposed liner and results in accelerated wear of the liners.

The second process in the mill whereby the chips of coal are ground into a fine powder is achieved by the mechanisms of attrition and abrasion. The fine grinding is performed by the smaller balls and occurs by rubbing the coal between the balls. The powdering of the coal is performed in the 'en Masse' region where grinding pressures are high. The powdered coal is then extracted by blowing hot air through one end of the mill. The coal dust is extracted out of the other end and is fed into classifiers to ensure that the particle size of the coal dust is small enough. If the coal dust particle size is too large (>75 μm) it is returned to the mill for further processing, otherwise it is is blown into the boilers for combustion.

CHAPTER 2

LITERATURE REVIEW

Nates[1], Powell[11] and Skorupa[19] published dissertations in the field of ball mill mechanics in the last 18 months (prior to April 1991). These dissertations are reviewed in this section.

Nates[1] performed an extensive literature review of work performed in the field of milling and the milling process. In addition to the literature review Nates developed theoretical models to model a particle on the inside of a rotating cylinder. Nates also performed experimental work in an attempt to verify the theoretical models. Powell[11] investigated the influence the liner design had upon the charge motion in a rotary mill. Powell's literature survey concentrated on charge motion, the techniques used to investigate it and the effect of the liner design on charge motion. Skorupa[19] investigated the wear of tube mill liners in the South African power industry.

2.1 An Investigation into the Parameters affecting the Performance of Tube Mills. Author: M. Nates[1]

This thesis was the first stage of a project to investigate the parameters affecting the performance of tube mills. Nates' thesis started with an in depth literature review. The next stage in Nates' thesis was the development of theoretical models of the motion of a single particle inside a rotating cylinder. Experimental work was then performed in an attempt to verify the theoretical models.

2.1.1 Literature Survey Performed by Nates

The aim of the literature review was to identify any areas of lesser expertise and to identify a logical starting point for the project as a whole. The literature survey is divided into five sections. The first included a brief description of the milling process and the terminology used to describe the behaviour of a mill charge. The second section covers ball paths and ball trajectories. The third and fourth sections deals with the behaviour of the 'en Masse' region. The third section emphasises the nature of charge slippage

and the fourth section covered charge surge. The last section discusses the radial segregation of the 'en Masse' region. A brief summary of each section will be given below. The section on general milling terminology is covered in the introduction to this thesis.

2.1.1.1 Ball Paths and Trajectories in a Tube mill

The authors reviewed by Nates and their contributions to the subject, as reported by Nates, are listed below.

Author(s)	Date	Contributions
White[2]	1905	-Experimental investigation. -First mathematical model.
Davis[3]	1909	-Extended White's theory. -Derived expressions for Point of Departure. -Theory of Centrifuging of charge at critical velocity. -Observation of balls in separate layers.
Haultain & Dyer[4]	1922	-Experimental investigation in an attempt to reproduce Davis theoretical results. -Charge did not centrifuge at critical velocity. -Occurrence of Radial Segregation observed.
Gow, Campbell & Coghill[5]	1929	-Challenged Davis Model. -Proposed new model. -New model includes bunching or pushing of balls by other balls. -Gow model predicts balls will travel further across mill than predicted by Davis.

Author(s)	Date	Contributions
Fahrenwald & Lee[6]	1931	-Critised Gow et al for "exaggerating conditions somewhat". -Derived expression for the Angle of Departure (AOD) that include the effect of friction.
Rose & Sullivan[7]	1958	-Rederived Davis model using different approach. -Davis ignored friction and ball interaction after the ball had left the liner. -Extended work to enable the prediction of charge shape. -Friction is included in new model.
McIvor[8]	1983	-Derived theoretical model for flight of single ball. -Include the effect of friction and lifter bar face-angle.
Vermeulen Olsen De Fine Schakowski[9]	1984	-Experimental testing using piezoelectric sensors placed in liners. -Theoretical modelling of ball paths including the effect of the adhesion forces.
Vermeulen[10]	1985	-Theoretical modelling of ball paths including the effect of lifter bars. -Performed experimental work. -Good correlation between theoretical and experimental results obtained.
Powell[11]	1988	-See Section 2.2.

2.1.1.2 Charge Slippage in a Tube Mill

Author(s)	Date	Contributions
Haultain & Dyer[4]	1922	-First to mention charge slippage. -Advocated the use of corrugated liners to prevent slippage.
Gow et al[5]	1929	-All reported from experimental work that slippage decreases with an increase in the percentage fill of a mill.
Gross[12]	1938	
Hukki[13]	1958	
Manz[14]	1972	-Experimental procedure to measure slip using electrical probes in mill. -Conclusions reached 1. Slip increases with mill speed. 2. Slip increases with power input to mill. 3. Slip can be decreased by using smaller balls which "key in" more easily than bigger balls.
Henein & Brimacombe Watkinson[15]	1983	-Experimental investigation in rotary kiln. -Difference between rotary kiln and mill is size of grinding media. -Identified six types of motion that occur in a mill.
Vermeulen & Howat[16]	1983	-Experimental work performed using rods in an attempt to negate end effects that occur in glass ended mills. -Found an increase in the amount of cataracting with the inclusion of lifter bars in a mill.

2.1.1.3 Charge Surging in a Tube Mill

Nates reported that the phenomenon of charge surge is a relatively unresearched field. The occurrence of surge in a mill is difficult to predict and if it occurs it can damage a mill and its drive mechanism. Nates included a brief overview on the subject of surge so that the complexities and uncertainties involved in determining charge motion can be appreciated. The authors, which Nates found to have investigated the subject, are Rose and Sullivan[7] and Vermeulen and Howat[17].

Rose and Sullivan developed a surge model in terms of the distance between the centre of the mill and the centre of gravity of the charge. Rose and Sullivan stated that the charge oscillated and that it moved both in the same direction and in the opposite direction to the mill rotation.

Vermeulen and Howat conducted an experimental investigation into the phenomenon of charge surge using high speed cinematography. They found that the charge did not display pendulum type behaviour, as reported by Rose and Sullivan[7], and at no time during the surge cycle did the charge move in the opposite direction to the mill rotation.

2.1.1.4 Radial Segregation in a Tube Mill

Nates stated that radial segregation is defined as division of the charge into separate zones. These zones differ according to element size and occur radially in a mill. Nates reported that the occurrence of radial segregation was reported by various authors (3,4,8,12).

Haultain and Dyer[3] were the first to comment on radial segregation. They observed during experimental work that at low speeds smaller particles would migrate to the centre of the mill. This phenomenon was reversed at high speeds.

Henien et al[18], in 1985, conducted an experimental investigation into the radial segregation in rotary kilns. Nityanand et al[19] extended Henien et al's work. Nityanand obtained results that agreed with the findings of

Haultain et al[3]. Nityanand developed a model that describes the various regions of the segregated charge.

2.1.2 Theoretical Models Developed by Nates

Nates developed theoretical models for three types of particle motion that can occur inside a rotating cylinder. The three types of motion considered are:

Pure Sliding	: Modelled using a Block
Pure Rolling	: Modelled using a Sphere
Combination of Rolling and Sliding	: Modelled using a Sphere

For the **Pure Sliding Model** the forces acting on the block are summed radially and tangentially to the liner. Three equations, Equations (2.1)-(2.3), are derived for the Reaction Force (R), the Tangential Frictional Force (T), and the Angular Velocity ($\dot{\theta}$). These forces and the directions in which they act are illustrated in Figure 2.1.

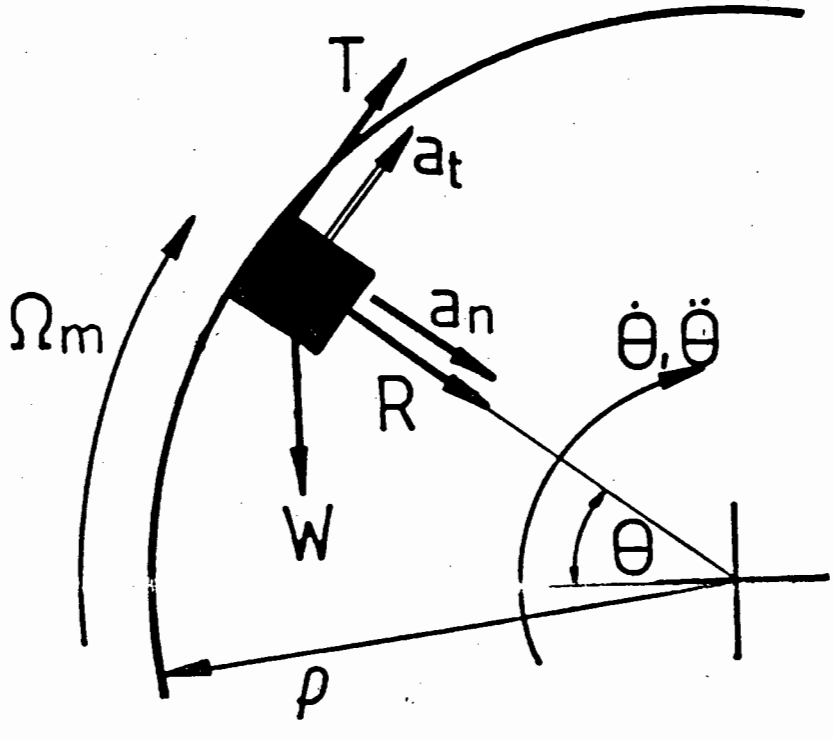

Figure 2.1: Orientation of the Forces acting on a Block[1]

Nates derived equations for the Reaction Force (R) and the Tangential Friction Force (T) by equating the forces that act on the block.

$$R = m\,\dot{\theta}^2\rho - m\,g\,\mathrm{Sin}(\theta) \qquad (2.1)$$

$$T = m\,\ddot{\theta}\,\rho + m\,g\,\mathrm{Cos}(\theta) \qquad (2.2)$$

Nates stated that prior to sliding the block sticks to the liner and the angular velocity ($\dot{\theta}$) of the block equals the angular velocity of the rotating mill (Ω_m). For this boundary condition the tangential and reaction forces can be calculated.

For Non-Sliding: $\dot{\theta} = \Omega_m$ (Ω_m = Constant) (2.3)

$$\ddot{\theta} = 0 \qquad (2.4)$$

$$\theta = \Omega_m\,t + \zeta \qquad (2.5)$$

where ζ = Initial Position of Block

By substituting the non-sliding conditions, Equations (2.3)-(2.5), into Equations (2.1) and (2.2) gives

$$R = m\,\Omega_m^2\,\rho - m\,g\,\mathrm{Sin}(\Omega_m\,t + \zeta) \qquad (2.6)$$

$$T = m\,\Omega_m\,\rho + m\,g\,\mathrm{Cos}(\Omega_m\,t + \zeta) \qquad (2.7)$$

Nates stated that once sliding has started the Tangential Frictional Force (T) is proportional to the Reaction Force (R) (ie $T = \mu R$). Equating these two forces, Nates derived the governing equation

$$\rho\,\ddot{\theta} - \mu\,\rho\,\dot{\theta}^2 + g\left[\,\mathrm{Cos}(\theta) + \mu\,\mathrm{Sin}(\theta)\right] = 0 \qquad (2.8)$$

Equation (2.8) is the equation of motion of a block sliding relative to a flat liner. Nates used an Euler Forward Step Approximation to numerically solve the governing equation.

The results obtained from the numerical solution of Equations (2.1), (2.2) and (2.8) are then compared to experimental results obtained from a test rig. The rig simulated a rotating cylinder with a flat liner.

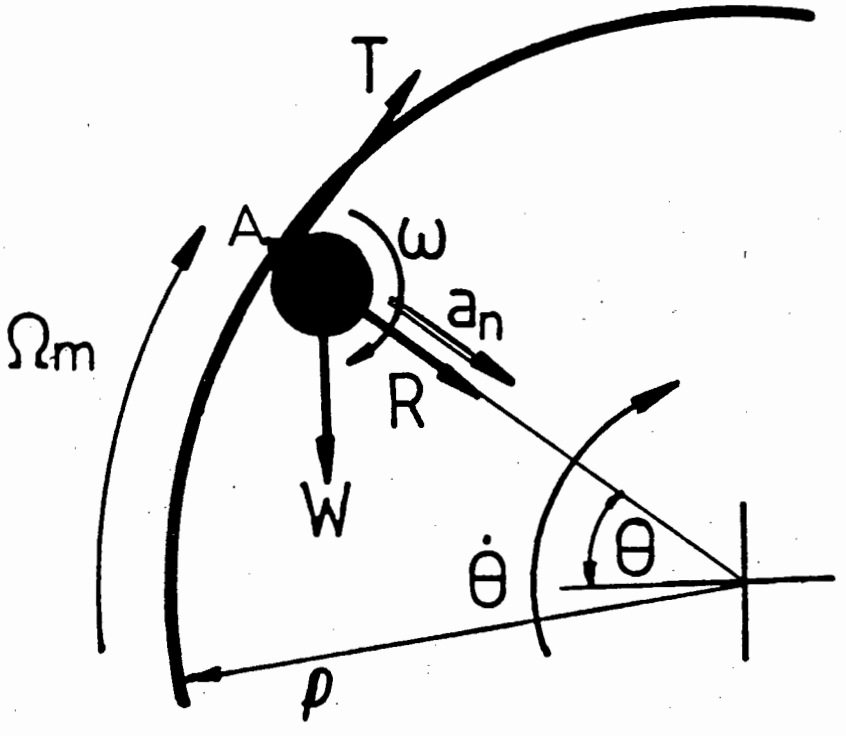

Figure 2.2: Orientation of Forces acting on a Sphere[1]

The second model that Nates formulated is for pure rolling. This model assumed that a sphere is rolling on the inside of a rotating cylinder. One of the preconditions is that no slip occurs between the spheres and the liner. Nates derived the equations for the pure rolling case in a similar manner to that for pure sliding. The orientation of the forces acting on the sphere are shown in Figure 2.2. The equations derived for the Tangential Friction Force (T) and the Reaction Force (R) are the same. The equation of motion for a block is no longer valid and Nates derives a new equation of motion. The equation derived takes the spin of the sphere into account. Nates summed the moments acting about the sphere centre, P:

$$I\,\dot{\omega} = T\,a \qquad (2.9)$$

where I = Second Moment of Inertia of a Sphere = $\frac{2}{5}\,m\,a^2$

T = Tangential Friction Force

a = Radius of Sphere

Substituting Equation (2.9) into Equation (2.2) yields

$$2\,\dot{\omega}\,a = 5\,\ddot{\theta}\,\rho + 5\,g\,\mathrm{Cos}(\theta) \qquad (2.10)$$

Nates stated that one of the conditions is that the sphere moves with pure rolling. Summing the velocity vectors acting at A (Point A, in Figure 2.3, is the point of contact between the sphere and liner) yields

$$\Omega_m\,\rho = \dot{\theta}\,(\rho - a) + \omega\,a \qquad (2.11)$$

Nates assumed that $\rho \gg a$ and therefore $(\rho - a) \approx \rho$.

$$\Omega_m\,\rho = \dot{\theta}\,\rho + \omega\,a \qquad (2.12)$$

Nates differentiated Equation (2.11), with respect to time, and substituted the differentiated equation into Equation (2.10). This yields

$$7\,a\,\dot{\omega} = 5\,g\,\mathrm{Cos}(\theta) \qquad (2.13)$$

Equations (2.12) and (2.13) are coupled and have to be solved simultaneously. In these equations the value for the coefficient of friction is not included in the calculation of the actual motion of the sphere. It is only used to calculate the values of the tangential and reaction forces. It is also used to ascertain whether the limiting friction ($T \leq \mu\,R$) has been exceeded.

The initial boundary conditions for the numerical solution of the governing equations (2.12) and (2.13) are the initial angular displacement [$\theta(0)$], the angular velocity [$\dot{\theta}(0)$] of the sphere about the mill centre and the initial angular velocity [$\omega(0)$] of the sphere about its centre. An Euler Forward Step Approximation is used to numerically solve the two simultaneous equations.

Nates stated that the model for sliding excluded the possibility of the block rolling whereas the rolling model excluded the possibility of the sphere sliding. Nates derived a third model that included the possibility of both the rolling and sliding of a particle. Nates used the same derivation as for the sliding to obtain the Reaction (R) and Tangential (T) forces. These can

be seen in Equations (2.1) and (2.2). As with sliding the assumption is made that $T = \mu R$ and hence combining Equations (2.1) and (2.2) yields Equation (2.14).

$$\rho \ddot{\theta} - \mu \rho \dot{\theta}^2 + g\left[\text{Cos}(\theta) + \mu \text{ Sin}(\theta)\right] = 0 \qquad (2.14)$$

If the particle is permitted to spin then taking moments about the centre yields

$$I \dot{\omega} = T a$$

Substituting for the Tangential Force (T) yields

$$\dot{\omega} = \frac{m a [\theta \rho + g \text{ Cos}(\theta)]}{I} \qquad (2.11)$$

where I = Second Moment of Inertia of the Particle

Nates, after formulation of the combined model, felt that a simple combination of the two individual models would not adequately portray the problem of the combined motion of the sphere.

2.1.3 Discussion of Nates' Models

Nates found that the formulation by Davis[2] was inadequate. This was because Davis neglected to include the affect of friction on the motion of the particle. The sliding model derived by Nates proved that Davis had assumed that the coefficient of friction between the block and liner to be infinite.

The sliding model predicted that there are two ways in which the block can be centrifuged to the liner. The first is that the block's angular velocity equals the rotational speed of the mill. The second is when the angular velocity of the block is less than the rotational speed of the mill (ie sliding is occurring). These two types of centrifuging are reproduced in the experimental work performed.

It was found that the pure rolling model is only valid for the initial period of the sphere's motion. This is because once the frictional force is exceeded then the sphere starts to slide. The model derived by Nates for the combined rolling and sliding of a particle does not model the situation adequately. Equations (2.8) and (2.14) are identical. This implies that the motion of a block sliding relative to a liner is equivalent to the motion of a sphere sliding relative to a liner. This is not the case and therefore the model for combined rolling and sliding cannot be valid.

It was found that the motion of a block is affected by variations in the coefficient of friction between the liner and the block and by variations in the mill rotational velocity. The effects of these changes on a block on a smooth liner can be seen in Figures 2.3 and 2.4. In Figure 2.3 the effects of a change for the coefficient of friction can be seen. The effect of increasing friction is to make the block move higher up the rotating cylinder prior to it leaving the liner. This in turn causes the block to have a higher tangential velocity and causes the block to be flung further across the mill. This also occurs if friction is kept constant and the mill speed is varied (Figure 2.4). The block's tangential velocity increases as the mill speed increases and therefore it is also flung further across the mill.

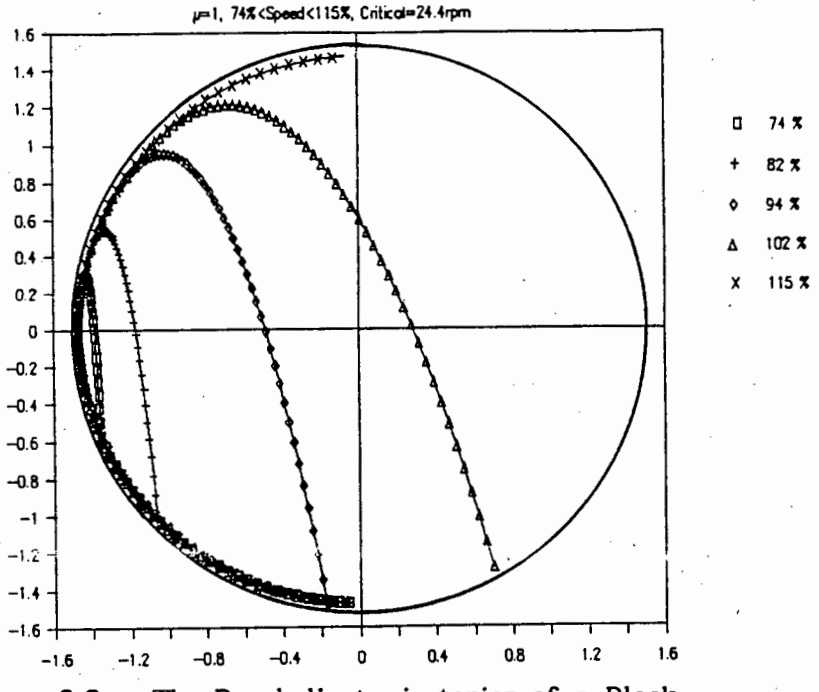

Figure 2.3: The Parabolic trajectories of a Block for varying Ω_m and constant μ. (μ=1)[1]

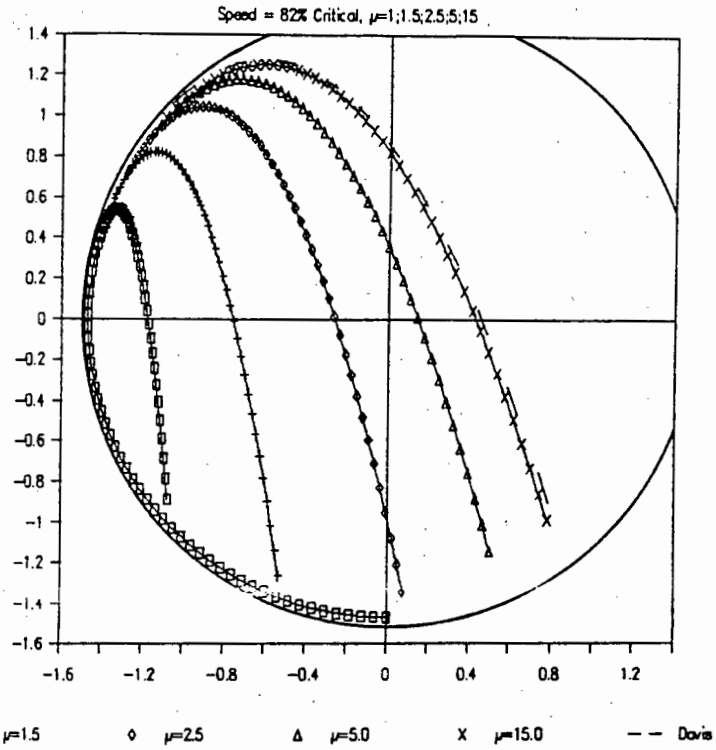

Figure 2.4: The Parabolic Trajectories of a Block for varying μ and constant Ω_m.
(Ω_m = 82% Critical)[1]

Nates performed experimental work to validate the pure sliding model and the pure rolling model. The results obtained from the experimental work, for a block on a flat liner, correlated with the numerical results. This led to the conclusion that the model derived for a block on a smooth liner is valid. No attempt was made to experimentally validate the combined rolling and sliding model.

Nates encountered difficulties in setting the initial boundary conditions for the experimental investigation of a sphere moving with pure rolling. Nates stated that the model for pure rolling would only be valid for a short period of time. In reality the coefficient of friction, between two steel surfaces, is approximately 0.35. Nates reported that if this is the case then the pure rolling model is valid for approximately 0.58 seconds.

Nates stated that the simple combination of the **Pure Rolling** and **Pure Sliding** models does not overcome the inadequacies of the two models. The resulting model ignores the influence of the particle's spin on the motion of the particle and reduces the model to that for a block on a flat liner.

PART 1 INTRO.

South Africa has one of the largest coal reserves in the world. This reserve is a mixture of low and high grade ores. South Africa pursues a policy of making the best use of its energy reserves and therefore relies on the use of progressively lower grades of coal in its new power stations. By pulverising the low grade ore the energy content of the coal is fully utilised. ESKOM decided that to utilise the lower grade coal milling plants would be used to crush the coal. The milling plants consist of tube mills approximately 5m in diameter and 8m in length.

The power station receives the coal ore in 30 mm sized pieces. This ore is then fed into the tube mills. The crushed ore exits the tube mill in the form of a fine powder. The average particle size of the pulverised coal is approximately 75 μm. The tube mills are charged with steel balls and the rotary action of the mill causes the steel balls to grind the ore to the required particle size. During the grinding process the balls and replaceable liners are worn away. The percentage fill of the mill has to be kept at an optimum and this is done by replacing the worn balls. This is done at a cost of approximately R1000 per mill per week. On average the new power stations have six boiler units and five mills per boiler. The sacrificial liners have an average lifetime of 35 - 40 thousand hours. The cost of replacing one set of liners is approximately R120 000 per mill. The cost of replacing the balls and liners in the early 1990's was estimated to be approximately R10 million per annum[1].

This prompted ESKOM to investigate ways of cutting the costs associated with tube mills. An investigation was initiated to determine the charge motion and wear characteristics of the balls and tube mill liners. The main objective of this research project is to develop a better understanding of the parameters that affect the motion of the mill charge. Once the charge motion of the mill is understood then a study of the nature of the wear of the balls and liners can be undertaken.

expertise so as to provide a logical starting point for the project. It was decided that a viable starting point for this project would be to develop a formulation that included the effects of friction on a particle's behaviour.

Nates' thesis forms the initial stages of the entire project. The initial stage of the project was limited, firstly, to the behaviour of a single particle. The reason for this is that a full understanding of the behaviour of a single particle is needed before a study can be undertaken into the behaviour of multiple particle systems. Secondly, the particle was modelled in a mill devoid of lifter-bars or liners. This was done to simplify the initial model. Finally, the effect of the interaction between the coal and the grinding media is ignored. The inclusion of the effect of the coal would transform the system into a multi-particle system and would not be a suitable starting point.

The aim of this thesis is to develop and test a model that incorporates the effects of friction and a corrugated liner on the behaviour of a single particle inside a rotating cylinder. Only a single particle will be investigated and the effects of the interaction between the coal and the balls will be ignored.

To achieve these objectives, the thesis develops formulations for some of the possible behaviour patterns of a single particle on a corrugated surface. The governing equations are derived using vector analysis. These governing equations are then solved numerically using a modified version of the program developed by Nates[1]. Experiments were conducted in an attempt to verify the derived model. Conclusions are drawn regarding the results obtained from the theoretical and experimental investigations. Finally recommendations have been made for possible areas of further research.

Chapter 2 contains a literature review of recently published dissertations. The authors reviewed were Nates[1], Powell[11] and Skorupa[19]. Nates investigated the behaviour of a single particle on the inside of a smooth rotating cylinder. Powell performed a theoretical and experimental

The research project was started by Nates[1] who conducted a literature review into milling with special regard to the charge behaviour within operating mills. The aim of the literature review was to identify areas of lesser expertise so as to provide a logical starting point for the project. It was decided that a viable starting point for this project would be to develop a formulation that included the effects of friction on a particle's behaviour.

Nates' thesis forms the initial stages of the entire project. The initial stage of the project was limited, firstly, to the behaviour of a single particle. The reason for this is that a full understanding of the behaviour of a single particle is needed before a study can be undertaken into the behaviour of multiple particle systems. Secondly, the particle was modelled in a mill devoid of lifter-bars or liners. This was done to simplify the initial model. Finally, the effect of the interaction between the coal and the grinding media is ignored. The inclusion of the effect of the coal would transform the system into a multi-particle system and would not be a suitable starting point.

The aim of this thesis is to develop and test a model that incorporates the effects of friction and a corrugated liner on the behaviour of a single particle inside a rotating cylinder. Only a single particle will be investigated and the effects of the interaction between the coal and the balls will be ignored.

To achieve these objectives, the thesis develops formulations for some of the possible behaviour patterns of a single particle on a corrugated surface. The governing equations are derived using vector analysis. These governing equations are then solved numerically using a modified version of the program developed by Nates[1]. Experiments were conducted in an attempt to verify the derived model. Conclusions are drawn regarding the results obtained from the theoretical and experimental investigations. Finally recommendations have been made for possible areas of further research.

Chapter 2 contains a literature review of recently published dissertations. The authors reviewed were Nates[1], Powell[11] and Skorupa[19]. Nates investigated the behaviour of a single particle on the inside of a smooth rotating cylinder. Powell performed a theoretical and experimental

investigation into the effect of liner design on the charge motion in a rotary mill. Skorupa investigated the wear of tube mill liners for the South African power industry.

In Chapter 3 the equations of motion for the behaviour of a block on a corrugated liner are derived. Two distinct types of motion can occur, namely the sliding of the block relative to the liner and the sticking of the block to the liner. The governing equations are solved using numerical methods.

In Chapter 4 a model is derived for the pure rolling of a sphere on a corrugated liner. A model is also derived for a sphere moving on a corrugated liner with a combination of rolling and sliding. The governing equations derived are not solved numerically.

Chapter 5 presents the results obtained from the numerical solution of the governing equations for a block on a corrugated liner are presented. The effects of the mill speed, coefficient of friction and the liner configuration on the angle of departure is investigated.

Chapter 6 explains the experimental investigation. In Chapter 7 a comparison between the experimental and theoretical results was performed and the findings are presented in this chapter.

Chapter 8 discusses the findings and observations made concerning the theoretical and experimental work performed.

1.1 General Milling Terminology.

Tube mills are used mainly in the mining and power industries to crush coal (power industry) and mineral bearing ore (mining) for further processing.

A cross section of a tube mill is shown in Figure 1.1. A mill charge consists of both coal ore and grinding media. The grinding media can consist of balls, rods or pebbles. The amount of charge in the mill is referred to as the Percentage Fill (J). The mill charge is divided into two distinct regions.

These regions are divided by the line AB. The region of the mill charge that falls below this line is known as the 'en Masse' region. The 'Angle of Repose' is the angle of line AB to the horizontal.

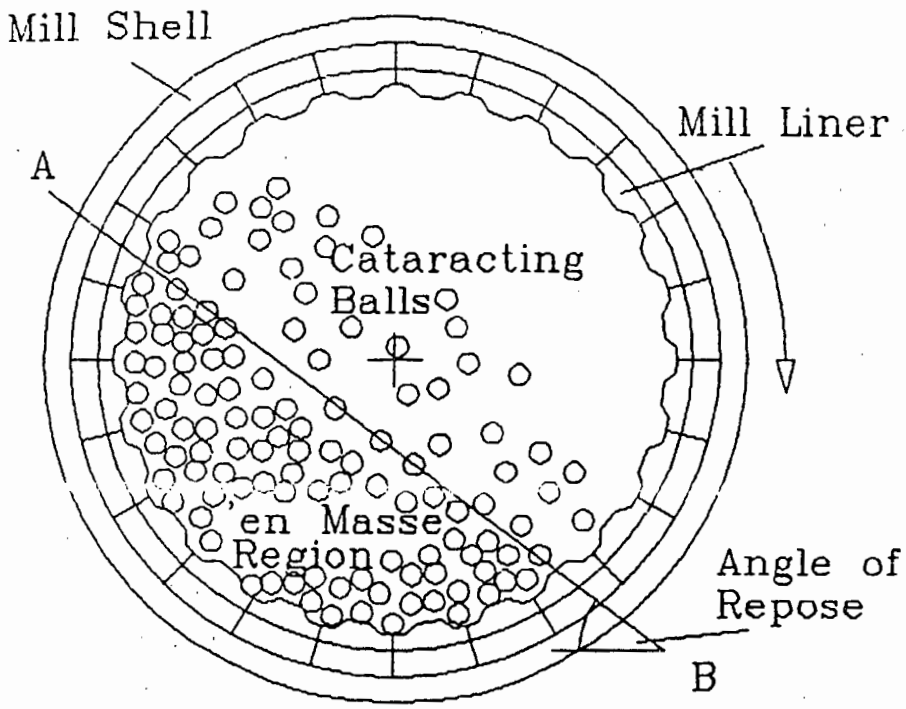

Figure 1.1: Cross-section through a tube mill[1].

The motion of the balls can be defined by using one of two terms, cataracting or cascading. A ball is defined as cataracting if it detached from the main body of the charge. If the ball does not leave the body of the charge but rolls down the charge face it is defined as cascading.

The point where the balls leave the charge is defined as the **Point of Departure** (POD). The angle of this point, above the horizontal through the mill centre, is known as the **Angle of Departure** (AOD). If the mill speed is increased then the AOD will also increase. The AOD will increase to a point (90°) where the charge no longer leaves the liner. This condition is known as centrifuging. The theoretical velocity at which this occurs was defined by Davis[4] as being the Mill Critical Velocity (N_c).

In tube mills coal ore is ground by a combination of abrasion, attrition and impact. The large portions of coal that are fed into the mill are initially broken up by the cataracting action of the larger balls impacting on the coal at the toe of the charge. The mill speed is controlled so that the cataracting balls impact on the toe of the charge. If the mill speed is too high then the balls impact on the exposed liner and results in accelerated wear of the liners.

The second process in the mill whereby the chips of coal are ground into a fine powder is achieved by the mechanisms of attrition and abrasion. The fine grinding is performed by the smaller balls and occurs by rubbing the coal between the balls. The powdering of the coal is performed in the 'en Masse' region where grinding pressures are high. The powdered coal is then extracted by blowing hot air through one end of the mill. The coal dust is extracted out of the other end and is fed into classifiers to ensure that the particle size of the coal dust is small enough. If the coal dust particle size is too large (>75 μm) it is returned to the mill for further processing, otherwise it is is blown into the boilers for combustion.

2.2 The Effect of Liner Design upon Charge Motion in a Rotary Mill. Author: M. Powell[11]

This thesis involved the theoretical and experimental investigation of the charge motion of an isolated rod or ball. It also investigated how the charge motion is influenced by the geometry of a flat faced lifter-bar. Factors such as face-angle, lifter-bar height and the coefficient of friction between the rod and lifter-bar are taken into account. The outer layer of the charge is the portion of the charge that is most affected by the liner configuration. For this reason the theoretical and experimental investigation concentrated on the outer layer.

Experimental work was performed in an attempt to validate the theory used. The experimental work was performed in a glass ended mill and the charge motion was filmed using a high speed camera. These experiments were performed for various configurations of lifter bars and the mill was run at speeds ranging from 60% to 100% of the mill critical velocity (N_c). The coefficient of friction was measured under simulated mill conditions for various liner-ball configurations. The amount of power drawn by the mill for the various configurations was also measured.

There is good correlation between the results obtained from the experimental and theoretical investigations. A problem was encountered with the value of the coefficient of friction used in the theory. It was found that this value was not of a high enough magnitude. This was evident from comparisons made between the theoretical and experimental results. The results obtained from the theory gave a very good representation of the outer charge motion.

Powell stated that previous work on the effect of lifter bars on the charge motion in a mill extended only to the point where the charge lifted or left the liner. The work by Powell included the flight of the ball or rod after departure. The impact point, where the ball collides with the other side of the mill, is also calculated. The importance of this is that it is preferable that the charge does not impact on the liner on the other side of the mill but rather on the toe of the mill charge. If the charge impacts on the exposed liner accelerated wear of the liner occurs.

The main findings by Powell are as follows:

1. There is an increase in the angle of departure of the charge as the height of the lifter bar is increased from zero to just greater than the radius of a grinding-element. Therefore to prevent slippage in a mill the lifter-bar height should be at least as high as a grinding-element radius. The AOD increases only until a critical lifter-bar height is reached, where upon no further increase in the AOD occurs.

2. An increase in lifter-bar face-angle results in a decrease in slip and an increase in the lift and AOD of the grinding elements. An increase in the AOD leads to an increase in the impact angle of the grinding media. Powell also stated that by making use of the effect of the face-angle a liner could be 'tuned' to allow the charge to impact on a desired point.

3. There is a linear relationship between the mill speed and the angle of impact.

Powell stated that some important facts regarding the effects of lifter-bar geometry on the charge motion had been discovered. The interaction between the three main variables (mill speed, lifter-bar height and lifter-bar face-angle) are summarised in Figures 2.5-2.7.

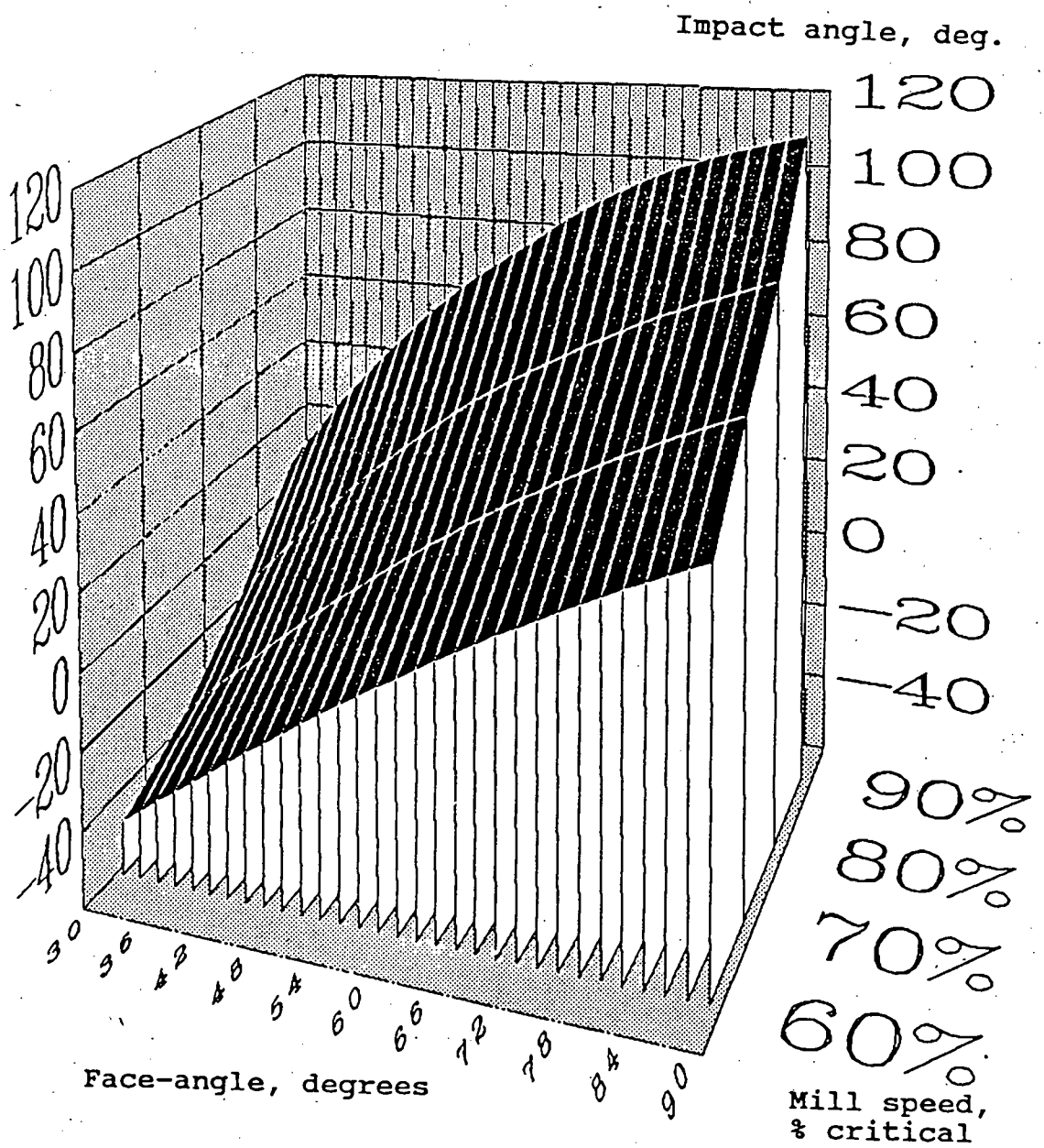

Figure 2.5: The combined influence of lifter-bar face-angle and mill speed upon the impact angle[11]

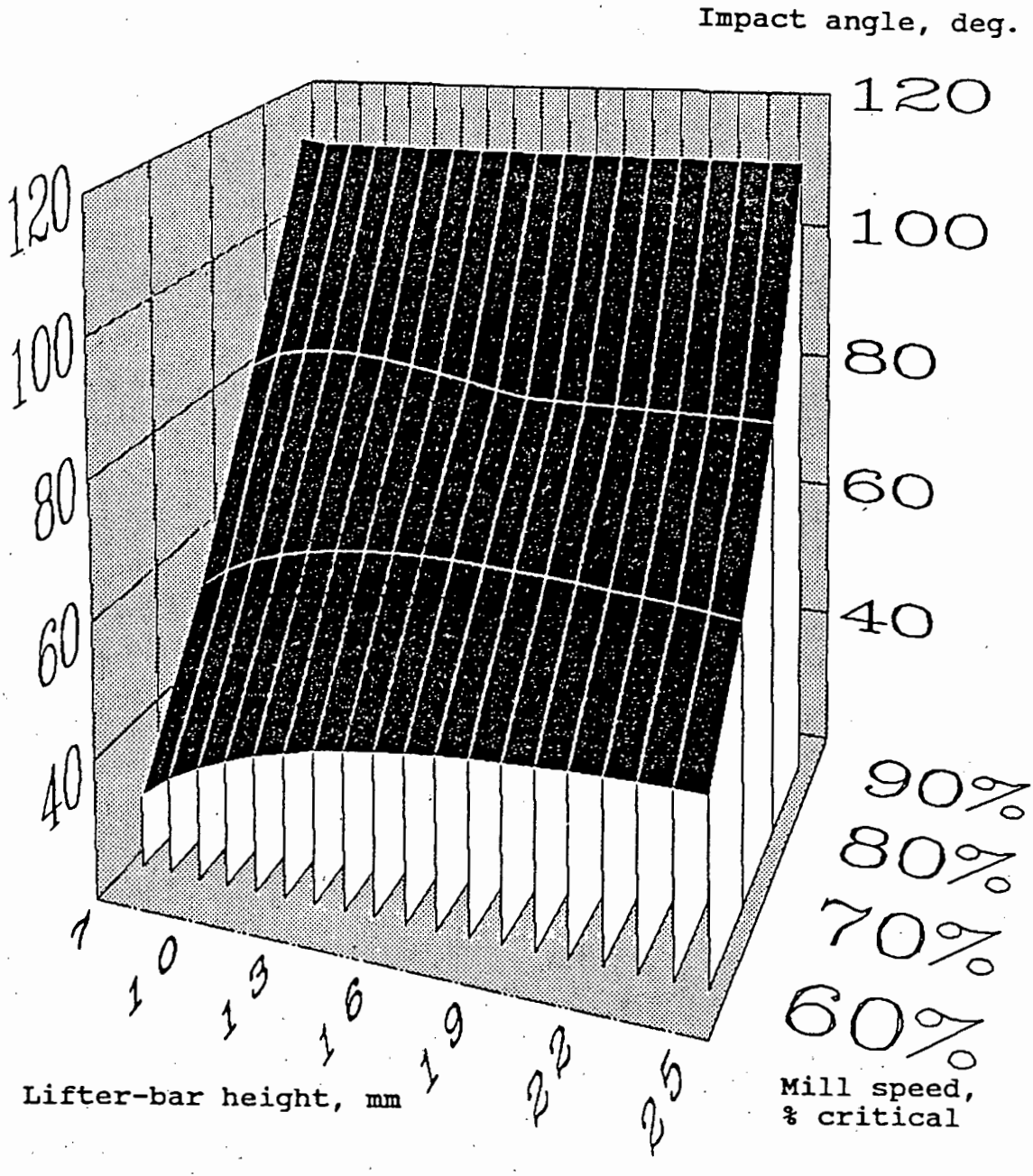

Figure 2.6: The combined influence of lifter-bar height and mill speed upon the impact angle[11]

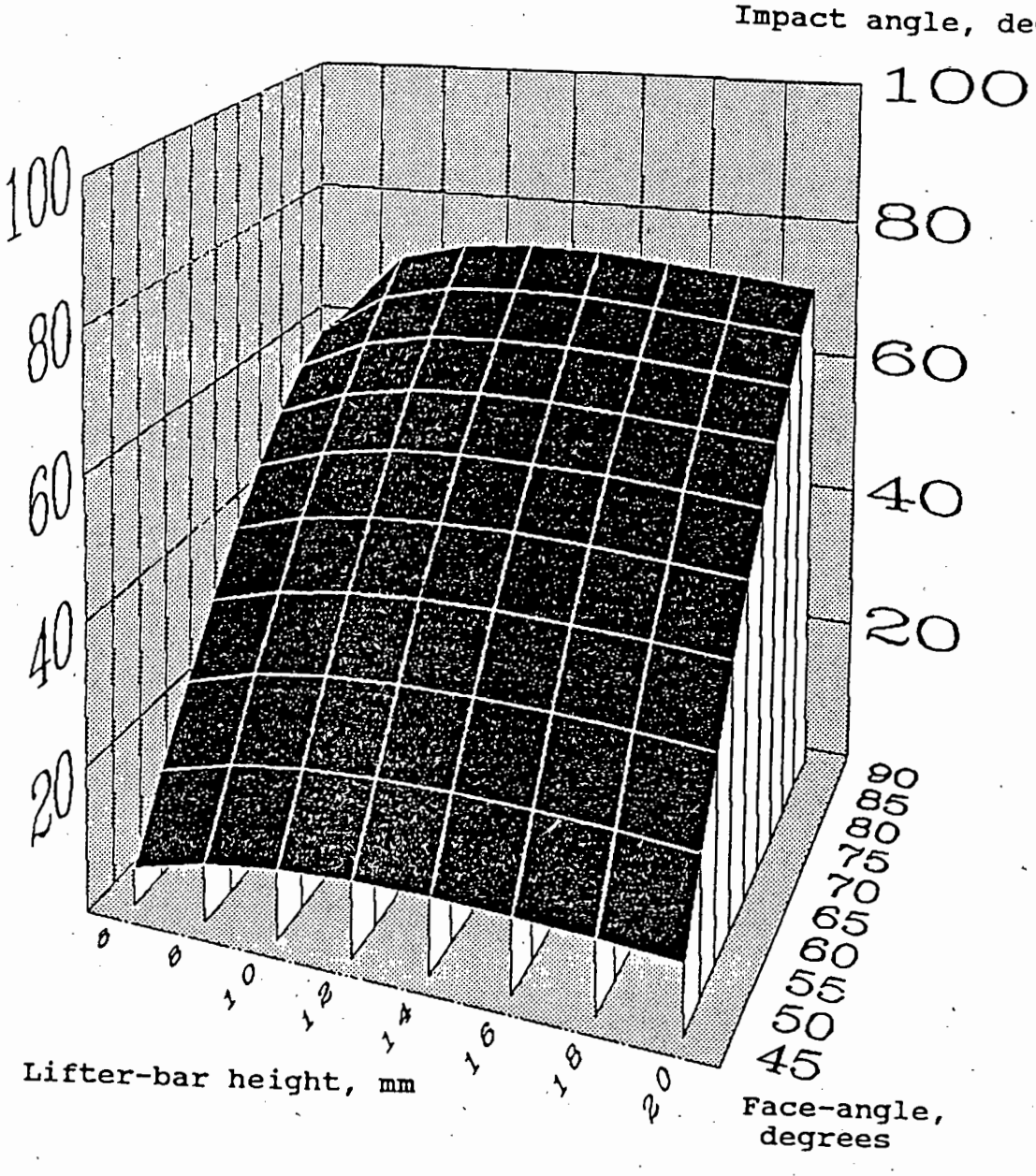

Figure 2.7: The combined influence of lifter-bar face-angle and face-angle upon the impact angle[11]

2.3 Wear of Tube Mill Liners for the South African Power Industry. Author: J.J. Skorupa[19]

A review of all general wear theories is performed. It was found that liner wear is produced by three mechanisms, namely: impact, sliding abrasion and corrosion. In air swept mills the first two are primarily responsible for the wear occurring. Wear by corrosion is only a problem in wet mills.

The wear by impact is created when the grinding media causes plastic deformation of the liner material to occur. This leads to a highly strained surface which fractures when further deformations of the surface occur. For this type of wear to occur sufficient energy has to be imparted by the impacting particle for plastic deformation of the surface to occur. The plastic deformation leads to hardening and subsequent imbrittlement of the liner material.

The sliding abrasion is caused primarily by a cutting action and also includes some wear by deformation. The mechanics of sliding wear can clearly be seen in Figure 2.8.

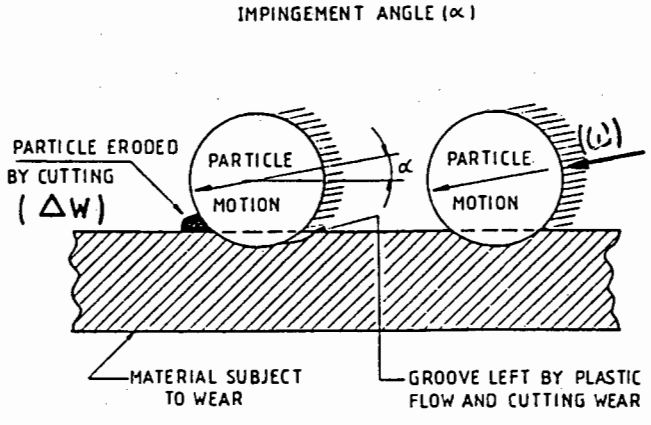

Figure 2.8: A Physical Model of Sliding Abrasion[19]

There are a large number of materials which can be used for the manufacture of liners and each material has varying degrees of resistance to wear. It is therefore important that the wear situation be thoroughly investigated before a liner material is chosen.

The wear inside the mill is influenced by the mill rotational velocity, the percentage fill of the mill and, most important, the liner profile or lifter-bar geometry. Skorupa reported that a number of studies have been performed to determine the wear resistance of various materials. These aforementioned factors were not considered in determining the wear resistance of the materials tested in the studies mentioned above.

2.3.1 Laboratory Investigation Performed to Determine the Wear Resistance of Various Metals

The following tests were performed by Skorupa to ascertain the properties of the various sample metals.

a) Metallurgical Evaluation
   1. Chemical Analysis
   2. Hardness

b) Wear Tests
   1. Rubber Wheel Abrasion Test
   2. Impact Abrasion Test
   3. Industrial Trials

In the industrial trials, liners in the shape of liner #1 (see Figure 2.9), were cast in nine different materials and placed in a tube mill that is in use at the Arnot Power Station. Before and after each test the liners were weighed and measurements of the height of the profile and liner thicknesses were taken.

In industrial tube mills there are two possibilities as to where the balls impact on the liner. The first possibility is when the ball impacts on the toe of the charge. In this instance the liner is protected by the layer of balls found at the toe of the charge. The second possibility is where the ball impacts just above the toe of the charge. Here the liner is only protected by a thin layer of coal. It was therefore decided that an electron microscope would be used to examine the material surface of the test liners. These photographs were then compared to photographs of a similar material which, under controlled laboratory conditions, had been subjected to the two mechanisms of wear mentioned above.

2.3.2. Conclusion

Skorupa reported, that by analyzing the results both statistically and by comparing them to the results obtained from classical grinding theory, that the design and experimental methods used were appropriate and consistent. There was no evidence of unreliability in the statistical analysis.

It is also shown that the principles of scaling the mill speed were valid. This was proven by laboratory tests using high speed photography. This is further supported by the close agreement of the results obtained from the industrial trials and the experimental work in the laboratory.

The liner shapes shown in Figure 2.9 were cast in a ceramic material and tested in a working tube mill. It was evident from these additional industrial trials that one of the liners showed superior wear performance characteristics. The recommendation is made that after some further testing, that liner #4 could replace the currently used liner #1.

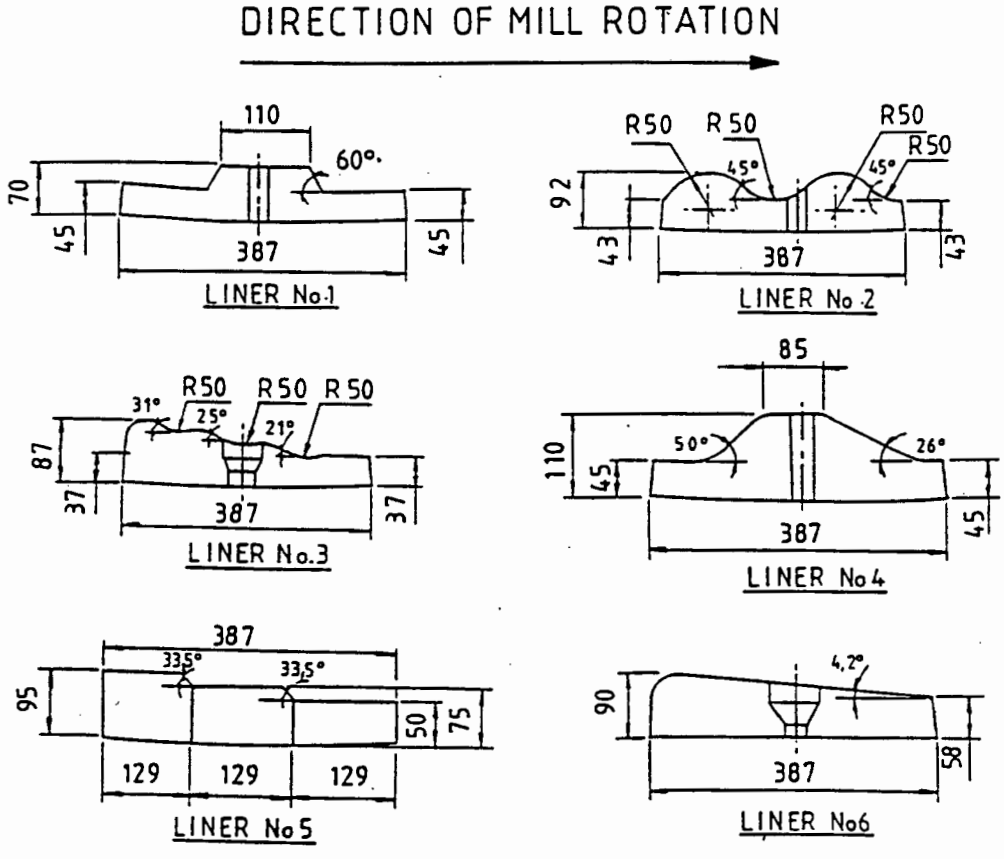

Figure 2.9: Mill Liner Profiles Tested[19]

CHAPTER 3

THEORETICAL ANALYSIS OF THE MOTION OF A BLOCK ON A CORRUGATED LINER

A particle in a mill can experience three distinct types of motion. It can either slide, roll or move with a combination of the two along a liner surface. Previous work has modelled these types of motion on a flat liner[1]. The next step was to include the effect that a corrugated liner has on a particle's motion.

3.1 Model Justification

A particle moving in free space has six degrees of freedom (DOF), three translational and three rotational. Nates[1] reported that previous investigators (3, 8, 10, 11) had ignored the out-of-plane travel of the particle and the system is then reduced to two dimensions (ie x and y directions). The resulting system consists of three degrees of freedom (two translational and one rotational). The rotational degree of freedom is the spin of the particle about an axis parallel to the mill axis.

The motion of a sphere on the inside of a rotating cylinder can be modelled by including the rotational DOF into the model. By restricting the rotational degree of freedom the system is reduced to two degrees of freedom. This is the equivalent of not allowing the ball to spin.

The two models investigated were for a block with two degrees of freedom (two translational DOF) and a sphere with three DOF (two translational and one rotational). It has been found that balls subjected to wear in the tube mills develop flat faces and become cubic in shape. The fact that they become cubic in shape leads to the conclusion that they cannot readily spin when moving along a liner. It is therefore justifiable to use a block shaped particle as a starting point for the analysis of a single particle on a corrugated liner in a rotating cylinder.

3.2 The Derivation of a Surface Function to Model a Corrugated Liner

By using Fourier Analysis any periodic liner shape can be approximated. The equation used for this analysis is shown below.

$$f(\beta) = \rho + \sum_{n=1}^{N} \left(c_n \text{Cos}(\zeta_n \beta) + d_n \text{Sin}(\zeta_n \beta) \right) \tag{3.1}$$

where N = number of terms

ρ = mean radius of liner

c_n = constant

d_n = constant

ζ_n = No of Corrugations per 360°

β = Relative Angular Position of Block

The initial function that will be used is a simple Cosine function. This liner function takes the form

$$f(\beta) = \rho + c_1 \text{Cos}(\zeta_1 \beta) \tag{3.2}$$

where c_1 = Amplitude of the Corrugations

ζ_1 = Frequency of the Corrugations

This equation, when plotted in polar coordinates, describes the liner surface. The values of ρ, c_1 and ζ_1 can be altered to change the shape of the liner used. This is illustrated in Figures 3.1 and 3.2.

The other liner that will be modelled is the liner found by Skorupa[19] to be the most wear resistant in industrial tests. The derivation of the Fourier Series Approximation for this liner can be seen in Appendix A. The liner used can be seen in Figure 3.3. When the governing equation (Equations 3.25) block were solved for this liner (derived from Skorupa[19]), it was found that the Fourier Series Approximation did not model the liner adequately. The shortcomings of the Fourier Series Approximation are discussed in Section 3.3.4.

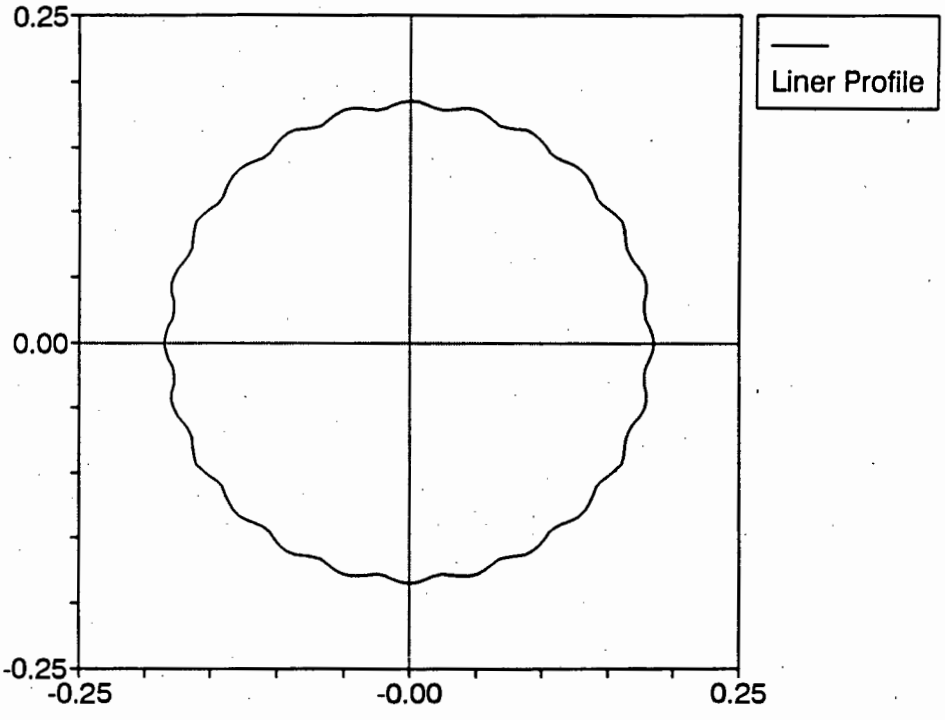

Figure 3.1: Liner Profile for the function
$f(\beta) = 0.1825 + 0.003\ \mathrm{Cos}(24\beta)$

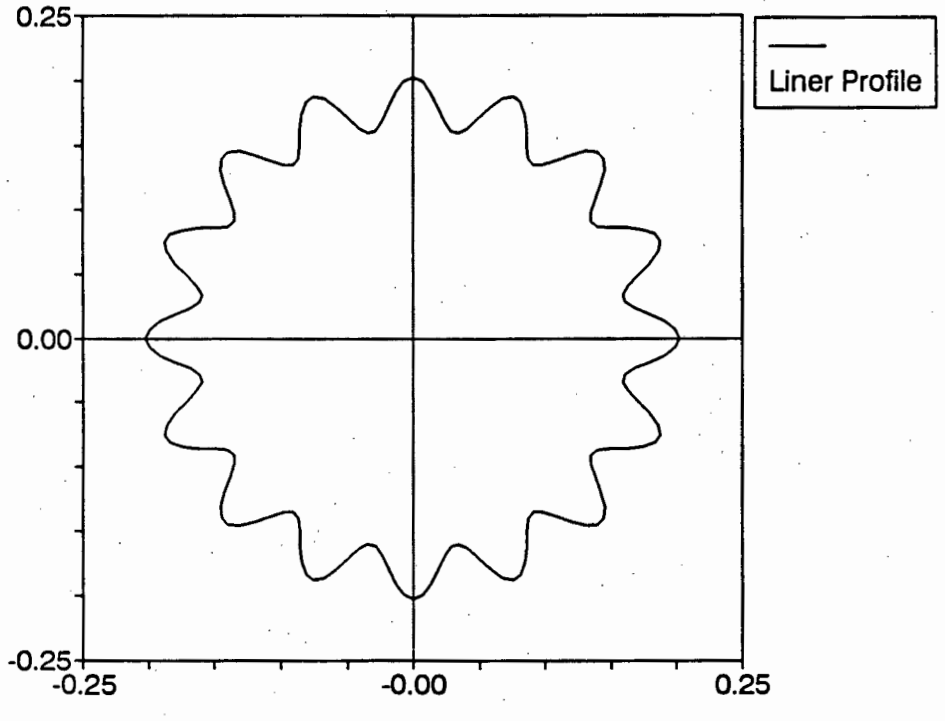

Figure 3.2: Liner Profile for the function
$f(\beta) = 0.1825 + 0.02\ \mathrm{Cos}(16\beta)$

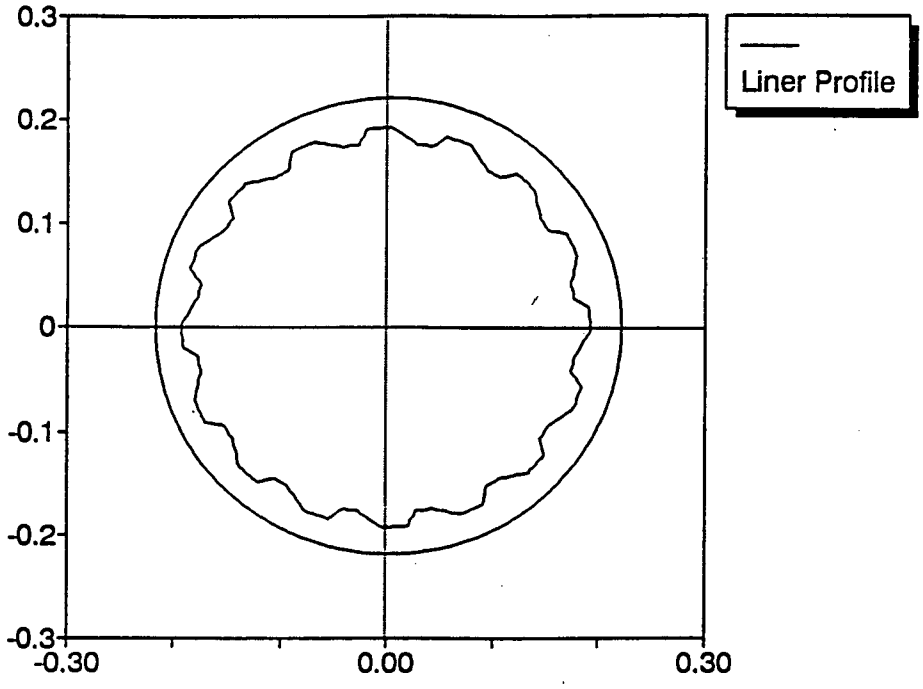

Figure 3.3: Liner Profile from Skorupa

3.2.1. Rotation Of the Liner

To rotate the liner the following equation is assumed

$$\beta = \phi - \Omega_m t \qquad (3.3)$$

Where β = Relative Angle of Displacement of a Particle

ϕ = Angular Position of a Particle

Ω_m = Rotational Speed of the Liner in rad s^{-1}

t = Time Elapsed from Release of Particle

During the formulation of the governing equation (Eqn 3.25) of a block on a corrugated liner the first and second derivatives, with respect to time, of Equation (3.1) are required. The first and second derivative of Equation (3.3) are also required. These are

$$\dot{\beta} = \dot{\phi}\ \Omega_m \qquad (3.4)$$

$$\ddot{\beta}\ \ddot{\phi} \qquad (3.5)$$

3.3 Derivation of the Equations Governing the Motion of a Block on a Corrugated Liner

There are two types of motion that can occur when a block is in contact with a rotating liner. The first is when the block moves with the same velocity as the liner (i.e. the block is sticking to the liner). The other type of motion that can occur is when the block does not move at the same velocity as the liner (i.e. the block is slipping relative to the liner).

3.3.1 Derivation of the Sliding Equations

It is necessary to ascertain the position of the block relative to its surroundings. The vectors that are used to describe the position of the block are shown in Figure 3.4.

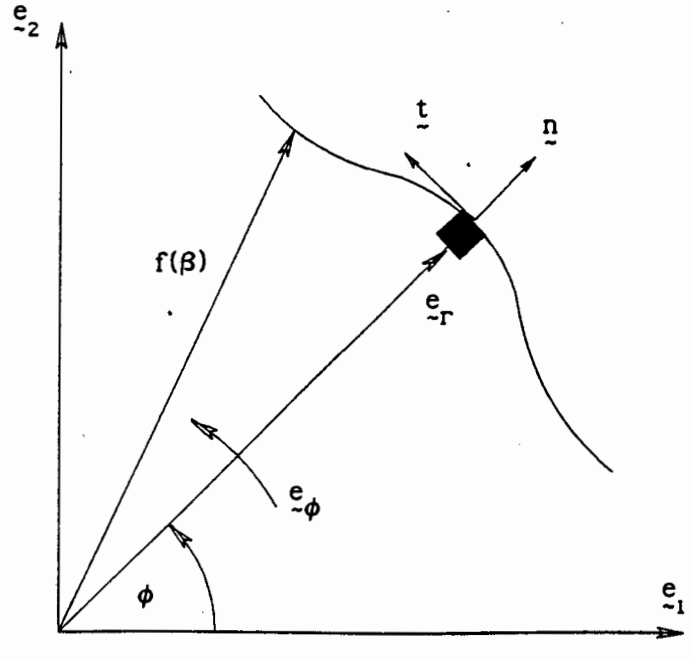

Figure 3.4: Vectors acting on a Block on a Corrugated Liner.

The position of the point of contact between the block and liner, in the cartesian coordinate system, is given by

$$\underset{\sim}{r}(x,y) = x\ \underset{\sim}{e}_1 + y\ \underset{\sim}{e}_2 \qquad (3.6)$$

where $\underset{\sim}{e}_1$ and $\underset{\sim}{e}_2$ are unit vectors

Equation (3.6) can be simplified into components of $f(\beta)$ in the x and y directions. This leads to Equation (3.7)

$$\underset{\sim}{r}(\beta) = f(\beta)\ \mathrm{Cos}(\beta)\ \underset{\sim}{e}_1 + f(\beta)\ \mathrm{Sin}(\beta)\ \underset{\sim}{e}_2 \qquad (3.7)$$

where $f(\beta)$ is defined in Equation (3.1)

Equation (3.7) can be converted to the polar coordinate system by introducing the radial and angular unit vectors: $\underset{\sim}{e}_r$ and $\underset{\sim}{e}_\phi$,

$$\underset{\sim}{e}_r = \mathrm{Cos}(\phi)\ \underset{\sim}{e}_1 + \mathrm{Sin}(\phi)\ \underset{\sim}{e}_2$$

$$\underset{\sim}{e}_\phi = -\mathrm{Sin}(\phi)\ \underset{\sim}{e}_1 + \mathrm{Cos}(\phi)\ \underset{\sim}{e}_2$$

The position of the block centre can then be expressed in vector form by

$$r(\beta) = f(\beta)\ \underset{\sim}{e}_r - a\ \underset{\sim}{n} \qquad (3.8a)$$

where a = Distance from block centre to liner

It is assumed however that $f(\beta) \gg a$, therefore Equation (3.8a) becomes

$$\underset{\sim}{r}(\beta) = f(\beta)\ \underset{\sim}{e}_r \qquad (3.8b)$$

Equation (3.8b) is used to ascertain the position of the block. It is also necessary to ascertain the velocity and acceleration of the block. This is done by taking the first and second derivatives, with respect to time, of Equation (3.8b). The first derivative is given by

$$\underset{\sim}{r}'(\beta) = \dot{\beta}\ f'(\beta)\ \underset{\sim}{e}_r + f(\beta)\ \dot{\underset{\sim}{e}}_r \qquad (3.8c)$$

But

$$\dot{\beta} = \dot{\phi} - \Omega_m$$

and

$$\dot{\underset{\sim}{e}}_r = \dot{\phi}\ \underset{\sim}{e}_\phi$$

Therefore Equation (3.8c) becomes

$$\dot{\underset{\sim}{r}}(\beta) = \left(\dot{\phi} - \Omega_m \right) f'(\beta)\, \underset{\sim}{e}_r + \dot{\phi}\, f(\beta)\, \underset{\sim}{e}_\phi \tag{3.9}$$

The second derivative with respect to time is given by

$$\ddot{\underset{\sim}{r}}(\beta) = \ddot{r}_r\, \underset{\sim}{e}_r + \ddot{r}_\phi\, \underset{\sim}{e}_\phi \tag{3.10}$$

$$\text{where } \ddot{r}_r = \ddot{\phi}\, f'(\beta) + \dot{\phi}^2 \left(f''(\beta) - f(\beta) \right) - 2\, \Omega_m\, \dot{\phi}\, f''(\beta) + \Omega_m^2\, f''(\beta)$$

$$\ddot{r}_\phi = \ddot{\phi}\, f(\beta) + 2\, \dot{\phi}^2\, f'(\beta) - 2\, \Omega_m\, \dot{\phi}\, f'(\beta)$$

All the forces acting on the block can be shown in vector form.

$$\underset{\sim}{F} = m\, \ddot{\underset{\sim}{r}} \tag{3.11}$$

The force vector $\underset{\sim}{F}$ comprises three components. These are the Normal Reaction Force ($\underset{\sim}{R}$), the Tangential Friction Force ($\underset{\sim}{T}$) and the Weight Component ($\underset{\sim}{W}$). This stated in equation form is

$$\underset{\sim}{F} = \underset{\sim}{R} + \underset{\sim}{T} + \underset{\sim}{W}$$

The forces, that act on the block are shown in Figure 3.5, and represented in the form

Normal Reaction Force $\quad \underset{\sim}{R} = -N_r\, \underset{\sim}{n} \tag{3.12}$

Tangential Friction Force $\quad \underset{\sim}{T} = N_t\, \underset{\sim}{t} \tag{3.13}$

Weight Component $\quad \underset{\sim}{W} = -\, m\, g\, \underset{\sim}{e}_2$

$$= -\, m\, g \left(\text{Sin}(\phi)\, \underset{\sim}{e}_r + \text{Cos}(\phi)\, \underset{\sim}{e}_\phi \right) \tag{3.14}$$

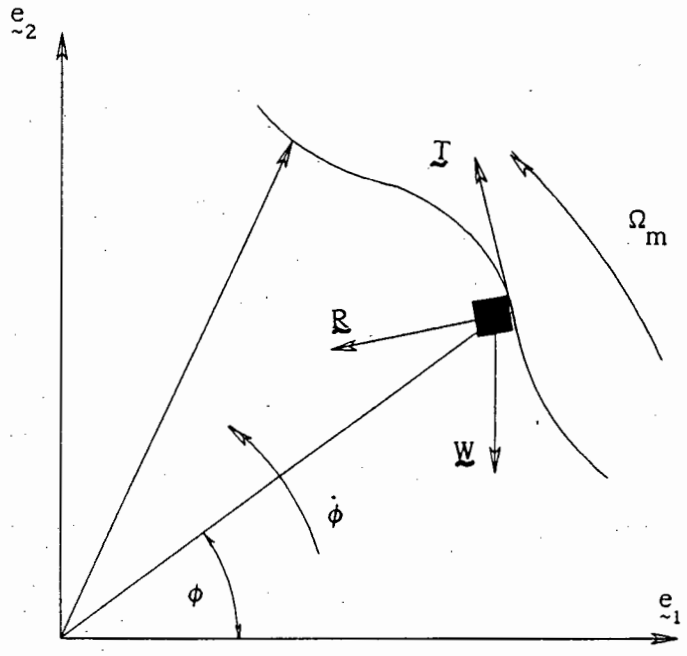

Figure 3.5: Orientation of the Forces Acting on a Block on a Corrugated Liner

The vectors $\underset{\sim}{n}$ and $\underset{\sim}{t}$ are the unit normal and tangent vectors to the liner surface. The derivation of the unit vectors is shown in Appendix B, and are

$$\underset{\sim}{n} = \alpha \left\{ f(\beta)\, \underset{\sim}{e}_r - f'(\beta)\, \underset{\sim}{e}_\phi \right\} \tag{3.15}$$

$$\underset{\sim}{t} = \alpha \left\{ f'(\beta)\, \underset{\sim}{e}_r + f(\beta)\, \underset{\sim}{e}_\phi \right\} \tag{3.16}$$

$$\text{where } \alpha = \frac{1}{\sqrt{f(\beta)^2 + f'(\beta)^2}}$$

Equations (3.10), (3.12), (3.13) and (3.14) are substituted into Equation (3.11). The resulting equation is then resolved into the radial and angular components.

Resolved in the e_r (radial) direction:

$$m \ddot{r}_r = - \alpha f(\beta) N_r + \alpha f'(\beta) N_t - m g \text{Sin}(\phi) \qquad (3.17)$$

Resolved in the e_ϕ (angular) direction:

$$m \ddot{r}_\phi = \alpha f'(\beta) N_r + \alpha f(\beta) N_t - m g \text{Cos}(\phi) \qquad (3.18)$$

Equations (3.17) and (3.18) are two equations in two unknowns (N_t,N_r). Solving for these two unknowns, the derived equations are

$$N_t = m \alpha \left[f'(\beta) \ddot{r}_r + f(\beta) \ddot{r}_\phi \right] + m g \alpha \left[f(\beta) \text{Cos}(\phi) + f'(\beta) \text{Sin}(\phi) \right] \qquad (3.19)$$

and

$$N_r = m \alpha \left[f'(\beta) \ddot{r}_\phi - f(\beta) \ddot{r}_r \right] + m g \alpha \left[f'(\beta) \text{Cos}(\phi) - f(\beta) \text{Sin}(\phi) \right] \qquad (3.20)$$

Equations (3.19) and (3.20) are used for both the *non-sliding* and *sliding* conditions. For the non-sliding condition the ball rotates with the same angular velocity as the mill (i.e. $\dot{\phi} = \Omega_m$). The angular displacement and acceleration of the ball can be calculated from

$$\dot{\phi} = \Omega_m \qquad (3.21)$$

Integrating Equation (3.21) with respect to time yields the angular displacement.

$$\phi = \Omega_m t + \xi \qquad (3.22)$$

where ξ = Starting Point of the Block

The acceleration is derived by differentiating Equation (3.21) with respect to time. This yields

$$\ddot{\phi} = 0 \tag{3.23}$$

The block will continue to rotate at $\dot{\phi} = \Omega_m$ until friction is exceeded. When this occurs Equations (3.21)-(3.23) are no longer valid, and the block will start to slide relative to the liner. It is assumed that the *Frictional Force* (N_t) between the block and the liner is directly proportional to the *Normal Reaction Force* (N_r). This is governed by

$$N_t = \mu N_r \tag{3.24}$$

By substituting Equations (3.19) and (3.20) into Equation (3.24), the governing equation for a block sliding on a corrugated surface is derived, and takes the form of a Second Order Differential Equation;

$$B \ddot{\phi} + C \dot{\phi} + D \dot{\phi}^2 + E = 0 \tag{3.25}$$

where $B = \dfrac{1}{\alpha^2}$

$$C = -2\Omega_m \left\{ f''(\beta) \left[f'(\beta) + \mu f(\beta) \right] - f'(\beta) \left[f(\beta) - \mu f'(\beta) \right] \right\}$$

$$D = 2 f'(\beta) \left\{ f(\beta) - \mu f'(\beta) \right\} + \left\{ f'(\beta) + \mu f(\beta) \right\} \left\{ f''(\beta) - f(\beta) \right\}$$

$$E = g \left\{ \left[f(\beta) - \mu f'(\beta) \right] \mathrm{Cos}(\phi) + \left[f'(\beta) + \mu f(\beta) \right] \mathrm{Sin}(\phi) \right\} + \Omega_m^2 f''(\beta) \left[f'(\beta) + \mu f(\beta) \right]$$

Equation (3.25) is in terms of ϕ (i.e. it has only one degree of freedom). As stated by Nates[1] it is evident from Equation (3.25) that the motion of the block is independent of the mass of the block. The mass only affects the values of N_r and N_t.

A comparison of the equations derived for a block on a corrugated liner and the equations derived by Nates[1] is shown below.

	von Bentheim	Nates
Reaction Force	N_r (Eqn 3.19)	$R = m \rho \dot{\phi}^2 - m g \, Sin(\phi)$
Tangential Force	N_t (Eqn 3.20)	$T = m \rho \ddot{\phi} + m g \, Cos(\phi)$
Governing Equation	$B\ddot{\phi} + C\dot{\phi} + D\dot{\phi}^2 + E = 0$	$\rho\ddot{\phi} - \rho\mu\dot{\phi}^2 + g(\mu Sin\phi + Cos\phi) = 0$

Table 3.1: Comparisons of Equations Derived by von Bentheim and Nates[1]

If the correct boundary conditions are substituted into the governing equation and the equations for the Tangential Force and Reaction Force, as derived in this thesis, then the formulation derived by Nates[1] is produced. This is shown in Appendix C.

3.3.2 Numerical Solution of Sliding Equations

The governing equation (Equation (3.25)) is a *second order, non-linear, homogeneous ordinary differential equation* (ODE). This equation is of a highly non-linear nature and therefore a numerical solution has been sought.

The governing equation can be decomposed into two first order differential equations. These two equations are then solved simultaneously using a Fourth-Order Runge-Kutta Method[20]. This method is used instead of the Euler Forward Step because the Fourth-Order Runge-Kutta Method is computationally more efficient. Due to its formulation larger time steps can be taken whilst retaining the same degree of accuracy as the Euler Forward Step. The procedure for the decomposition of the second order differential equation is shown in Appendix D. The following equations were used in the numerical solution

$$\phi_{n+1} = \phi_n + h\,\dot{\phi}_{n+1} \tag{3.26}$$

$$\dot{\phi}_{n+1} = \dot{\phi}_n + h\,\ddot{\phi}_{n+1} \tag{3.27}$$

$$\ddot{\phi}_{n+1} = (k_1 + 2\,k_2 + 2\,k_3 + k_4)/6 \tag{3.28}$$

Where $k_1 = -h\,(C_n u_1 + D_n u_1^2 + E_n)/B_n \quad ; u_1 = \dot{\phi}_n$

$k_2 = -h\,(C_n u_2 + D_n u_2^2 + E_n)/B_n \quad ; u_2 = \dot{\phi}_n + 0.5 \cdot k_1$

$k_3 = -h\,(C_n u_3 + D_n u_3^2 + E_n)/B_n \quad ; u_3 = \dot{\phi}_n + 0.5\,k_2$

$k_4 = -h\,(C_n u_4 + D_n u_4^2 + E_n)/B_n \quad ; u_4 = \dot{\phi}_n + k_3$

h = Time Step

n = Present Increment

n+1 = Next Increment

B, C, D, E as stated in Equation (3.25)

When solving a differential equation numerically it is necessary to have boundary conditions. The initial boundary conditions for the governing equation, Equation (3.26), are the block's initial position (ϕ) and angular velocity ($\dot{\phi}$) at time t = 0. The program allows these values to be specified prior to solving the ODE.

During the solution of the differential equation a point is reached where the block starts to slide. Just prior to the onset of sliding the block's angular velocity equals the mill rotational velocity ($\Omega_m = \dot{\phi}$) and its angular acceleration is zero ($\ddot{\phi} = 0$). Until the point of sliding the Tangential Friction Force (N_t) is directly proportional to the Normal Reaction Force (N_r).

Therefore the theoretical point of slipping can be obtained from:

$$N_t = \mu\, N_r \tag{3.24}$$

Substituting for N_t and N_r, in Equation (3.24), and using the conditions that occur at the point of slipping, $f(\phi) = \rho_1$ and $f'(\phi) = f''(\phi) = 0$, yields

$$J \ddot{\phi} + K \dot{\phi} + L \dot{\phi}^2 + M = 0 \qquad (3.30)$$

where $J = \rho_1$

$K = 0$

$L = - \mu \rho_1^2$

$M = \rho_1 \, g \left\{ \text{Cos}(\phi) + \mu \, \text{Sin}(\phi) \right\}$

But $\dot{\phi} = \Omega_m$ and $\ddot{\phi} = 0$, therefore Equation (3.30) becomes

$$g \left\{ \text{Cos}(\phi) + \mu \, \text{Sin}(\phi) \right\} = \rho_1 \, \mu \, \Omega_m^2 \qquad (3.31)$$

Equation (3.31) is solved using the solving routine on a Hewlett Packard 28S scientific calculator. The results obtained from the solution of this equation is defined as ϕ_{slip} and is the angular position at which the block starts to slide for the given mill speed and given coefficient of friction.

Various end conditions have to be imposed so that the numerical solution of the ODE can be terminated. For a block moving on a corrugated liner there are two possible end conditions. These are

1. The block leaves the liner and follows a parabolic trajectory.
2. The block becomes centrifuged to the liner.

It is assumed that when $N_r < 0$ then the block has left the liner. When the block has left the liner it will travel in a parabolic trajectory until it impacts on the liner. The initial velocity of the block when it leaves the liner is calculated from Equation (3.9). The velocities of the block, at the start of the parabolic flight, in the x and y direction are

$$v_x = (\dot{\phi} - \Omega_m) \, f'(\beta) \, \text{Cos}(\phi) - \dot{\phi} \, f(\beta) \, \text{Sin}(\phi) \qquad (3.32)$$

$$v_y = (\dot{\phi} - \Omega_m) \, f'(\beta) \, \text{Sin}(\phi) + \dot{\phi} \, f(\beta) \, \text{Cos}(\phi) \qquad (3.33)$$

Energy is transferred from the liner to the block via the frictional force. As the coefficient of friction is increased so the energy transfer between the liner and block increases. It is also evident that as the amplitude (ie height) of the liner is increased so will the energy transfer between the liner and block increase. The higher the blocks kinetic and potential energy the higher the block will travel up the liner prior to departure from the liner. The time taken for the block to reach the Point of Departure **(POD)** will depend on the coefficient of friction as well as the configuration of the liner.

The point of departure can occur anywhere between -90° and 90°. In the model developed by Nates[1] the block could only leave the liner above the horizontal ($\phi > 0$). In the model developed for a block on a corrugated liner a block can leave the liner prior to it reaching the horizontal ($\phi < 0$). This is only possible if the magnitude of the relative velocity, between the block and the liner, is large enough (ie $\dot{\phi} << \Omega_m$). This will cause the block, on reaching the peak between two troughs, to leave the liner.

A block is described as being centrifuged when $\phi \approx 90^{\circ}$ and $\dot{\phi} > 0$. There are two types of centrifuging that can occur. The first is when a block slides relative to the liner. When this occurs the block is actually slipping relative to the liner. This type of centrifuging is known as *Slipping Centrifuging*. The other type of centrifuging is when the block travels at the same speed as the liner (i.e. $\dot{\phi} = \Omega_m$) and the block is known as being *Totally Centrifuged*. This type of centrifuging occurs if the coefficient of friction and/or the speed of the mill are large. A block becomes totally centrifuged when the block reaches the top of the mill (ie $\phi = 90^{\circ}$).

3.3.3 Computer Implementation of the Numerical Solution of the Governing Equations for a Block on a Corrugated Liner

The Runge-Kutta type methods (of which the Euler Method is a special case) are called single-step methods because they only use the information from the last step computed. In this way they have the ability to perform the next step with a different time step and are ideal for solving equations where only the initial conditions are known. The Fourth-order Runge-Kutta method is used to solve the governing differential equation.

The program used is a modified version of the one used by Nates[1]. The program is written in Fortran 77 and was implemented on a main frame computer. This required that the program developed by Nates[1] had to be transferred and a number of minor changes had to be made. These changes were necessitated due to there being slight differences between the main frame and PC based Fortran 77. The main frame was not able to support the graphics routines used by Nates[1]. The main frame did not have any equivalent graphics routines so it was decided that the graphical output of the block behaviour would be sacrificed in the interests of computational speed. Figure 3.6. contains a simplified flow chart of the computer program.

The program can be divided into four main parts. These are:

1. Input of Variables.
2. Solution of Governing Equations.
3. The Step-wise Solution of the Parabolic Flight.
4. Output to the Data Files.

At start of the program the user is given the opportunity to name the output data file. The facility to change the input variables (initial conditions) from within the program was included to enable the user to change the input variables easily. Once the data output file has been initialized then the initial conditions are written to the output file.

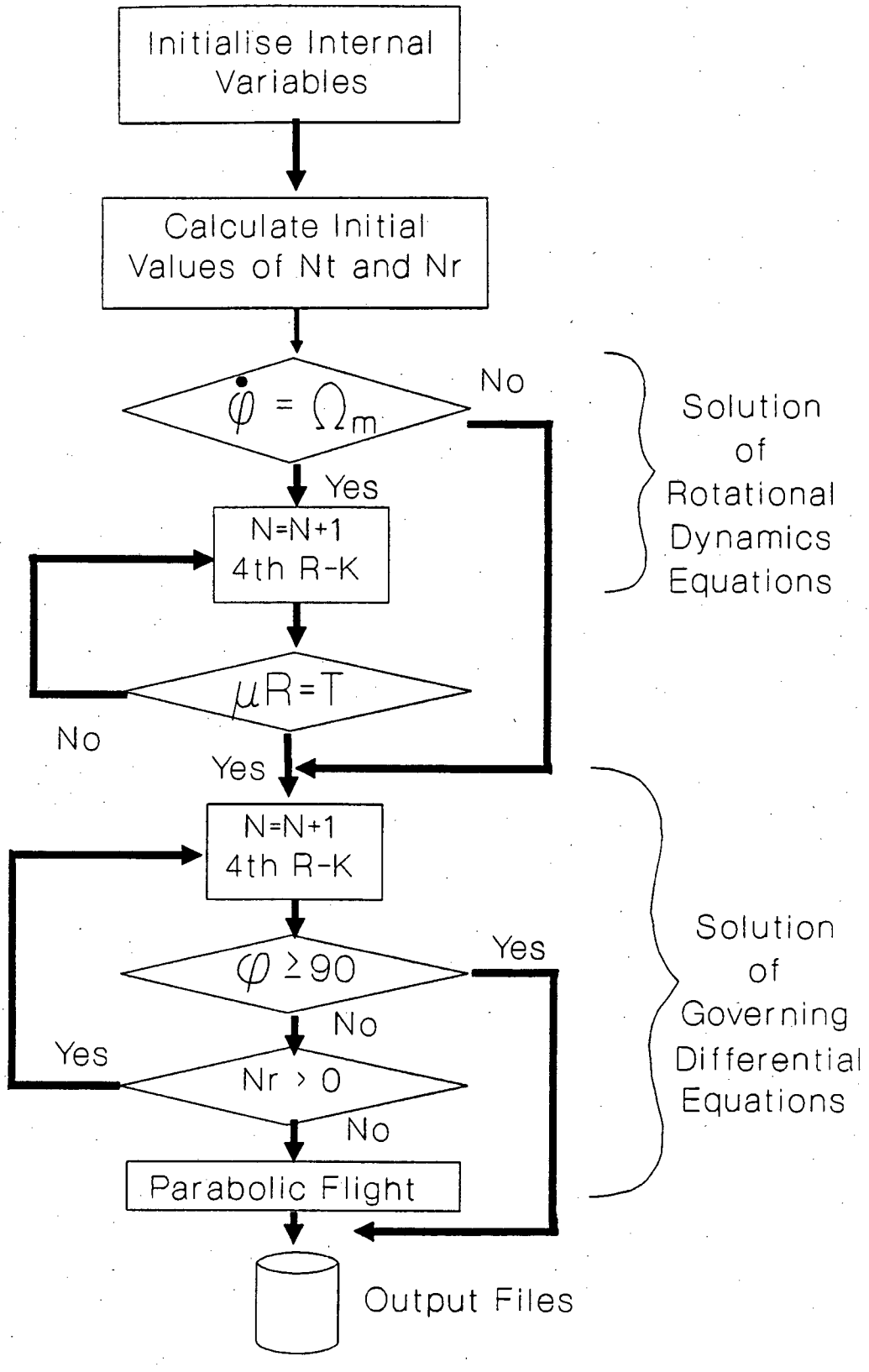

Figure 3.6: Computer Program Flow Chart

The second part of the program is the section where the solution of the governing equations is solved. The block can move with the same velocity as the liner ($\dot{\phi} = \Omega_m$) or if the block is sliding relative to the liner ($N_t \geq \mu N_r$). A flag is used to determine whether the block is sticking or sliding relative to liner. If the block is sticking to the liner then the governing equations used are simple rotational dynamics equations (Equations (3.20)-(3.23). A check is made following each time step to determine whether the block has started to slide. If it has started to slide then the flag is changed and the governing equations for a sliding block are solved.

For both the non-sliding and sliding equations the values for the liner function and its derivatives has to be calculated. This was done in a separate subroutine, called "FUNCTION.FOR". The equations for the three liner configurations were defined in three separate files with differing file names. These file names were changed to "FUNCTION.FOR" for each liner configuration studied. The solution of the governing equations for the sliding of the block was also performed in a separate subroutine. Two checks are made at the end of each time step. These are to ascertain whether the block has centrifuged to the liner ($\phi \geq 90^\circ$) or if it has left the liner ($N_r \leq 0$). If the block has left the liner then it is assumed that the block will follow a parabolic path. A flag is set when the block leaves the liner and the program branches into the fourth part of the program which performs the step-wise solution of the parabolic flight of the block. This is terminated when the block impacts on the liner after completion of its parabolic flight.

The fifth part of the program writes the numerical results to file. These values, which are calculated after each time interval, are stored in an array and written to the output file once the solution of the governing equation is terminated.

3.3.4. Numerical Implementation of the Skorupa Liner Function

The liner shape that was found by Skorupa[19] to be the most wear resistant was modelled using a Fourier Series. The solution of the theoretical model produced results that did not correlate with results obtained from the other liner configurations modelled. This was substantiated when the experimental work for the Skorupa liner was performed. On investigation, it was found that the Fourier function modelled the liner satisfactorily but the first and second derivatives showed large deviation from the intended values.

In Figure 3.7 a comparison is made between the Fourier function and the series of straight lines used to define the Skorupa liner. These straight lines define the correct liner shape. There is a close correlation between the Fourier function and the straight lines. In Figure 3.8 a comparison is made between the first derivatives. It can be seen that the first derivative of the Fourier function correlates closely to the first derivative of the straight lines. The first derivative of the Fourier function does however oscillate about the ideal value. The second derivatives of both the Fourier function and straight lines are compared in Figure 3.9. It can be seen that the second derivative for the series of straight lines is equal to zero. The second derivative for the Fourier function oscillates between an approximate values of 40 and -40. The oscillation of the first and second derivatives leads to there being inconsistencies occurring in the calculation of the constants for the governing equation (Equation 3.25).

There are two possible solutions available to solve this problem. The first was to use more Fourier terms to define the liner surface. The second was to use a series of straight lines. As it was not feasible to increase the number of Fourier terms, it was decided that straight lines would be used to define the liner surface.

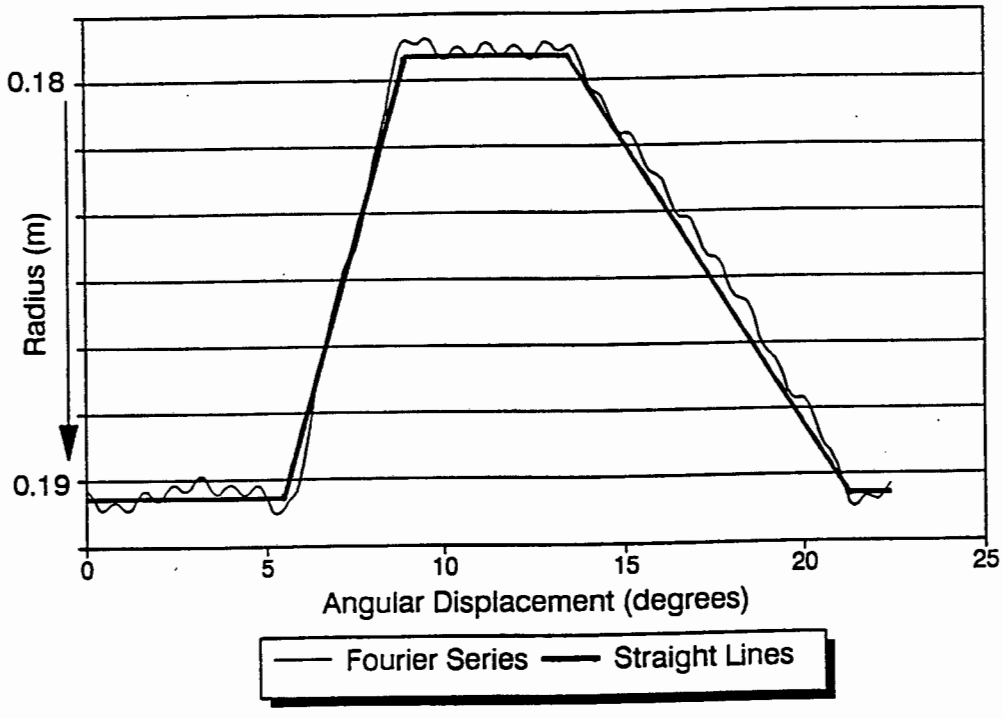

Figure 3.7: Comparison of Liner Functions Describing the Skorupa Liner

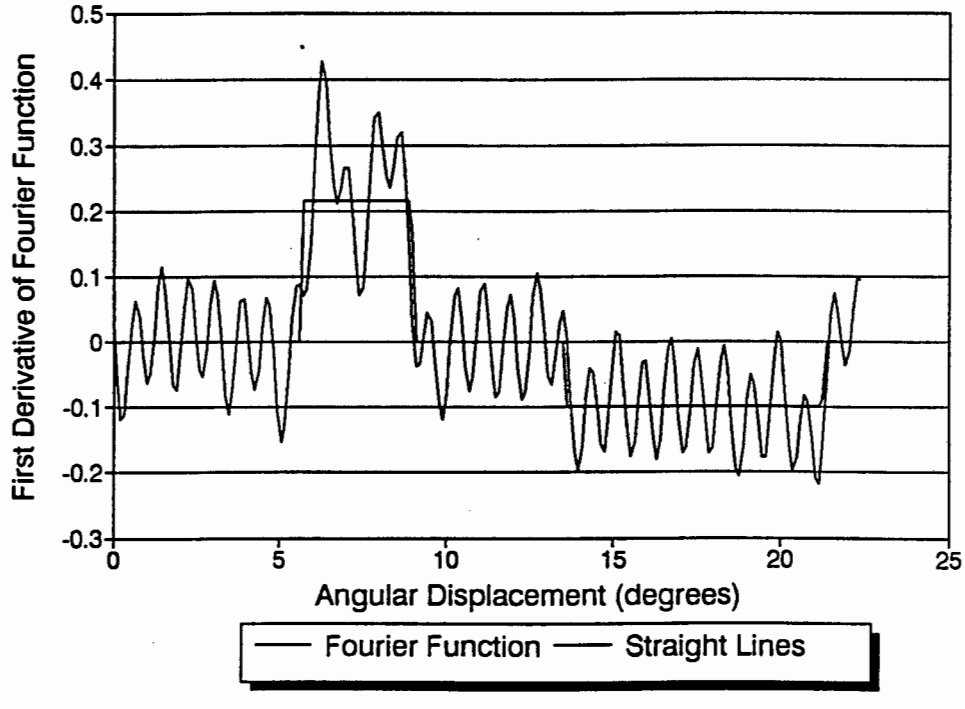

Figure 3.8: Comparison of the First Derivative of the Liner Functions Describing the Skorupa Liner

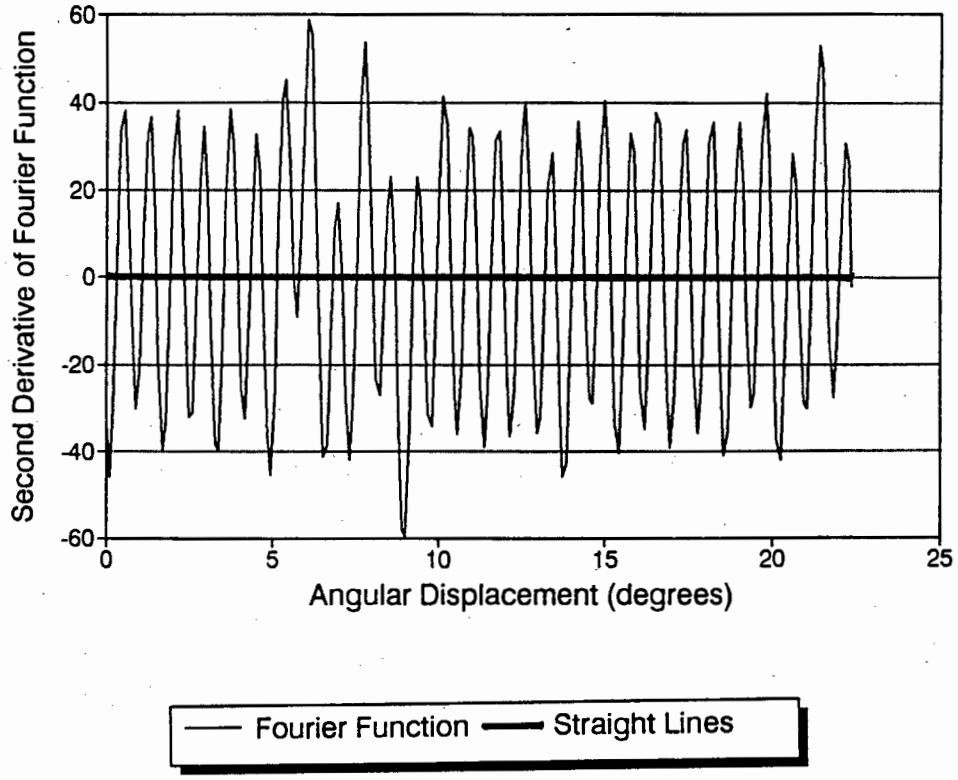

Figure 3.9: Comparison of the Second Derivative of the Liner Functions Describing the Skorupa Liner

The numerical solution of the governing equations for the C8 liner showed that a block does not leave its initial trough prior to departure from the liner. A trough is defined as the section of liner between two peaks or crests of a liner. Only one corrugation (from trough to trough) of the SK Liner was modelled. The block's initial position is at $\phi = -90^{\circ}$ and once it starts to slip its rotational velocity is always less than the mill rotational velocity ($\dot{\phi} < \Omega_m$). The section of liner modelled is shown in Figure 3.10.

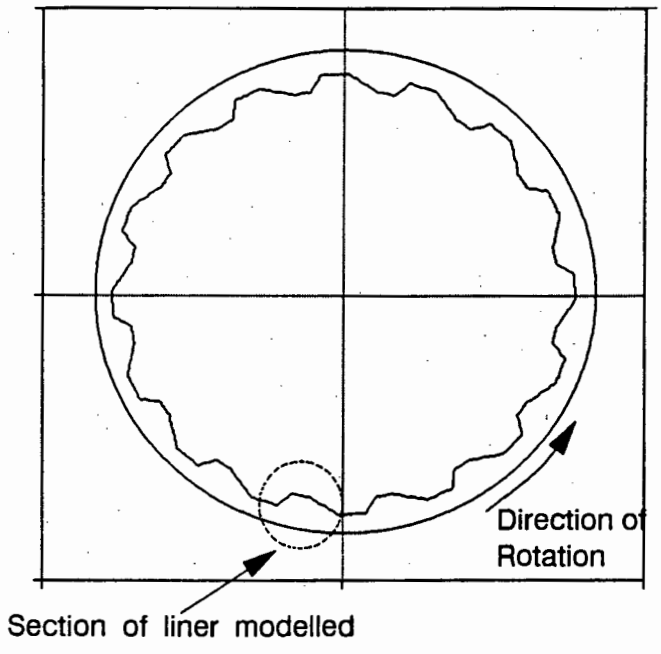

Figure 3.10: Section of Skorupa Liner Modelled using Straight Lines

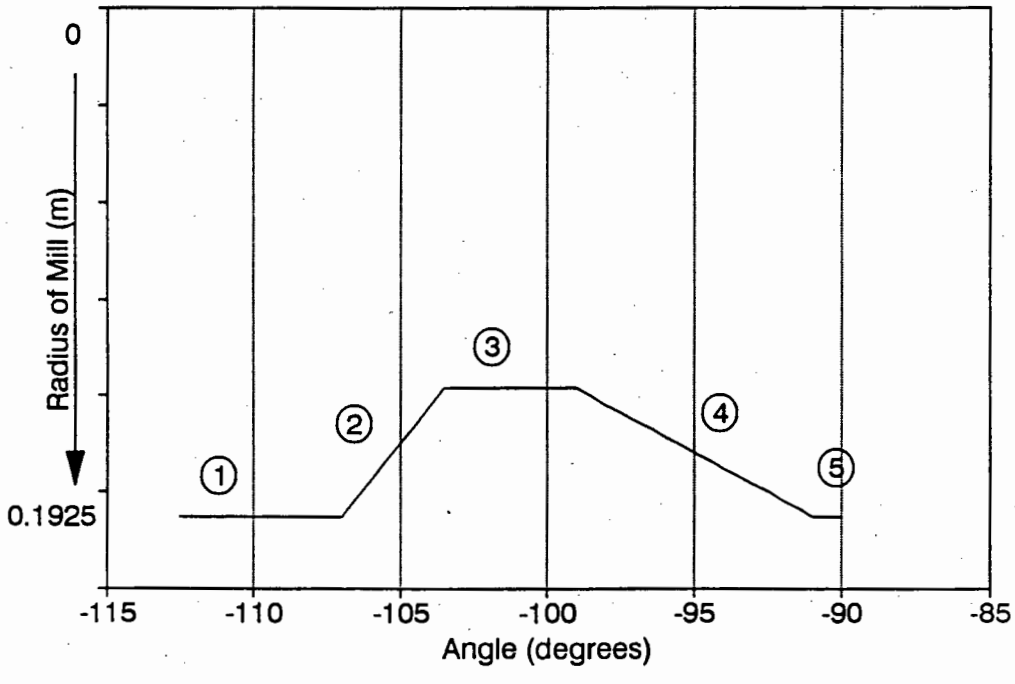

Figure 3.11: Schematic of the Section of the Skorupa Liner Modelled

The liner profile is defined using the position of the block relative to the liner. The position of the block is defined using β (see Equation 3.3) and the liner function and its derivatives are calculated using the equations shown in Table 3.2. These equations require that β be given in radians.

Section No refers to Figure 3.11.

Sec. No	Skorupa Liner Section
1:	$-112.5^\circ \le \beta \le -107^\circ$ $f(\beta) = 0.1925$ $f'(\beta) = 0$ $f''(\beta) = 0$
2:	$-107^\circ \le \beta \le -103.5^\circ$ $f(\beta) = -0.21773 * \beta - 0.21410$ $f'(\beta) = -0.21773$ $f''(\beta) = 0$
3:	$-103.5^\circ \le \beta \le -99^\circ$ $f(\beta) = 0.1792$ $f'(\beta) = 0$ $f''(\beta) = 0$
4:	$-99^\circ \le \beta \le -91^\circ$ $f(\beta) = 0.09524 * \beta + 0.34379$ $f'(\beta) = 0.09524$ $f''(\beta) = 0$
5:	$-91^\circ \le \beta \le -90^\circ$ $f(\beta) = 0.1925$ $f'(\beta) = 0$ $f''(\beta) = 0$

Table 3.2: Table of Equations used to Model Skorupa Liner

CHAPTER 4

THEORETICAL ANALYSIS OF THE MOTION OF A SPHERE ON A CORRUGATED LINER

In the previous section the motion of a block was investigated. The block has only one degree of freedom namely its angular velocity ($\dot{\phi}$). The sphere has however two degrees of freedom. These are its' angular velocity ($\dot{\phi}$) and the rotation of the sphere [i.e. spin (ω)] around its own axis. The spin of the particle is accounted for in this analysis.

The two types of motion that can occur are pure rolling and a combination of rolling and sliding. These two types of motion are modelled but are not solved numerically.

4.1 Derivation of the Equations of Motion for Pure Rolling of a Sphere on a Corrugated Liner

The position vector used to describe the position of the sphere are shown in Figure 4.1. The position of the sphere can be defined in vector form as

$$\underset{\sim}{r}(\beta) = f(\beta)\ \underset{\sim}{e}_r \qquad (3.8)$$

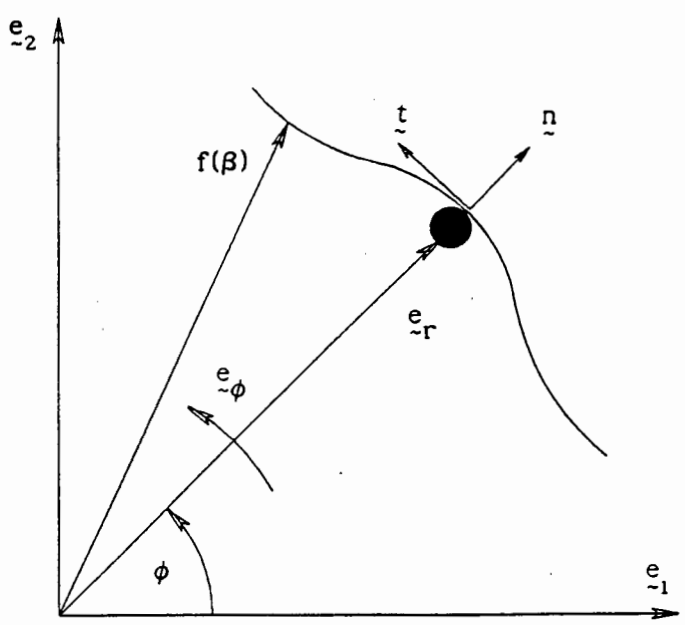

Figure 4.1: Directional Vectors of a Sphere

The first and second derivatives with respect to time will then give the velocity and acceleration of the sphere. These are

$$\dot{\underset{\sim}{r}}(\beta) = \left(\dot{\phi} - \Omega_m \right) f'(\beta)\, \underset{\sim}{e}_r + \dot{\phi}\, f(\beta)\, \underset{\sim}{e}_\beta \tag{3.9}$$

$$\ddot{\underset{\sim}{r}}(\beta) = r_r\, \underset{\sim}{e}_r + r_\phi\, \underset{\sim}{e}_\phi \tag{3.10}$$

where $r_r = \ddot{\phi}\, f'(\beta) + \dot{\phi}^2 \left(f''(\beta) - f(\beta) \right) - 2\, \Omega_m\, \dot{\phi}\, f''(\beta) + \Omega_m^2\, f''(\beta)$

$$r_\phi = \ddot{\phi}\, f(\beta) + 2\, \dot{\phi}^2\, f'(\beta) - 2\, \Omega_m\, \dot{\phi}\, f'(\beta)$$

The forces that act on the sphere are shown in Figure 4.1.

Normal Reaction Force $\quad \underset{\sim}{R} = -N_r\, \underset{\sim}{n}$ (3.12)

Tangential Friction Force $\quad \underset{\sim}{T} = N_t\, \underset{\sim}{t}$ (3.13)

Weight Component $\quad \underset{\sim}{W} = -\, m\, g\, \underset{\sim}{e}_2$

$$= -\, m\, g \left(\mathrm{Sin}(\phi)\, \underset{\sim}{e}_r + \mathrm{Cos}(\phi)\, \underset{\sim}{e}_\phi \right) \tag{3.14}$$

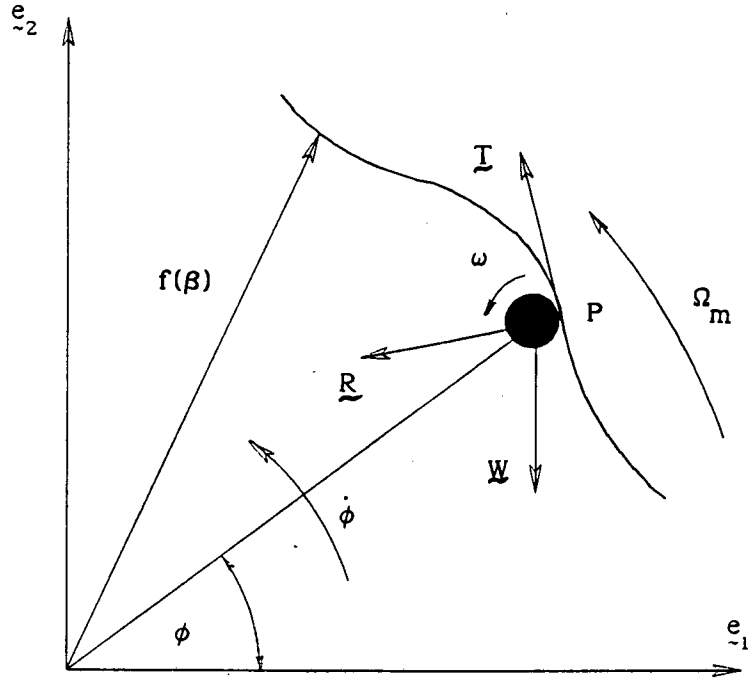

Figure 4.2: Orientation of Forces Acting on a Sphere

The forces can then be equated using Newton's Second Law (*THE CONSERVATION OF MOMENTUM).* The forces are equated in Equation (3.15). It is then possible to solve for N_r and N_t, the Normal Reaction Force (N_r) and the Tangential Friction Force (N_t). The equations derived are

$$N_t = m\,\alpha\left[f'(\beta)\,r_r + f(\beta)\,r_\phi\right] + m\,g\,\alpha\left[f(\beta)\,\mathrm{Cos}(\phi) + f'(\beta)\,\mathrm{Sin}(\phi)\right] \tag{3.19}$$

and

$$N_r = m\,\alpha\left[f'(\beta)\,r_\phi - f(\beta)\,r_r\right] + m\,g\,\alpha\left[f'(\beta)\,\mathrm{Cos}(\phi) - f(\beta)\,\mathrm{Sin}(\phi)\right] \tag{3.20}$$

These are the same as those obtained in the analysis of a block on a corrugated liner.

If the sphere is allowed to spin, then by taking the moments about the centre of the particle,

$$I\,\dot{\omega} = N_t\,a \tag{4.1}$$

The moment of inertia can be changed, depending on the shape of the particle used (i.e. the particle must still be able to roll, but could be a sphere or cylinder). For this investigation the moment of inertia is defined as that for a sphere. The moment of inertia for a sphere is

$$I = \frac{2}{5}\,m\,a^2$$

Substituting Equation (3.19) into Equation (4.1) and assuming the particle to be a sphere yields

$$\dot{\omega}\,a = \frac{5}{2}\,\alpha\left\{\left[f'(\beta)\,r_r + f(\beta)\,r_\phi\right] + g\left[f(\beta)\,\mathrm{Cos}(\phi) + f'(\beta)\,\mathrm{Sin}(\phi)\right]\right\} \tag{4.2}$$

It is required that the particle moves with *Pure Rolling.* This condition can be met by taking the sum of the moments about the point P (Figure 4.2), which gives

$$\dot{r}(t) + \omega\, a\, \underset{\sim}{t} = \Omega_m\, f(\beta)\, \underset{\sim}{e}_{\phi} \tag{4.3}$$

Substituting Equation (3.16) into Equation (4.3) and resolving tangentially to the liner (i.e. Dot equation (4.3) with $\underset{\sim}{t}$) yields

$$\omega\, a = -\frac{1}{\alpha}\dot{\phi} + \frac{1}{\alpha}\Omega_m \tag{4.4}$$

Differentiating Equation (4.4) with respect to time yields

$$\dot{\omega}\, a = -\frac{1}{\alpha}\ddot{\phi} + \dot{\phi}^2\left\{-\alpha\, f'(\beta)\left(f(\beta) + f''(\phi)\right)\right\} +$$

$$\dot{\phi}\left\{2\,\alpha\,\Omega_m\, f'(\beta)\left(f(\beta) + f''(\beta)\right)\right\} + \Omega_m^2\left\{-\alpha\, f'(\beta)\left(f(\beta) + f''(\beta)\right)\right\} \tag{4.5}$$

By substituting Equation (4.5) into Equation (4.2) it is possible to eliminate $\dot{\omega}$. The derived equation is

$$B\,\ddot{\phi} + C\,\dot{\phi} + D\,\dot{\phi}^2 + E = 0 \tag{4.6}$$

where $B = -\frac{7}{2}\frac{1}{\alpha}$

$$C = 7\,\alpha\,\Omega_m\, f'(\beta)\left(f(\beta) + f''(\beta)\right)$$

$$D = -\frac{7}{2}\,\alpha\, f'(\beta)\left(f(\beta) + f''(\beta)\right)$$

$$E = -\alpha\,\Omega_m^2\, f'(\beta)\left(f(\beta) + f'(\beta)\right)$$

$$-\frac{5}{2}\,\alpha\left[f(\beta)\,\mathrm{Cos}(\phi) + f'(\beta)\,\mathrm{Sin}(\phi)\right]$$

When the conditions used by Nates[1] are substituted into Equation (4.6), then the equations derived by Nates[1] is obtained. This can be seen in Appendix E.

4.2 Derivation of the Equations of Motion for a Combination of Rolling and Sliding of a Sphere on a Corrugated Liner

In Section 3 the possibility of the particle rolling was excluded. This led to the modelling of a block on a corrugated liner. In this section the possibility of rolling has been included. Here a sphere was modelled and Pure Rolling was assumed. The next step is to include the possibility of the sphere both Rolling and Sliding relative to the liner. The sphere would in reality start moving with Pure Rolling.

Using the same derivation as for the sliding of a block (Section 3.3.1), the resulting equations for N_r and N_t are

$$N_t = m\,\alpha\left[f'(\beta)\,r_r + f(\beta)\,r_\phi\right] + m\,g\,\alpha\left[f(\beta)\,\mathrm{Cos}(\phi) + f'(\beta)\,\mathrm{Sin}(\phi)\right] \tag{3.19}$$

and

$$N_r = m\,\alpha\left[f'(\beta)\,r_q - f(\beta)\,r_r\right] + m\,g\,\alpha\left[f'(\beta)\,\mathrm{Cos}(\phi) - f(\beta)\,\mathrm{Sin}(\phi)\right] \tag{3.20}$$

The spin of the sphere can be calculated by taking the moments about the centre of the sphere. This yields an equation for the rotational speed of the sphere about the centre of the sphere.

$$I\,\dot{\omega} = N_t\,a \tag{4.1}$$

Assuming that the particle is a sphere, where $I = \frac{2}{5}\,m\,a^2$, it is possible to solve for $\dot{\omega}$.

$$\dot{\omega}\, a = \frac{5}{2}\,\alpha \left\{ \left[f'(\beta)\, r_r + f(\beta)\, r_\phi \right] + g \left[f(\beta)\, \mathrm{Cos}(\phi) + f'(\beta)\, \mathrm{Sin}(\phi) \right] \right\} \tag{4.2}$$

As for sliding of a block , the assumption that $N_t = \mu\, N_r$ can be made. Thus combining Equations (3.19) and (3.20) yields

$$B\,\ddot{\phi} + C\,\dot{\phi} + D\,\dot{\phi}^2 + E = 0 \tag{4.7}$$

where $B = \dfrac{1}{\alpha^2}$

$$C = -2\,\Omega \left\{ f''(\beta) \left[f'(\beta) + \mu\, f(\beta) \right] - f'(\beta) \left[f(\beta) - \mu\, f'(\beta) \right] \right\}$$

$$D = 2\, f'(\beta) \left\{ f(\beta) - \mu\, f'(\beta) \right\} + \left\{ f'(\beta) + \mu\, f(\beta) \right\} \left\{ f''(\beta) - f(\beta) \right\}$$

$$E = g \left\{ \left[f(\beta) - \mu\, f'(\beta) \right] \mathrm{Cos}(\phi) + \left[f'(\beta) + \mu\, f(\beta) \right] \mathrm{Sin}(\phi) \right.$$
$$\left. + \Omega^2\, f''(\beta) \left[f'(\beta) + \mu\, f(\beta) \right] \right.$$

Equation (4.7) is the governing equation of motion for a sphere moving on a corrugated liner. The spin of the sphere, once it has started to slide, is determined using Equation (4.2). Equations (4.2) and (4.7) can be solved using a Fourth-Order Runge-Kutta method. A further stage in the overall project would be to attempt to solve these equations.

CHAPTER 5

DISCUSSION OF THE RESULTS FROM THE NUMERICAL SOLUTION OF THE EQUATIONS OF MOTION FOR A BLOCK ON A CORRUGATED LINER

The computer analysis was performed to determine the effect various parameters had on the motion of a block on a corrugated liner. The parameters that were varied were the time step (h), the coefficient of friction (μ) and the speed of the mill (Ω_m). The coefficient of friction is restricted to values of between 0 and 1. This is because in reality the value for μ cannot be greater than 1. The effect of the amplitude of the liner on the motion of the block was also investigated. The effect of the mass of the block on the block's motion was not investigated. This was because Nates [1] found that the mass of the block did not have any effect on the motion of a block. This can also be seen in the equations derived in Section 3. In the derivation the mass (m) parameter is eliminated during the derivation of the governing differential equation.

The initial conditions for the numerical tests performed were as follows:

1. The block starting position was $\phi(0) = -90^{\circ}$. The liner was so positioned that the block always started in a trough (i.e. the block always starts on a surface similar to that of a flat liner). The starting position of the block is shown in Figure 5.1.

2. The blocks initial angular velocity equalled the rotational velocity of the mill ($\dot{\phi}(0) = \Omega_m$).

The first parameter that was varied was the time step (h). The objective of varying the time step is to determine a time step which gave accurate results, yet did not increase the computational time significantly. The time step that was found to be the most suitable was δt=0.001 seconds. This value was chosen by varying the value of δt and observing the results obtained.

The second independent variable parameter was the coefficient of friction. The difference between the static and kinetic coefficients of friction was assumed to be negligible. The values used for the coefficient of friction ranged from 0 to 1.

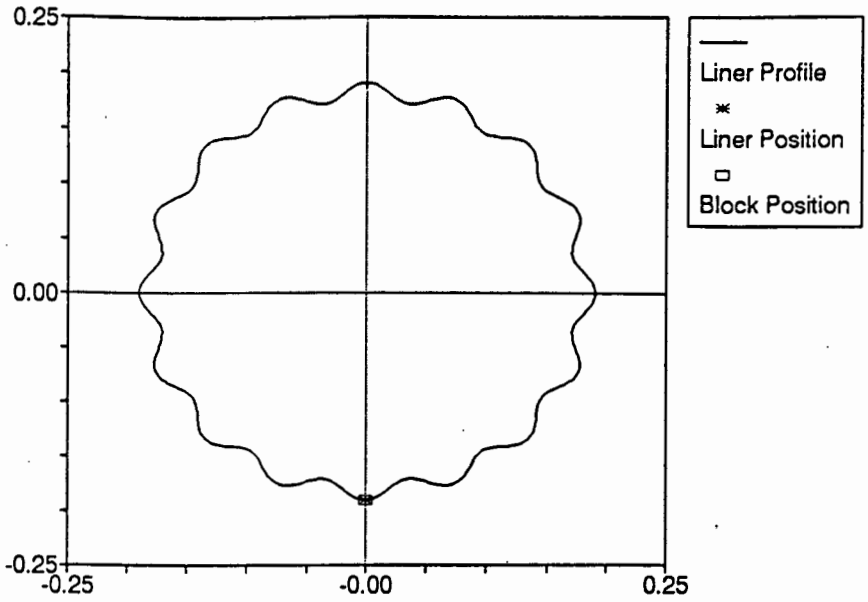

Figure 5.1: Starting Position of the Block on a Corrugated Liner

A study was done as to how the block's motion is affected by the amplitude of the cosine liner. The program was run for two different speed and two different coefficient of friction settings. The coefficients of friction used were 0.5 and 1 whilst the mill speeds used were 35 rpm (50% of Davis' Critical Velocity) and 70rpm (100% of Critical Velocity). The results obtained are shown in Figure 5.2.

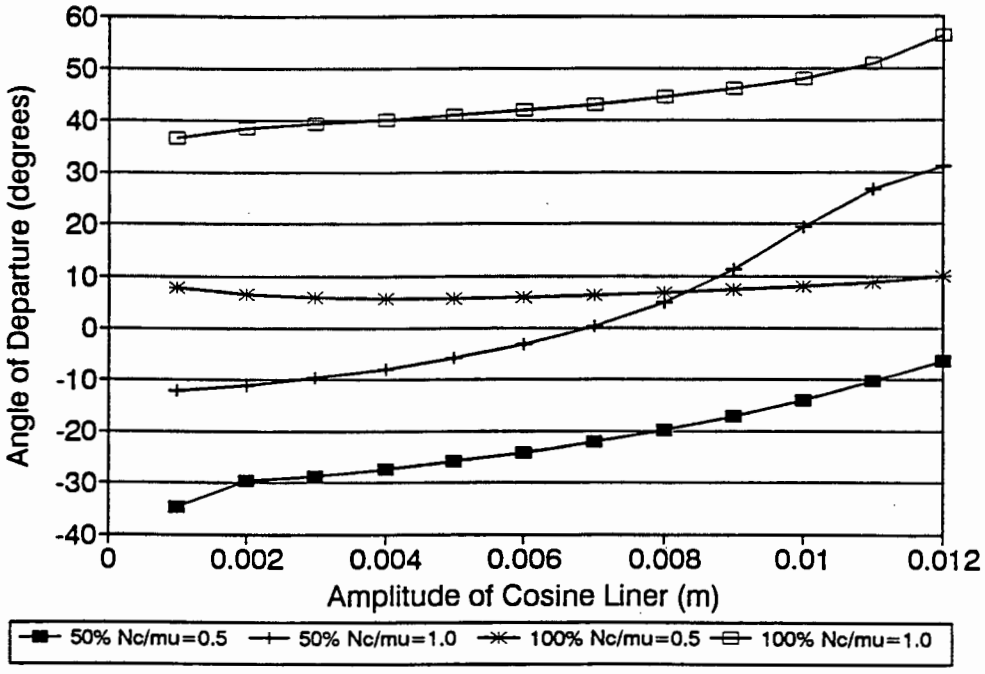

Figure 5.2: Graph of Angle of Departure vs Amplitude of a Cosine Liner of varying Amplitude

The results obtained clearly showed that the liner configuration does have an influence on the Angle of Departure. The behaviour of the block for each liner configuration is also dependent on the coefficient of friction. For three of the cases studied the AOD increases with an increase in the amplitude of the liner. In one of the cases (N_c=100% and μ=0.5) the AOD initially decreases but starts to increase at a liner amplitude of approximately 0.005m.

It is evident that the AOD for a liner of 0.001m amplitude, where the mill speed equals 35 rpm (50% N_c) and the coefficient of friction = 0.5, is not consistent with the other results for the same mill speed and coefficient of friction. This can be ascribed to the block leaving its initial trough. The angular distance from peak to trough, for the Cosine Liners, is 11.25°. For this particular case the difference between the AOD and the block's initial position is 32.3°. For all the other liner amplitudes tested, for the given conditions, the block did not leave its initial trough. This can be seen in Figure 5.3a. In Figure 5.3b the point of departure of the block relative to its initial position is shown. It can be clearly seen that the block leaves the initial trough and travels down the liner prior to departure.

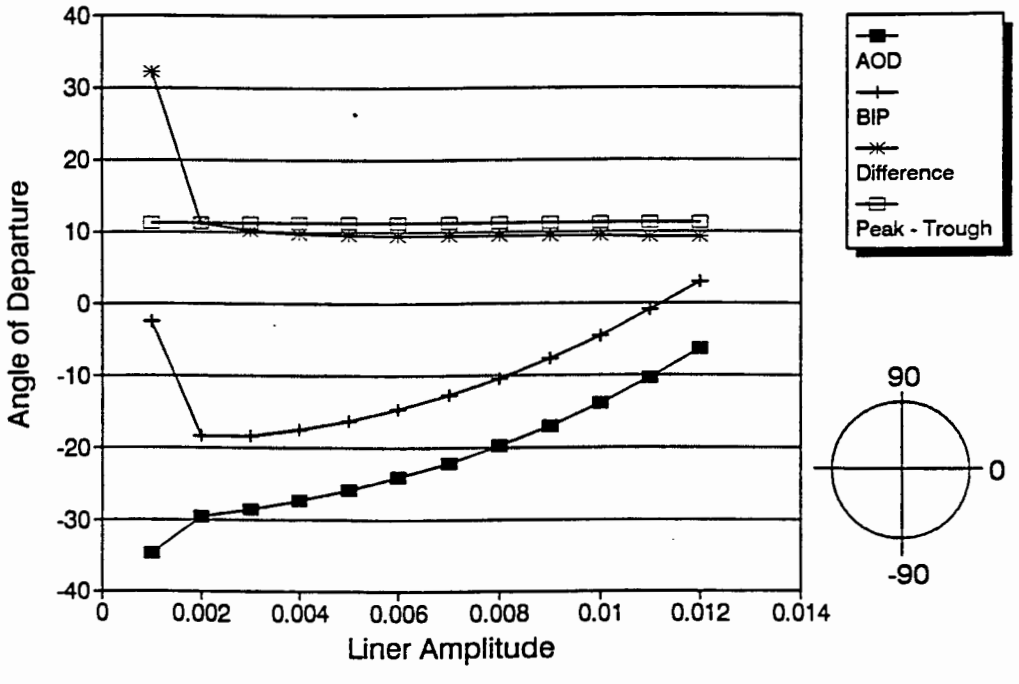

Figure 5.3a: Angular Displacement of a Block Relative to its Starting Position

BIP :- Block Initial Position

Peak - Trough :- Angular Distance from Peak to Trough of a Corrugation

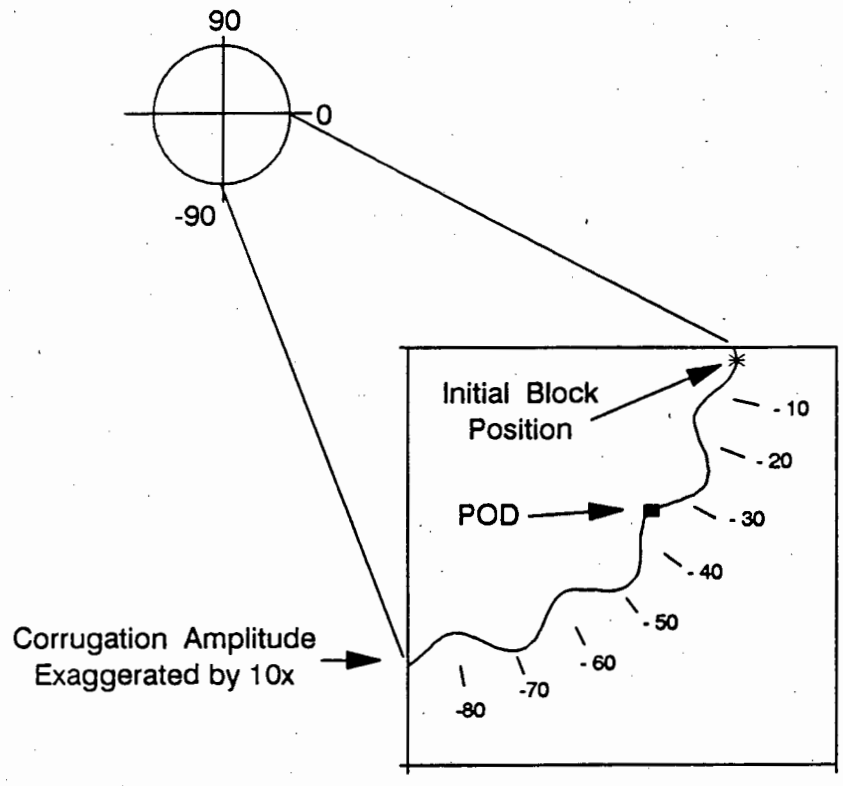

Figure 5.3b: Position of Block Relative to its Starting Point

Three liner configurations were studied as to how variations in mill speed (Ω_m) and friction (μ) affected the motion of the block. The liner configurations investigated are designated as follows:

C3 - A Cosine Liner with a corrugation amplitude of 0.003m
C8 - A Cosine Liner with a corrugation amplitude of 0.008m
SK - The Skorupa Liner developed from Skorupa's PhD. Thesis

The coefficient of friction is varied from 0.2 to 1. The value for the rotational velocity of the mill is varied from 10 rpm to 80 rpm (*14% to 114% of the Davis Critical Velocity* N_c).

An emphasis was made on the effect on the blocks ending conditions (i.e. its Point of Departure (**POD**)). The behaviour of the block prior to departure from the liner was also investigated. This was done to investigate the block's motion relative to the liner.

It is evident in Figure 5.4 that for a C3 liner, as the coefficient of friction increases the Angle of Departure also increases. The behaviour of the block for a mill speed of 10 rpm (14% N_c) does not follow the same pattern as the other data plots. On investigating the motion of the block prior to its departure from the liner it became evident that the block would either stay in the trough it started in or it could slide over the peak and into the next trough. For a mill speed of 25 rpm (36% N_c) and μ = 0.2 the block travels out of its initial trough whilst for all the other values of friction and mill speed the block remains in its initial trough.

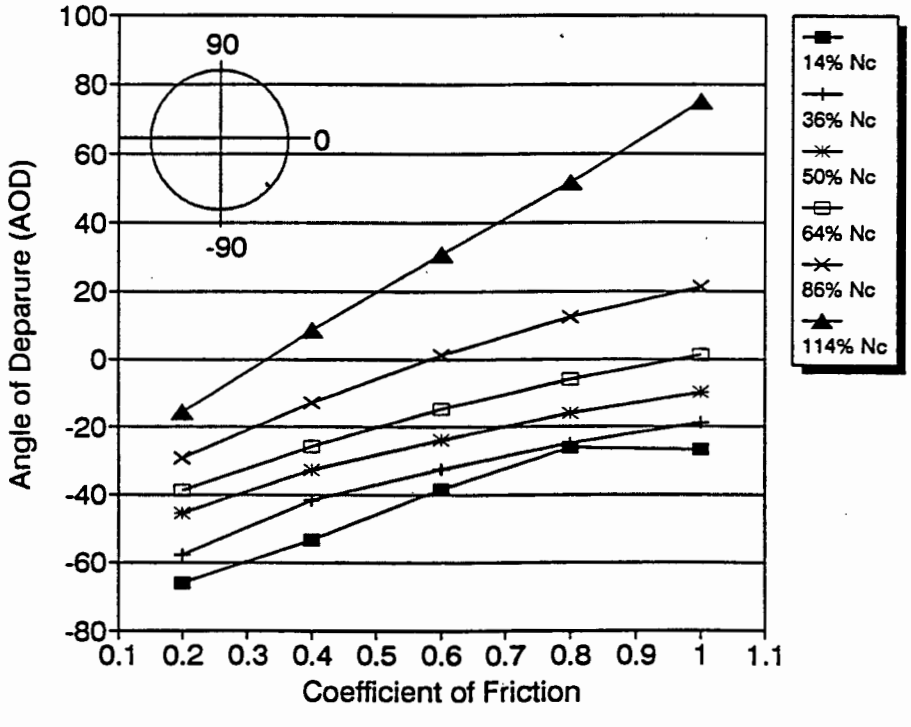

Figure 5.4: Graph of Angle of Departure vs the Coefficient of Friction for the C3 Liner

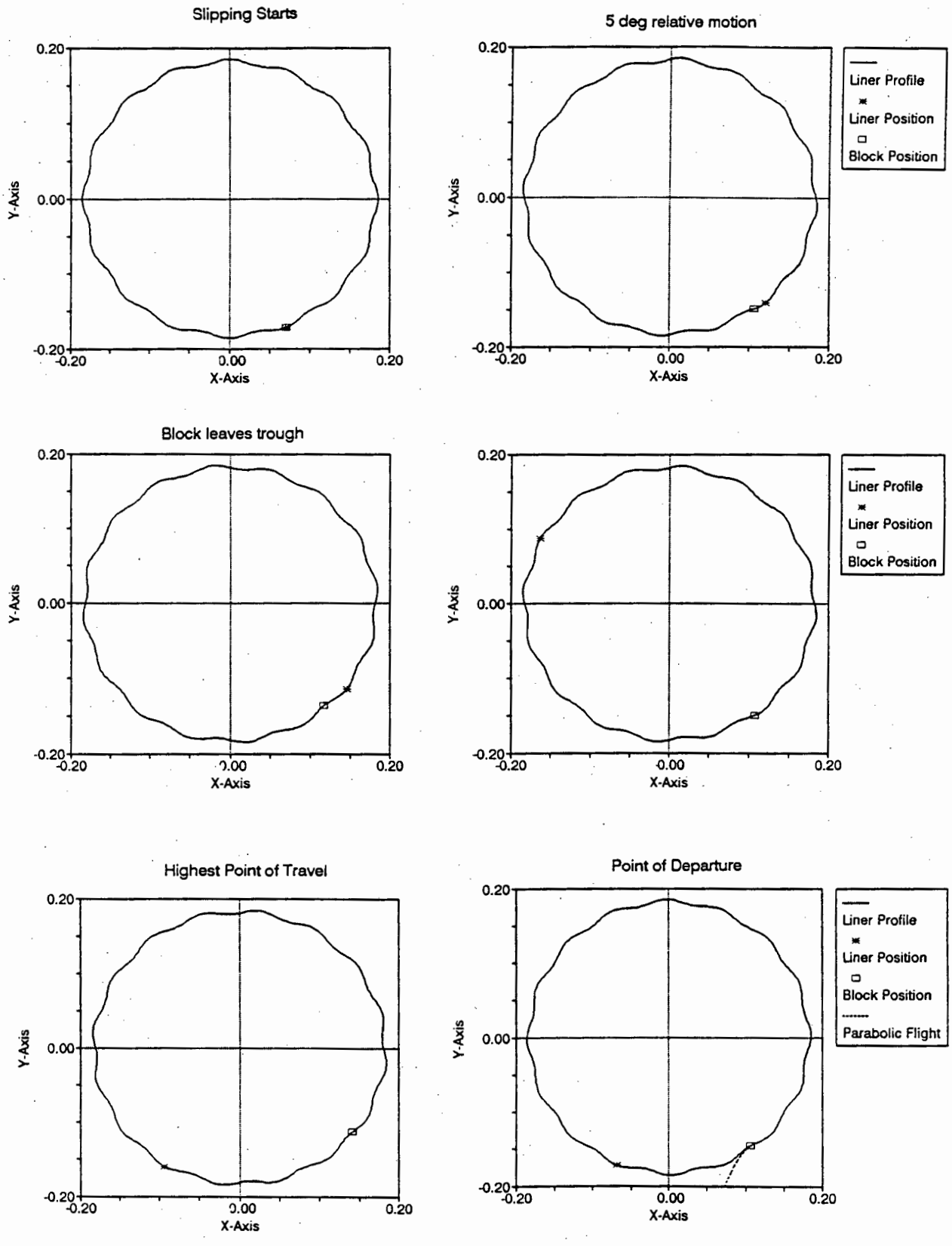

Figure 5.5: Path of Block Travelling on a C3 Liner.
(μ = 0.4, Ω_m = 10 rpm (N_c=14%))

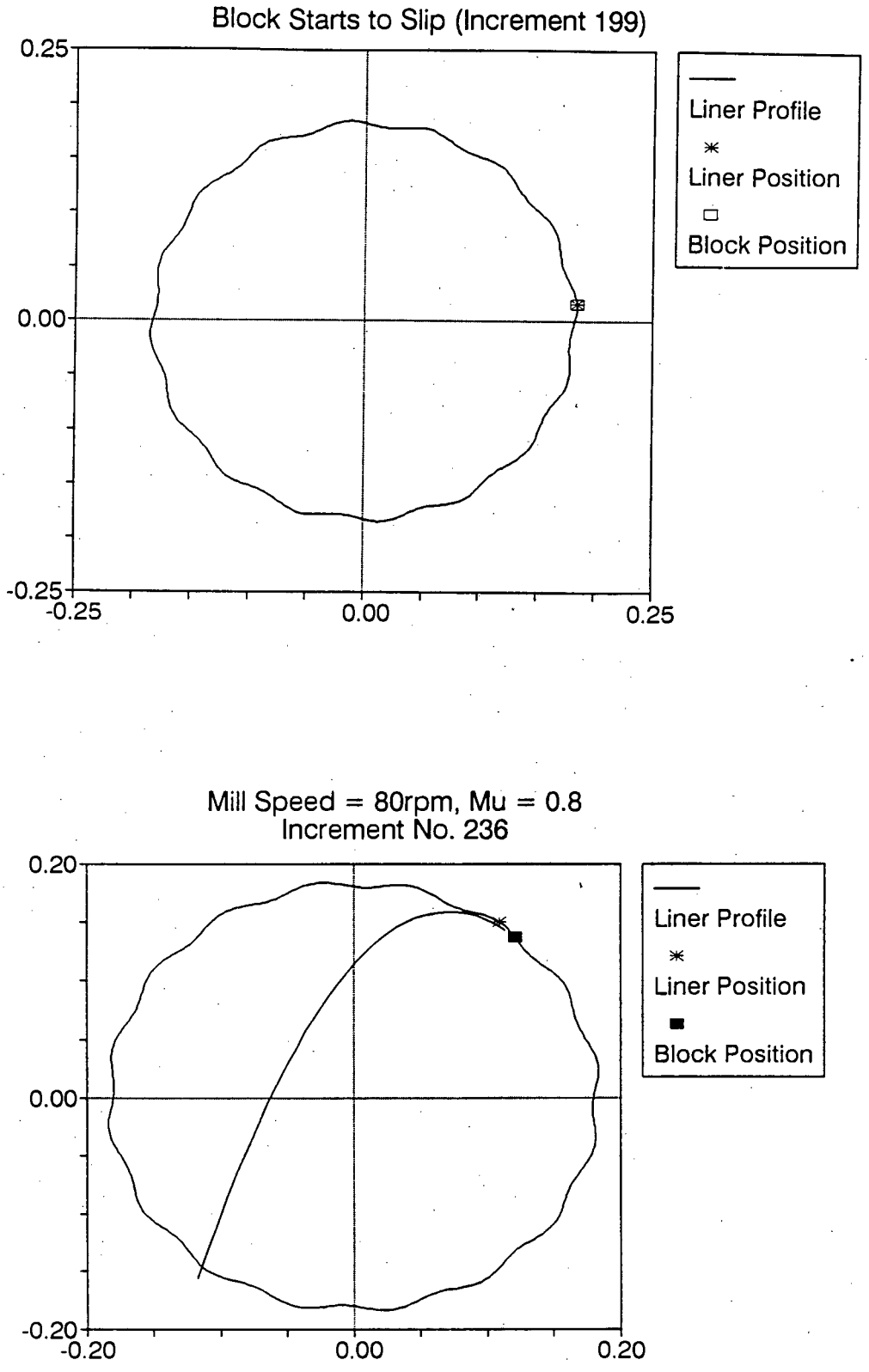

Figure 5.6: Path of Block Traveling on a C3 Liner.
(μ = 0.8, Ω_m = 80 rpm (N_c=114%))

In Figure 5.5 an example is shown where the block is moving relative to the liner and moves out of its original trough. The sequence of diagrams shows the block as it moves out of its original trough until it departs the liner. The fact that the block can leave the liner before it has reached the horizontal ($\phi \leq 0$) can be attributed to the liner corrugations acting as a ramp. In other words the block will only leave the liner if the velocity of the block down the liner is large enough for the given liner configuration.

In Figure 5.6 an example is shown where the block does not leave its initial trough and the angle of departure is above the horizontal ($\phi \geq 0^{\circ}$). This can be attributed to the high coefficient of friction and high rotational velocity of the mill.

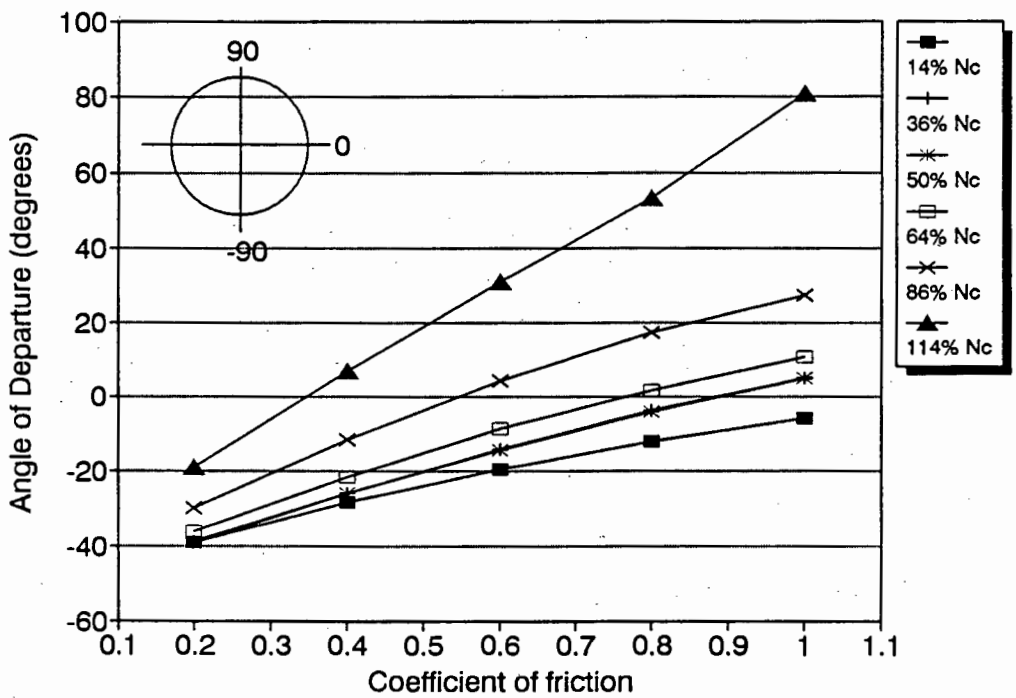

Figure 5.7: Graph of Angle of Departure vs the Coefficient of Friction for a C8 Liner

In Figure 5.7 the results for the Angle of Departure (AOD) for the C8 liner are displayed. The block's AOD increases as the coefficient of friction (μ) and mill rotational velocity (Ω_m) increases. The block does not leave its initial trough for any of the cases studied. This can be attributed to the

fact that the magnitude of the liner amplitude does not allow the block to leave the initial trough. The block does come close to being centrifuged when it reaches 81.1°. The centrifuging velocity for the C8 liner is 95 rpm (135.7% N_c).

In Figure 5.7 it can be noted that the points of departure for 25 rpm (36% N_c) and 70 rpm (50% N_c) coincide. In Figure 5.8 the rotational velocities of the block at the POD are shown. Although the Points of Departure coincide it is noted that the angular velocity of the block, at the POD, does increase with an increase in the mill rotational velocity. This can be attributed to an increase in the block's kinetic energy as the mill rotational speed increases.

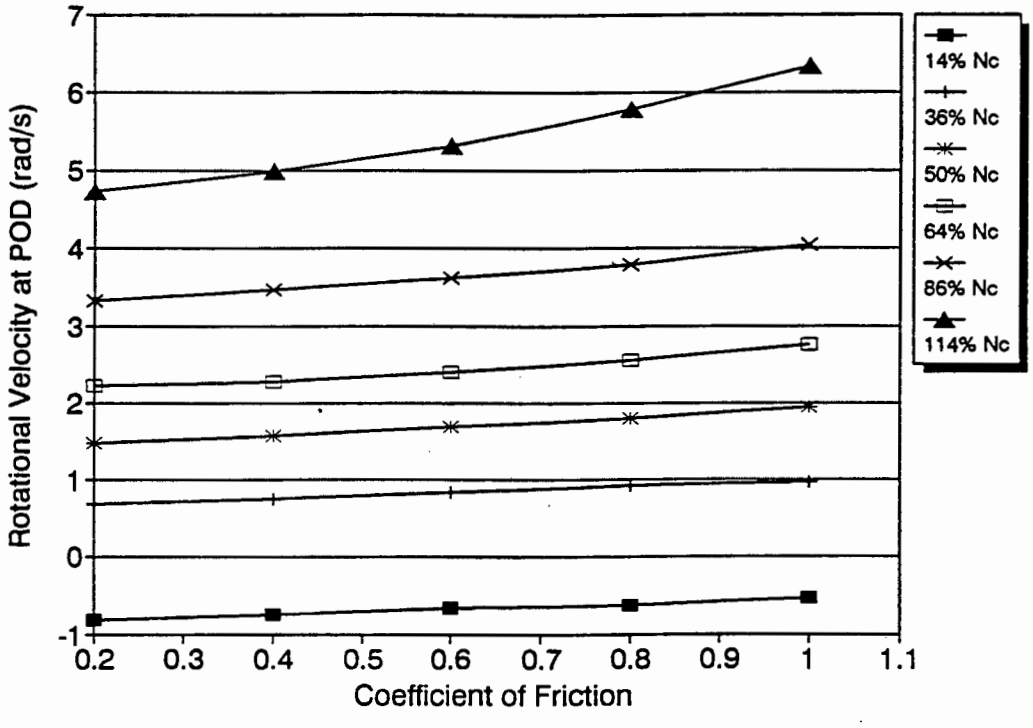

Figure 5.8: Graph of Rotational Velocity of the block at the POD vs the Coefficient of Friction

The third liner modelled was the liner derived from Skorupa[19]. The close resemblance between the C8 liner and the SK liner is shown in Figure 5.9.

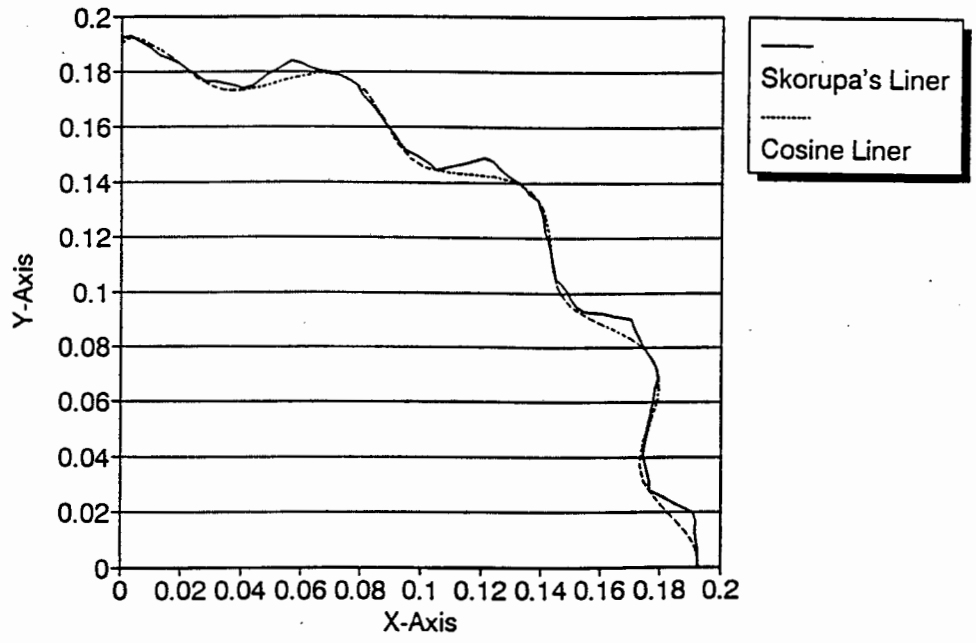

Figure 5.9: Comparison of SK and C8 Liner

In Figure 5.10 the Angles of Departure for the SK liner are shown. It must be noted that the AOD for initial conditions, 10 rpm (14% N_c) and μ = 0.2, is not included in Figure 5.10. This is because the block leaves its starting trough. As stated in Section 3.3.4, the SK liner has only been modelled for one corrugation. The block's angle of departure increases as the coefficient of friction (μ) and mill rotational velocity (Ω_m) increases. The block remains in its initial trough for all but one of the cases studied.

In Figure 5.11 a comparison is made between the AOD's of the SK Liner and the C8 liner. In the comparison it can be seen that there is a good correlation between the results. For 80 rpm (114% N_c) and μ = 1 the block on the SK liner centrifuges to the liner whilst the block on the C8 liner leaves the liner at 81.1°.

The next analysis investigated the effect the liner configuration had on the block's trajectory. An investigation is also conducted as to how the trajectory is affected by a change in the coefficient of friction (μ) and mill speed (Ω_m).

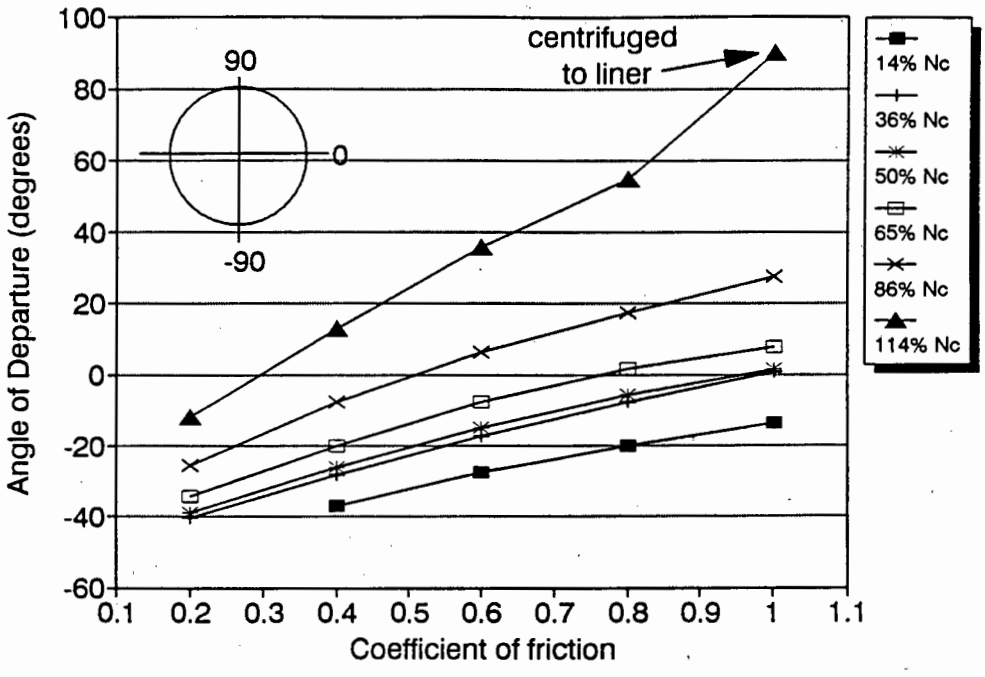

Figure 5.10: Graph of AOD vs the Coefficient of Friction for SK Liner

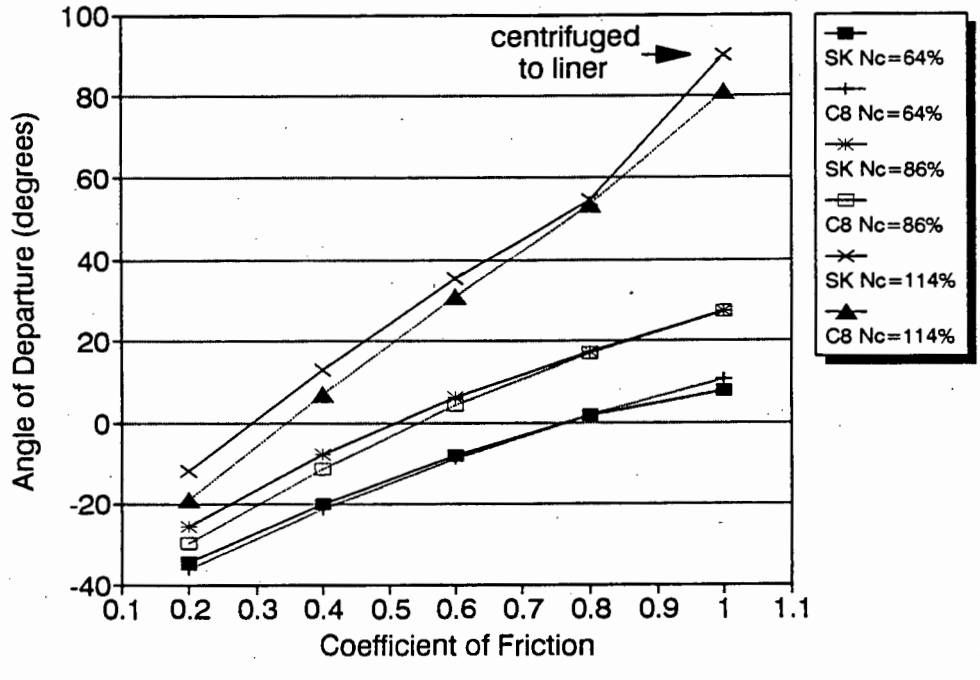

Figure 5.11: A Comparison of the AOD for the SK and C8 Liner

In Figure 5.12 a comparison of the trajectories, at two different mill speeds (N_c = 86% and N_c = 114%), is made for the three different liner configurations used. These results are for a coefficient of friction of 0.8. For both mill speeds the trajectories of the SK and C8 liners are close together. The block travelling on the C3 liner does not travel as far across the mill as the blocks travelling on the C8 and SK liners. The reason for this is that the block travelling on the C3 liner has a lower rotational velocity than the other blocks at the POD. The lower rotational velocity, at the POD, is the result of the larger amount of slip that occurs between the block and liner on the C3 liner. The higher amplitude of the corrugations on the C8 and SK liners means that there is greater resistance to the blocks attempt to slide down the liner. It is evident that C8 and SK lines are inversed for 86% N_c and 114% N_c. The author has not made an attempt to explain this phenomenon.

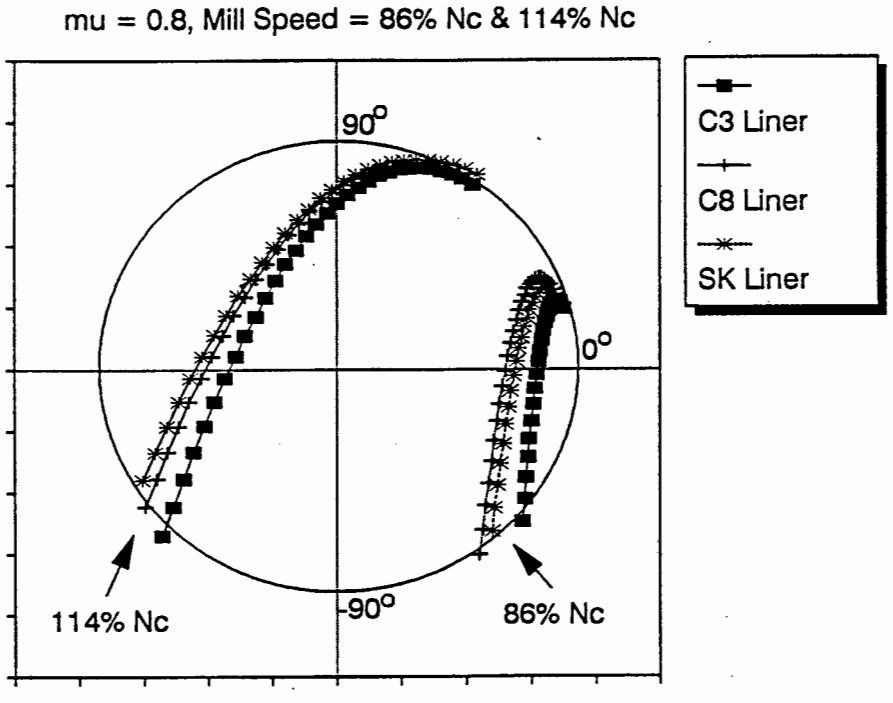

Figure 5.12: A Comparison of the Parabolic Trajectories for varying Liner Configurations

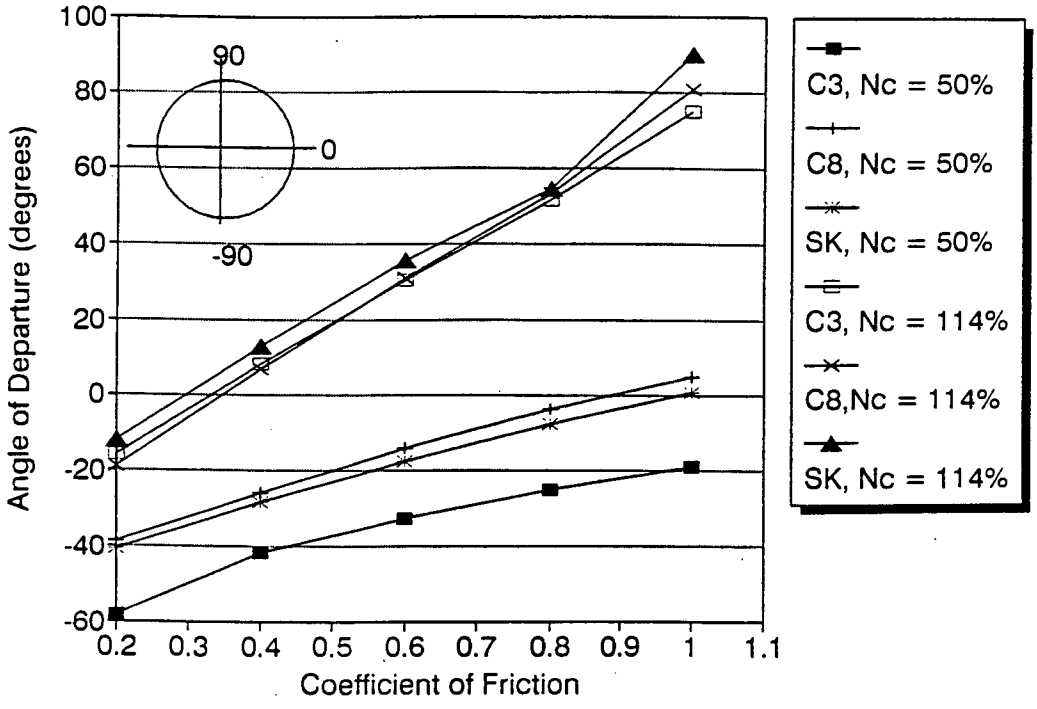

Figure 5.13: A Comparison of the AOD for varying Liner Configurations

The amount of slip prior to departure is also dependent on the mill velocity. This can be seen in Figure 5.13. For higher velocities (114% N_c) the AOD's for block are approximately the same. For a mill speed of 35 rpm (50% N_c) the blocks travelling on the C8 and SK liners leave the liner at approximately the same point. The block travelling on the C3 liner leaves its initial trough whilst the blocks on the C8 and SK liners do not move out of their initial trough.

5.1 DISCUSSION OF NUMERICAL SOLUTION

The motion of a block in a rotating cylinder is dependent on three variables. They are: the liner configuration, the coefficient of friction (μ) and the mill speed (Ω_m).

The liner configuration is the variable that most affects the efficiency with which energy is transferred from the rotating mill shell to the mill charge. The inclusion of the liner into a mill prevents the charge slipping and reduces the wear of the liners and grinding media. It was found that for a given set of initial conditions that as the amplitude of the Cosine liner increased so did the AOD. It is therefore reasonable to assume that as the liner amplitude increases that there is an increase in the efficiency of the energy transfer between the mill shell and the grinding media. It was noted that the rate of change of the AOD, with an increase in the liner amplitude, was also affected by the coefficient of friction. The block left its initial trough for only one of the initial conditions tested.

It is noted that with an increase in the coefficient of friction and mill speed the Angle of Departure of the block also increases. There is good correlation between the results for the AOD's of a block for the C8 and SK liner. An increase in the coefficient of friction leads to an increase in resistance to the block's sliding and this contributes to an increase in the efficiency of the energy transfer between the mill shell and the grinding media. A change in the mill speed does not affect the efficiency of the energy transfer but contributes to a change in the block's behaviour. With an increase in the mill speed the amount of energy that is transferred from the mill shell to the grinding media also increases.

By controlling these conditions (mill speed, coefficient of friction and liner configuration), the correct milling conditions can be achieved. These conditions are that enough slipping of the mill charge occurs to allow for the fine grinding of the coal. An increase in the amount of slipping accelerates the rate of wear of the mill liner and grinding media.

CHAPTER 6

EXPERIMENTAL RATIONALE AND PROCEDURE

The reason for performing experimental work was to ascertain whether the results obtained from the theoretical model were correct. This section is divided into three sections. The first section covers the reasons and aims of the experimental work. The second section will discuss the experimental apparatus used and the third section will describe how the experimental work was performed.

6.1 Experimental Rationale

An experimental investigation was performed so that a comparison of the theoretical predictions and experimental results could be made. The main difference to the formulation derived by Nates[1] is that the new formulation includes the effect of the liner configuration on the particle's motion.

The object of the experimental investigation was to determine the response of the block to differing environmental conditions. The conditions varied are: the speed of the mill (Ω_m) and the coefficient of friction (μ). Nates[1] found that the mass of a particle has no influence on its motion. It was suspected that with the inclusion of a corrugated liner that the blocks motion would be affected by the block geometry. An investigation was performed to ascertain the effect of the block geometry.

It is envisaged that the reaction of the block with specific reference to the sliding will be measured for initial conditions where the block is at the bottom of the mill [$\phi(0) = -90^\circ$] and moving at the same angular velocity as the mill [$\dot{\phi}(0) = \Omega_m$]. These conditions were chosen as they are the same conditions that were modelled in the theoretical analysis. The conditions chosen also allowed various specific results to be ascertained. These are the angle of slip (ϕ_{slip}), Angle of Departure (AOD) and the onset of centrifuging. The path of the block once it has left the liner is assumed to be parabolic. Nates reported that various authors (3,4,7,11) have experimentally investigated particle trajectories. It was decided that no investigation into particle trajectories would be performed.

6.2 Experimental Apparatus

The test rig to be used consists of an axially mounted mild steel drum. The drum has a diameter of 0.405m and a depth of 0.1m. As this investigation involves only one particle, and no liquid or coal charge, the test mill was left open at one end. This facilitates the easy observation of the particle's motion.

Figure 6.1 contains a photograph of the experimental apparatus used. Clearly visible is the steel drum. The $\frac{1}{4}$ hp electric motor used to drive the steel drum is partly obscured by the steel drum. The variac, an electrical speed control device, is seen on the left. The rotational speed of the shaft is measured using an optical switch in conjunction with a slotted disk and frequency counter. The disk has 60 slots cut in it and the displayed frequency is the shaft speed in RPM. The slotted disk is visible at the back of the shaft in Figure 6.1.

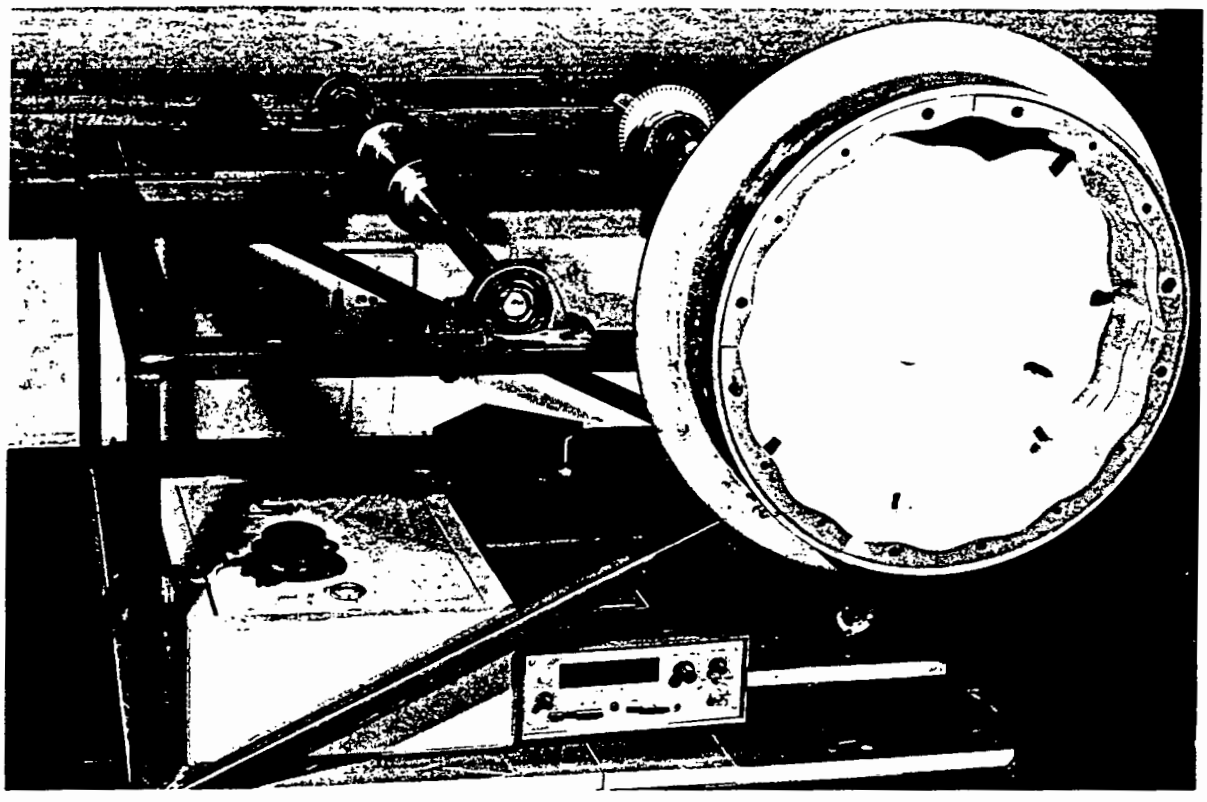

Figure 6.1: Photograph of Experimental Apparatus.

The liners used in the test rig were manufactured out of PVC (Polyvinyl Chloride) plastic. The author manufactured the liners using a Computer Numerically Controlled (CNC) milling machine. Two liner configuration were made. These were

1. A liner with a shape of a Cosine function
2. A liner derived from one of the liners used by Skorupa[19]

The liner is divided into quadrants so as to simplify the manufacturing process as well as the installation. Figure 6.2 contains a photograph of a quadrant from each liner. The holes that are visible in each liner quadrant were made during the manufacturing process. The two larger holes were used to fasten the PVC blank to the milling machine whilst the two smaller holes, found between the larger holes, were used to locate the PVC blank.

A polystyrene backdrop, see Figure 6.3, was made so that the angular position of the block could be easily observed. To allow the block's AOD to be easily measured the backdrop is marked in 5° intervals. The notation used on the backdrop is in accordance with the notation used in the theoretical discussion. Included in the backdrop were areas where test information could be displayed. A position for the frequency counter was also included.

In the theory for a block on a corrugated liner the assumption is made that there is no rotation of the particle. This condition was modelled using a block of steel. This prohibits the particle from rolling.

The two sets of blocks used in experimental tests had different masses and dimensions. These physical dimensions can be seen in Table 6.1. The difference in size between the two sets of blocks can be ascribed to a layer of cloth on the one set.

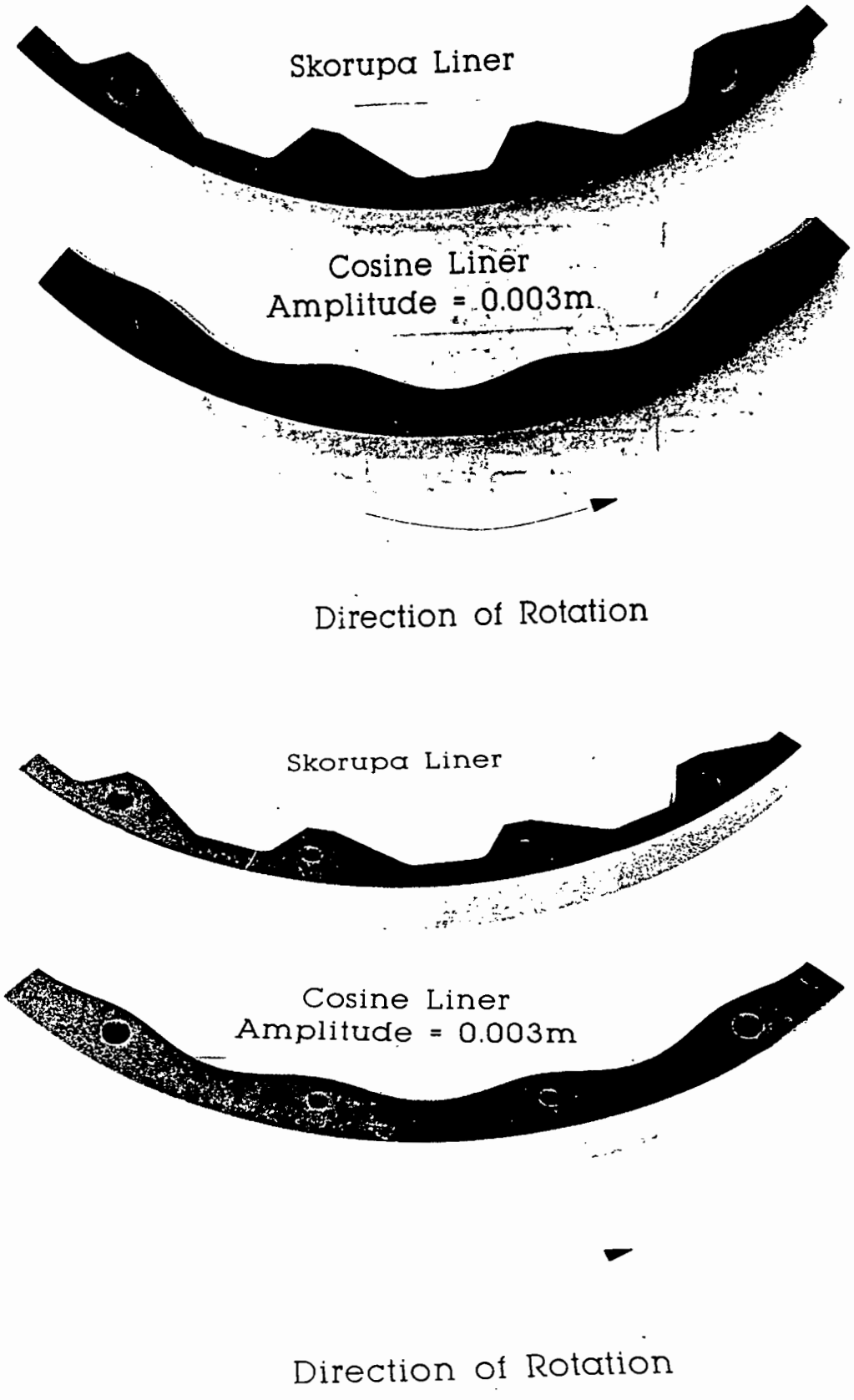

Figure 6.2: Photographs of Experimental Liner Configurations used

Block	Mass (g)	Dimensions (mm)
BSP	28.3	16x16x16
SSP	7.4	10x10x10
BCP	30.2	17x17x17
SCP	6.3	11x11x11

Table 6.1: Tabulation of the Physical Dimensions of the Blocks

The coefficient of friction between the blocks and liner was varied by covering one set of blocks with cloth. The blocks used in the experimental tests are designated as follows:

BSP :- Large Block with Steel-PVC liner interface
SSP :- Small Block with Steel-PVC liner interface
BCP :- Large Block with Cloth-PVC liner interface
SCP :- Small Block with Cloth-PVC liner interface

A video camera and recorder were used to capture the block's motion. The position of the video camera relative to the test rig can be seen in Figure 6.3. A video camera was used instead of a high speed camera because a video camera allows for almost instant replay and allows for the immediate identification of problem areas.

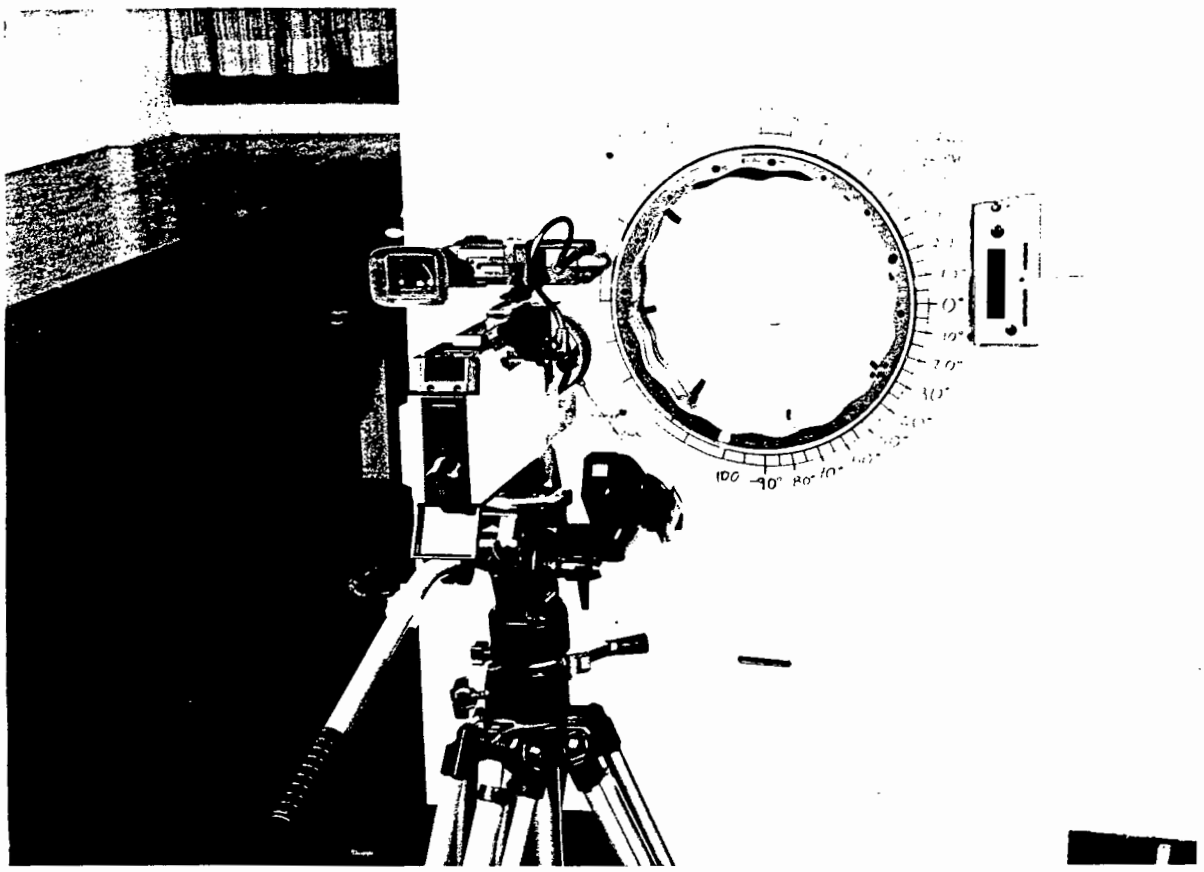

Figure 6.3: Layout of Experimental Equipment

6.3 Experimental Procedure

The experimental procedure was divided into three sections. The initial experimental work that had to be performed was to determine the coefficients of friction between the blocks and the PVC liner. The second and third sections involved the experimental tests on the Cosine and Skorupa liners respectively.

The investigation used the initial conditions described in Section 6.1 and evaluated the block's response when each of the chosen independent physical parameters was altered. The three conditions that were altered were Ω_m, μ and the block geometry.

Batches of tests were run for each of the two liner configurations. In Table 6.2 the batches of tests performed on each liner configuration is shown.

	C8 Liner		SK Liner	
Surface	Steel	Cloth	Steel	Cloth
Large Block	•	•	•	•
Small Block	•	•	•	

Table 6.2: Experimental Test Performed for each Liner Configuration

No tests were performed with the small cloth covered block for the Skorupa liner. This was because it was found that for the two steel blocks that the geometry of the block did not adversely affect the motion of the block on the liner.

For each liner configuration the motion of the block was evaluated and the following experimental results were obtained from the video recording of the tests.

1. The measurement of the Coefficients of Friction for each surface,
2. The determination of the Angle of Departure for each surface,
3. The determination of the Angle of Slip and
4. The centrifuge speed of the test mill.

The angle of slip (ϕ_{slip}) and the angle of departure (AOD) of each block was analysed using the recorded video. Figure 6.4 contains a photograph of a sample frame taken from the video recording. The liner shown is the Cosine liner with an amplitude of 0.003m. The mark visible at -100° was used as a reference point. The angle of slip (ϕ_{slip}) is determined by observing the relative motion between the block and the mark on the drum. When the block starts to leaves the liner below the horizontal it begins to tumble. The angle at which the block starts to tumble is assumed to be the angle of departure. When the block leaves the liner above the horizontal (0°), it is possible to see a gap opening between the liner and the block The angle at which the gap was first visible was assumed to be the Angle of Departure.

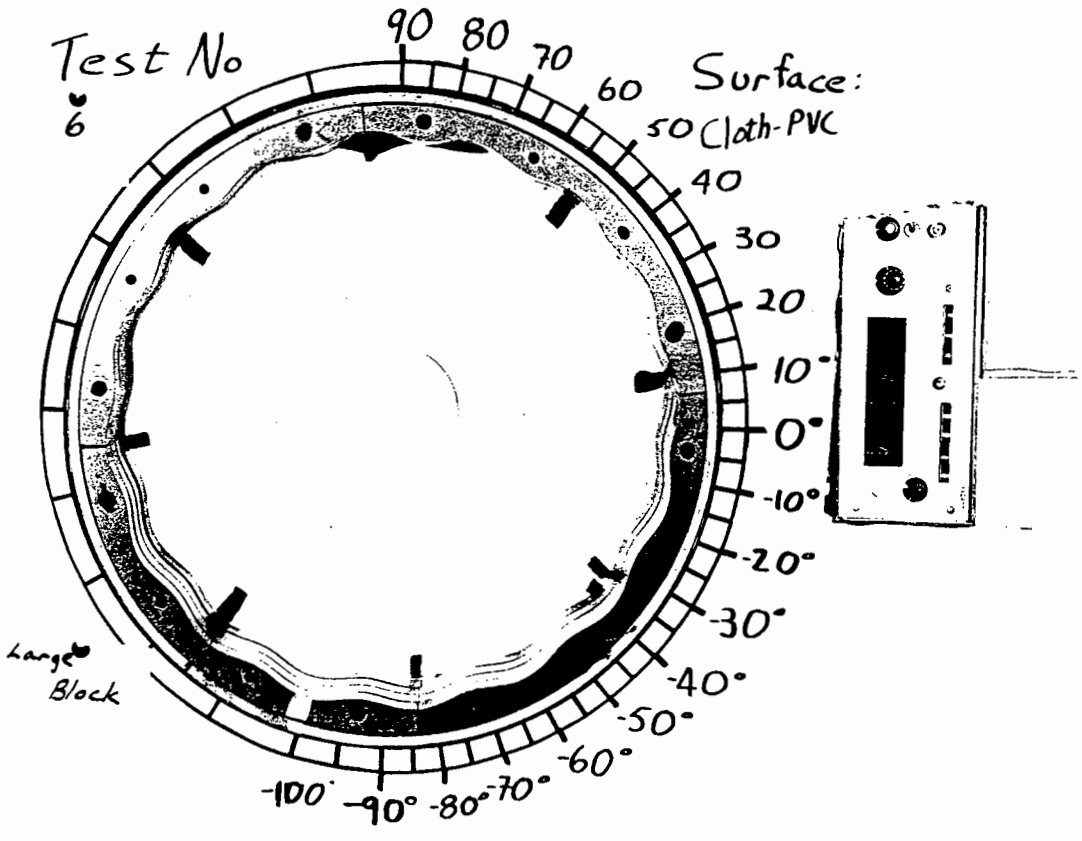

Figure 6.4: Photograph of Sample Video Recorded Frame

CHAPTER 7

PRESENTATION AND DISCUSSION OF THE EXPERIMENTAL RESULTS.

This section is divided into two main sections. Each of these sections presents the relevant experimental data for the two liner configurations tested. These experimental results will then be compared with the results obtained from the theoretical predictions. For all the results the mill speed is quoted as a percentage of the Mill Critical Velocity (N_c) as defined by Davis[3].

7.1. Determination of the Coefficient of Friction for each Liner Configuration and Liner Block Interface.

7.1.1 Determination of the Coefficient of Friction the C3 Liner.

As stated in Section 6.2 the coefficient of friction was varied by covering the blocks with cloth. It was necessary to determine the coefficient of friction, between the block and PVC liner, so that a comparison can be made between the experimental and theoretical predictions.

From Equation 3.25 an expression can be derived to calculate the coefficient of friction. By defining

$$\dot{\phi} = \ddot{\phi} = f'(\beta) = f''(\beta) = 0$$

and

$$f(\beta) = \rho$$

then Equation 3.25 reduces to

$$\mu = \text{Cot}\ (\phi) \qquad (6.1)$$

If $\phi < 0$ then $\mu = -\text{Cot}\ (\phi)$ (6.2)

The evaluation of the coefficients of friction were done by placing the block at the bottom of the stationary mill ($\phi = -90^{\circ}$). The mill was then rotated

slowly until the block started to slide. The coefficient of friction could then be calculated using Equation 6.2.

For each liner-block configuration ten observations of the Angle of Slip were made. The mean of the Angle of Slip was then calculated and a Student or "T" test was used to statistically determine a 90% Confidence Interval. These results are presented in Table 7.1.

Block	Mean Angle	Mean μ	Uncertainty Range (°)	Uncertainty in μ
BSP	-71.4°	0.337	-74.90° → -67.90°	0.270 → 0.406 (±20%)
SSP	-69.9°	0.366	-73.82° → -65.98°	0.290 → 0.446 (±21%)
BCP	-60.7°	0.561	-62.89° → -58.50°	0.512 → 0.613 (±9%)
SCP	-60.2°	0.573	-61.59° → -58.81°	0.541 → 0.605 (±6%)

Table 7.1: Tabulation of the Coefficient of Friction for the C3 Liner.

The values, for the coefficient of friction, that will be used in the theoretical predictions will be restricted to within uncertainty limits shown in Table 7.1.

This is because small uncertainty in ϕ_{slip} will lead to a large uncertainty in the coefficient of friction. This is due to the nature of the Cotan function (Equation 6.2) used to calculate the coefficient of friction (μ).

7.1.2 Determination of the Coefficient of Friction for SK Liner

The evaluation of the coefficients of friction for the SK liner was ascertained using the same method used for the C3 liner. These results are presented in Table 7.2.

Block	Mean Angle	Mean μ	Uncertainty Range ($^\circ$)	Uncertainty in μ
BSP	-69.6°	0.371	$-74.73^\circ \rightarrow -64.87^\circ$ (±9%)	0.273 → 0.469 (±26%)
SSP	-64.1°	0.486	$-70.40^\circ \rightarrow -58.41^\circ$ (±10%)	0.356 → 0.615 (±27%)
BCP	-59.7°	0.584	$-62.39^\circ \rightarrow -57.18^\circ$ (±5%)	0.523 → 0.645 (±10%)

Table 7.2: Tabulation of the Coefficient of Friction for the SK Liner

The values, for the coefficient of friction, that will be used in the theoretical predictions will be restricted to within uncertainty limits shown in Table 7.2.

7.2 Experimental Results for the C3 Liner

7.2.2 Angle of Departure of a Block on a C3 Liner

It was possible to determine when the block left the liner by observing the blocks motion. If the block leaves the liner prior to reaching the horizontal ($\phi < 0$) it does not have a pronounced flight path and only leaves the liner for a short period of time. When the block comes back into contact with the liner it starts to tumble. This phenomenon was used to establish the *Point of Departure* of the block when the filmed results were examined. If however the block left the liner above the horizontal then the *Point of Departure* was easily visible. This was due to the fact that a clear separation between the liner and block was visible.

Tests were performed to determine the *Angle of Departure* (AOD) of the block for two surfaces and two different block geometries. It was decided that an investigation should be performed to determine whether the motion of the block was affected by its geometry. This is because the liner is of such a shape that for large amplitudes the block's edges could be in contact with the liner and not the block surface. This would in turn interfere with the motion of the block. The first aim of the experimentation is thus to determine whether the blocks motion is affected by its geometry.

The experimental data is listed in Appendix E. Each data sample was analysed statistically using a Student distribution with a 90% confidence level. In Appendix E the number of data points (N) and the mean of each data sample are listed. The upper and lower confidence levels and the theoretical predictions are also listed.

Figure 7.1 contains a plot of the AOD versus the Mill Speed. Two sets of data are compared on the same set of axes.

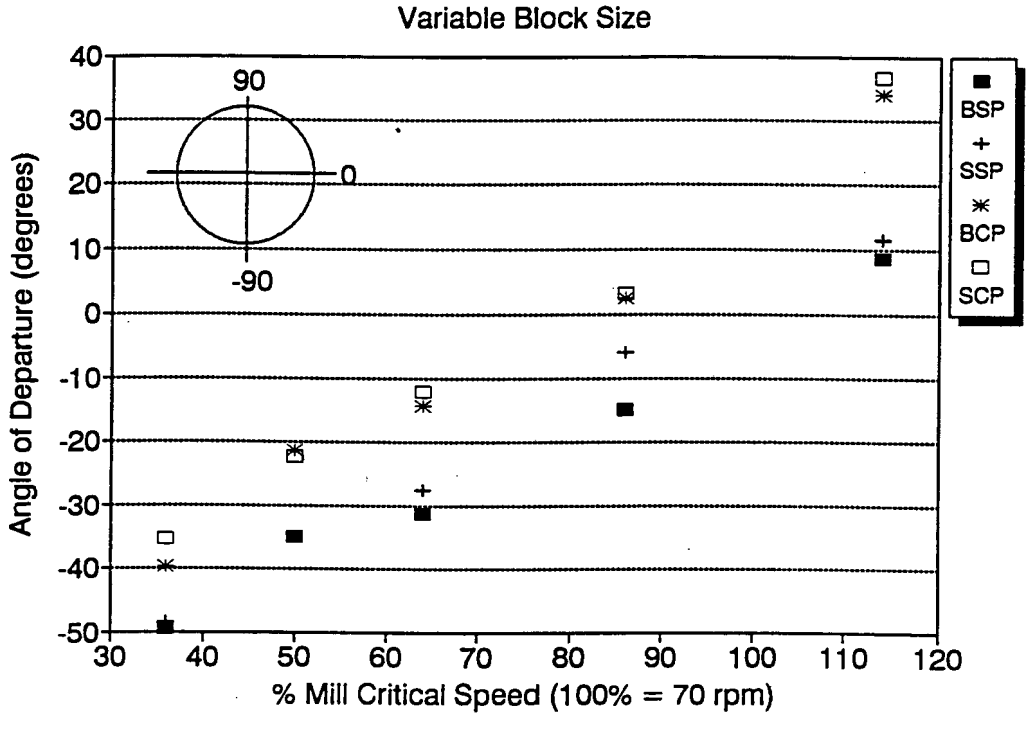

Figure 7.1: Graph of Angle of Departure versus Mill Speed for four different blocks on two Different Surfaces

It is evident from Figure 7.1 that there is good correlation between the AOD of the large and small blocks. For the steel blocks the greatest difference between the AOD of the large and small blocks is 9°. The greatest difference in the AOD of the large and small cloth covered blocks is 3°.

A subjective inspection of the steel blocks was performed and the author noted that there was a slight difference in the surface finish of the blocks. This did not occur on the cloth covered blocks because the blocks were covered in the same type of material. Even though there are these discrepancies in the coefficients of friction there is still good correlation of the angles of departure between the large and small blocks.

Therefore it is reasonable to assume that blocks of varying geometry exhibit a similar response on a liner-block interface with a constant coefficient of friction. It is also evident that the theoretical prediction that the block's motion is independent of its mass is confirmed. For the C3 liner tested, a change in the geometry of the block does not affect the block's motion. It is thought however that if the amplitude of the liner increases to such an extent that the block size is out of proportion to the distance between corrugation peaks then the size of the block will influence the block's motion. The motion of the block will also be governed by the liner configuration used. If the liner being used has sharp corners or sudden changes in slope then the larger block will have a greater tendency to topple.

The second series of tests were performed to examine the change in the *Angle of Departure* (AOD) as the mill speed (Ω_m) and the coefficient of friction (μ) were varied. In Figure 7.2 the results for the two liner-block interfaces are plotted. For each interface the mean value for the experimentally determined AOD's are plotted. The confidence intervals as determined from the Student Distribution tests are also plotted.

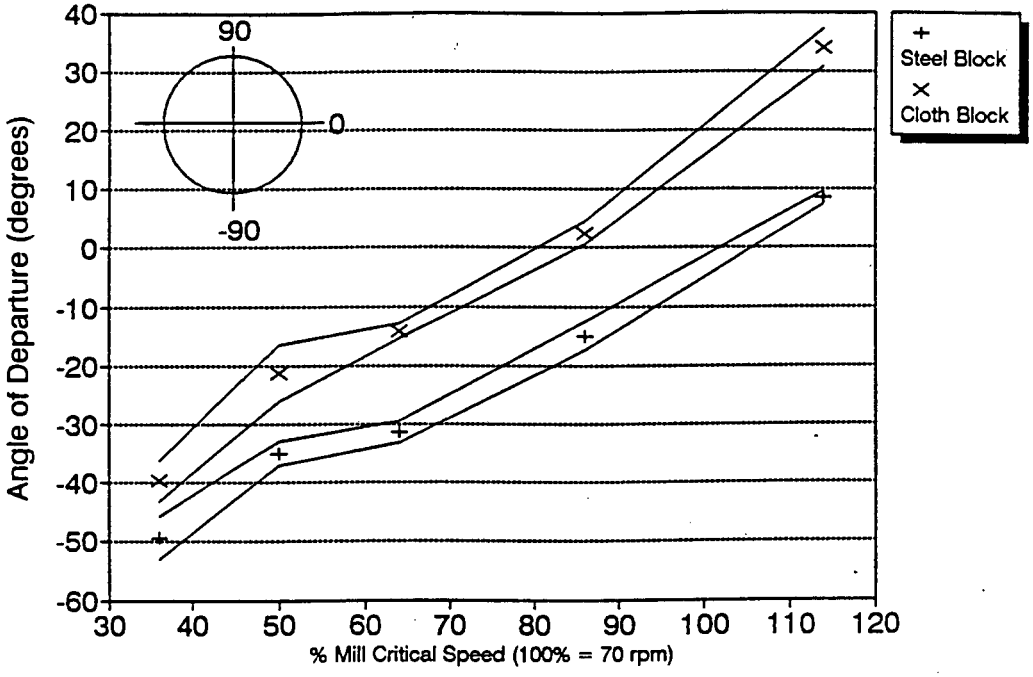

Figure 7.2 Graph of Angle of Departure versus Mill Speed for a large block, showing a 90% Confidence range for the C3 Liner

The difference in the upper and lower confidence levels is never greater than 7.8°. The 90% confidence range indicates that if the experiments were repeated, under the same conditions, that nine out of ten times similar results should be obtained. The confidence interval is larger at the lower and higher mill speeds.

At the lower mill speeds (36% → 50% N_c) it is difficult to determine accurately the *Point of Departure* (POD) of the block. The POD could only be determined once the block had left the liner and had started to tumble. A problem detecting the POD at high mill speeds (86% → 114% N_c) was also encountered. At high mill speeds the recorded image of the corrugated liner becomes "blurred" and the point where the block leaves the liner is difficult to detect. This problem was partially overcome by painting the observed face of the block a different colour to the liner.

A comparison of the experimental results and theoretical predictions are compared in Figure 7.3. The experimental results are the mean values shown in Appendix E. The theoretical values are obtained from the numerical solution of the governing equations shown in Section 3.3.1. The experimentally determined coefficients of friction are used for the calculation of the theoretical predictions. These theoretical predictions are then compared to the results obtained from the experimental work. For each case the top and bottom curves correspond to the upper and lower limits of the theoretical AOD which was determined using the experimentally determined coefficients of friction.

It is evident, from Figure 7.3, that the experimentally determined AOD's fall within or close to the theoretically predicted range of AOD's. Therefore it is reasonable to assume that the theoretical model developed for the C3 liner does satisfactorily predict the point of departure of the block from the liner. It is not known whether this holds true for any corrugated liner that is modelled. Additional experimental work has been performed to determine if the theoretical model does satisfactorily predict the AOD for different liner configurations. The additional experimental work is discussed in Section 7.3.

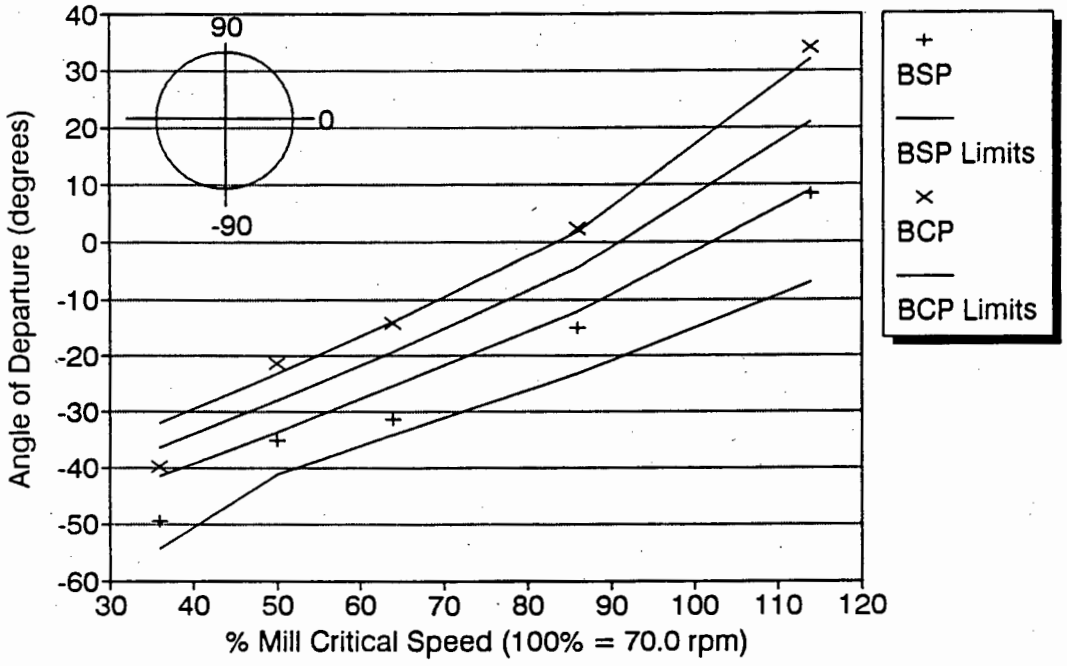

Figure 7.3 Graph of Angle of Departure versus Mill Speed on C3 Liner

7.2.3 Angle of Slip of a Single Block on a C3 Liner

If a block is placed in a mill and its initial conditions are:

1. Initial rotational speed of the block equals the mill speed ($\Omega_m = \dot{\phi}$).
2. Initial position is at the bottom of the mill ($\phi = -90^\circ$)

then it will continue to move with the same speed as the mill until the limiting friction has been exceeded ($N_t \geq \mu N_r$). The point where sliding starts to occur can be calculated theoretically using Equation (3.31) and is known as the *Angle of Slip* (ϕ_{slip}).

In Figures 7.4 and 7.5 the theoretical and experimental results for the BSP and BCP blocks are compared. The theoretical predictions are displayed as the upper and lower confidence interval. This interval was calculated using the coefficients of friction obtained from the experimental procedure. The experimental results are represented by the 90% confidence interval derived from the experimental tests.

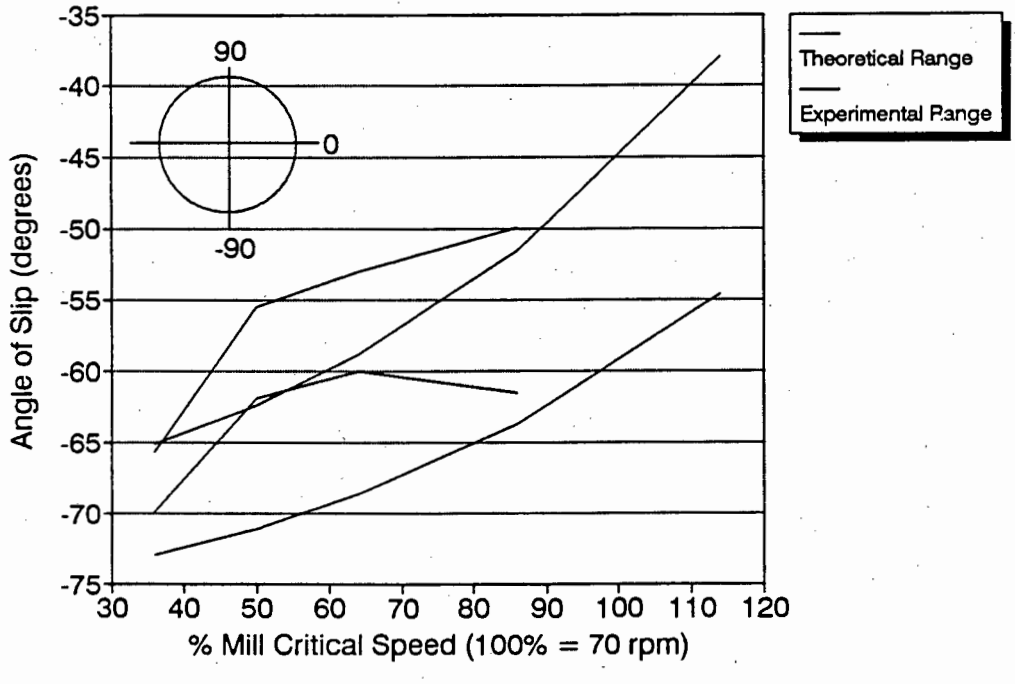

Figure 7.4: Graph of Angle of Slip versus Mill Speed for the BSP blocks on a C3 liner

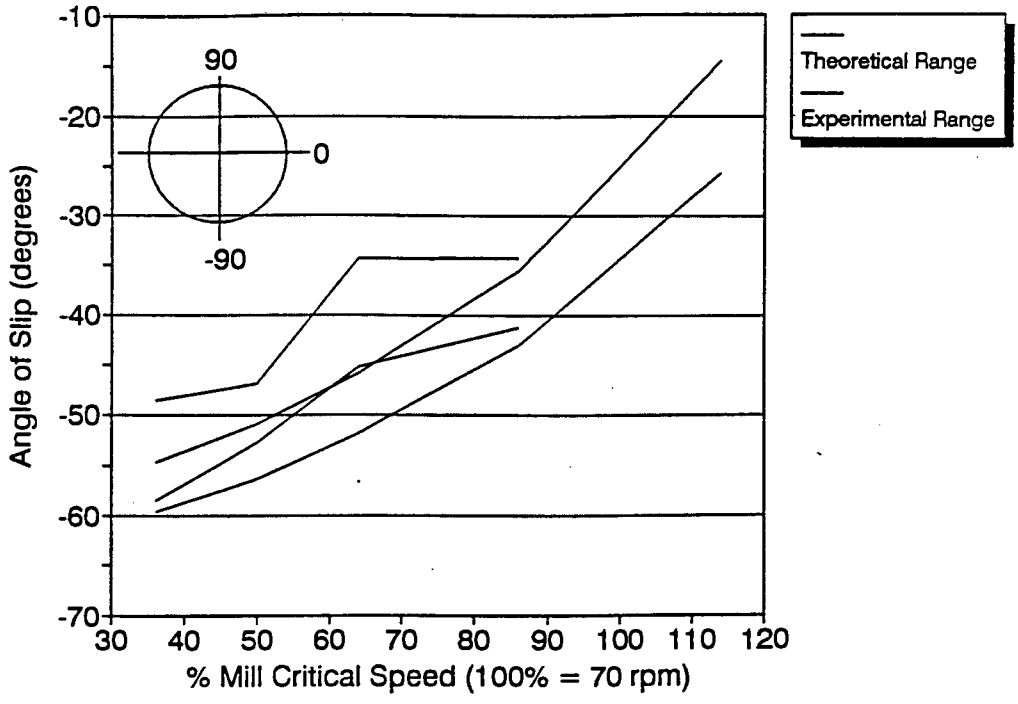

Figure 7.5: Graph of Angle of Slip versus Mill Speed for the BCP blocks on a C3 Liner

Although the confidence intervals of the experimental results and theoretical predictions overlap for the BSP blocks, the correlation between the results is not good. The mean of the experimental values of ϕ_{slip} for the BSP blocks is on average 5% higher than the theoretical values for. The confidence intervals of the experimental results and theoretical predictions for the BCP blocks only overlap for N_c = 86%. For the BCP blocks the mean of the experimental results is 9% higher than the mean of the theoretical predictions. It is noticeable that the confidence intervals for the experimental results lie above the theoretical predictions.

In both Figures 7.4 and 7.5 it can be seen that the experimental range lies above the theoretical prediction. This can be ascribed to the fact that in the experimental investigation it is difficult to ascertain at which point the block has started to slip relative to the liner. The onset of slip can only be identified once the block has moved approximately 2.5° relative to its starting point.

It is evident that the angle of slip increases with an increase in mill speed as well as with an increase in the coefficient of friction.

7.3 Experimental Results for the SK Liner.

The experimental investigation performed on the SK liner was restricted to the determination of the Angle of Departure of the block from the liner. No attempt was made to determine the Angle of Slip (ϕ_{sllp}) for the SK liner. The block does not move relative to the liner and therefore $f(\beta)$, $f'(\beta)$ and $f''(\beta)$ does not change. Therefore prior to the block sliding the block is not influenced by the liner configuration.

7.3.1. Angle of Departure of a Block on a SK Liner.

The point of departure of the block from the SK liner was determined in the same manner as that for the C3 liner. Tests were performed to determine the angle of departure of the block on two different surfaces. An investigation of the effect of the block geometry on the motion of the block was not performed. It was intended that the effect of the block geometry would be studied for the BSP and SSP blocks. After the tests were performed it was found that the values of coefficients of friction between the blocks and the liner were not similar. On closer investigation of the two blocks it was found that the blocks did not have a similar surface finish. The author is of the opinion that this is what contributed to the different coefficients of friction.

A comparison of the experimental results and theoretical prediction for the three blocks tested are shown in Figures 7.6, 7.7, and 7.8. The experimental values are the mean values shown in Appendix F. The theoretical values are obtained from the numerical solution of the governing equations. For each case the top and bottom curves correspond to the upper and lower limits of the theoretical AOD's. The theoretical AOD was calculated using the experimentally obtained coefficients of friction.

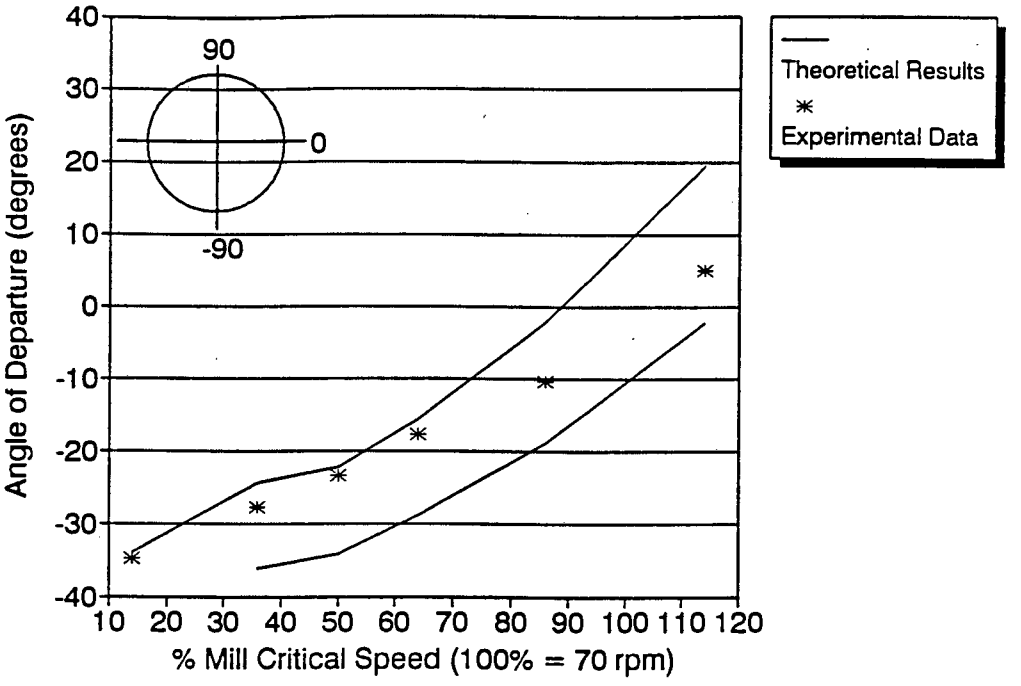

Figure 7.6: Graph of Angle of Departure vs Mill Speed for the BSP block for SK liner

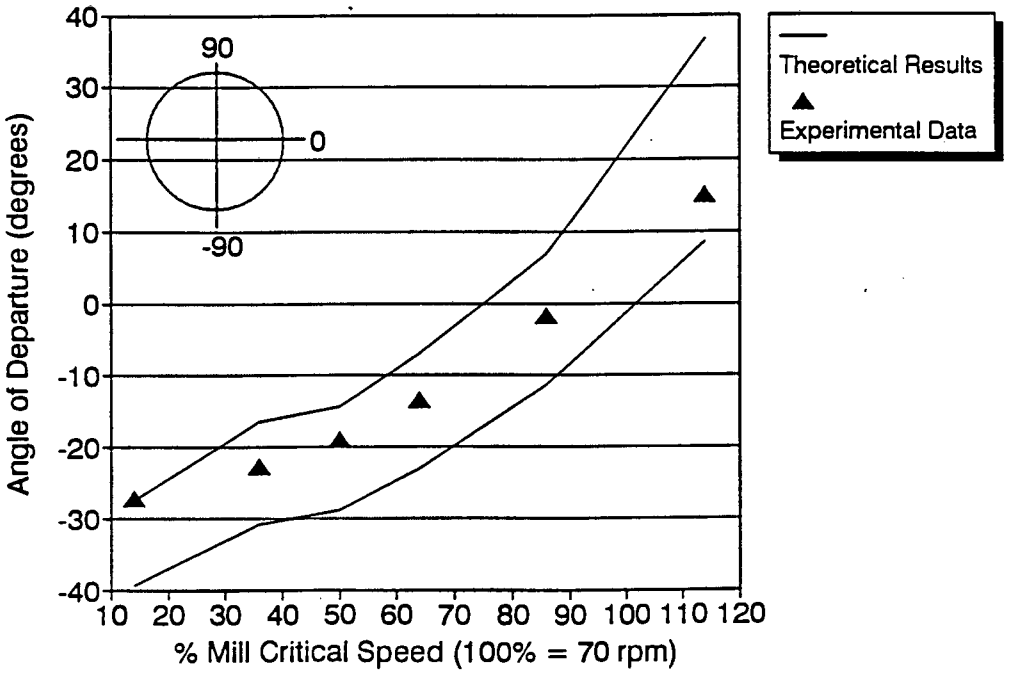

Figure 7.7: Graph of Angle of Departure vs Mill Speed for the SSP block for SK liner

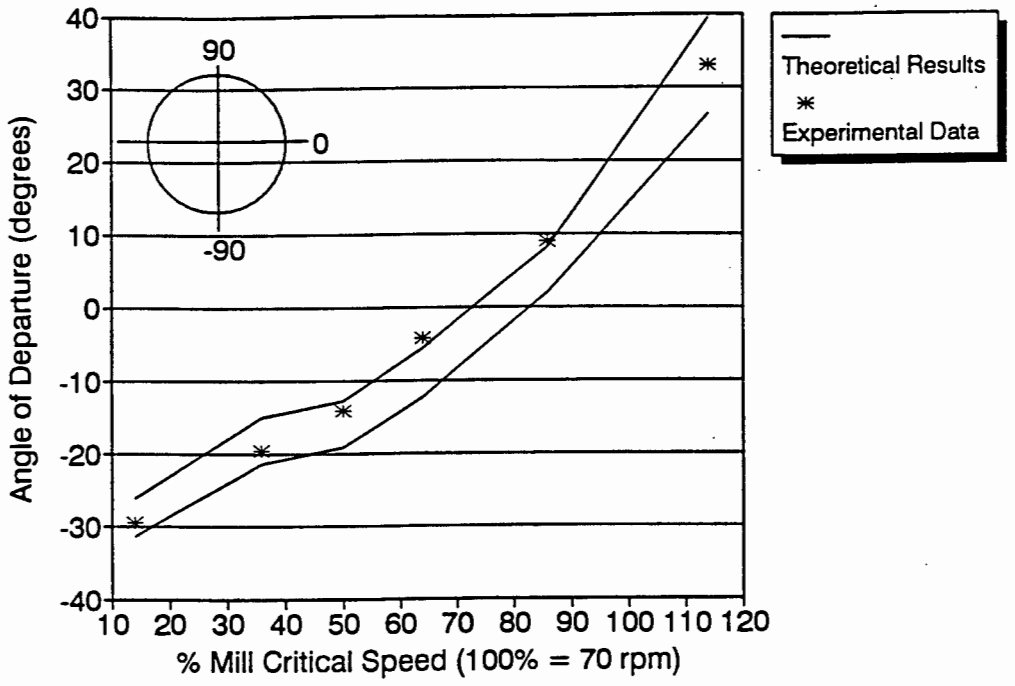

Figure 7.8: Graph of Angle of Departure vs Mill Speed for the BCP block for SK liner

It is evident from Figures 7.6, 7.7 and 7.8 that there is good correlation between the experimentally obtained AOD's and the theoretically predicted AOD's. It is therefore reasonable to assume that the model developed for the SK liner does satisfactorily predict the POD of the block from the liner. The comparison of experimental results and theoretical predictions for two different liner configurations confirms that the theoretical model does satisfactory predict the motion of a block on a corrugated liner. The experimental and theoretical results for both the C3 and SK liners correlate and it is therefore reasonable to assume that the theoretical model will satisfactorily predict the behaviour of a block on any periodic liner configuration.

CHAPTER 8

DISCUSSION

8.1. Discussion of Theoretical and Experimental Results

The main objective of this thesis was to develop a theoretical model that describes the motion of a particle on a corrugated liner on the inside of a rotating cylinder. The model accounted for the coefficient of friction and mill speed. Models for the motion of a block and sphere were developed.

The model derived for the motion of a block on a corrugated liner reduces to the formulation derived by Nates[1] if it is assumed that $f(\beta) = \rho$ (ie the amplitude of the Cosine liner is equal to zero). The governing equations for the block on a corrugated liner were numerically solved using the Fourth-Order Runge-Kutta method. No attempt was made to solve the governing equations for a sphere on a corrugated liner.

The motion of the block is dependent on the liner configuration, the coefficient of friction (μ) and the mill speed (Ω_m). The amplitude of the liner has a direct influence on the Angle of Departure (AOD) of the block. The increase in the AOD as the liner amplitude increases in also dependent on the coefficient of friction and the mill speed. The liner amplitude, mill speed and coefficient of friction also governs whether the block will remain in its initial trough or whether it will slide over a corrugation peak and slide into the next trough. Of the three liner configurations tested (C3, C8 and SK) the block left its initial trough only for a low coefficient of friction (μ = 0.2) and low mill speed (10 rpm, N_c = 14%).

For all three liner configurations tested the AOD increases with an increase in the coefficient of friction and mill speed. The increase in the coefficient of friction increases the efficiency with which energy is transferred from the mill shell to the mill charge. The increase in mill speed increases the amount of energy available and therefore increases the AOD of the block.

An experimental investigation of the motion of a block on a corrugated liner was undertaken in an attempt to verify the theoretical model developed. The

experimental AOD's, for both the C3 and SK liners, correlated well with the theoretically predicted AOD's. It is therefore reasonable to assume that the theoretical model derived for the prediction of the behaviour of a block on a corrugated liner is valid.

If the experimental and theoretical Angles of Slip for the C3 liner are compared it is evident that the experimental results are, on average, 55% higher than the theoretically predicted Angles of Slip. From this observation it can be stated that the procedure used to predict the Angle of Slip was not adequate. The exact point where the block starts to slip is not easily observable. The onset of slip is only observed once the block has moved approximately 2.5° relative to its starting position. It was evident from the experimental investigation that as the Angle of Slip increases that there is an increase in the Angel of Departure of the block.

8.2 Comparison of Theoretical Results for a Block on a Corrugated Liner to Theoretical Results for a Block on a Flat Liner

A comparison between the results obtained for this thesis and the results obtained by Nates[1] reveal that a for low mill speeds and coefficients of friction the block, modelled by Nates, will rise up the side of the rotating cylinder until it starts to slide. It continues to rise up the liner with a positive angular velocity until the angular velocity ($\dot{\phi}$) is equal to zero. The block then starts to slide down the liner with a negative angular velocity ($\dot{\phi}$) until a point is reached where the $\dot{\phi}$ is again equal to zero. Once this point is reached the block starts to accelerate up the rotating cylinder wall. This process is repeated until the block either rises above the 0° or reaches a steady state where the block does not rise any higher up the liner.

With the model for a block on a corrugated liner the block does start to slide down the liner but the block always has a positive angular velocity (ie The block will always travel in the same direction as the liner). This phenomenon occurs for all AOD's where the block leaves the liner below 0°. The block can leave the liner below 0° because the difference between the mill rotational speed and the block's angular velocity is great enough to allow the block to leave the corrugation.

The phenomena mentioned above can be seen in Figure 8.1. A comparison is made between the AOD's of a block on a flat liner and that of a block on a C3 and SK liner. The difference in the AOD for the block on a flat liner and the blocks on the corrugated liner is ascribed to the fact that the blocks on the corrugated liner does not oscillate but leaves the liner as soon as it travels out of its initial trough.

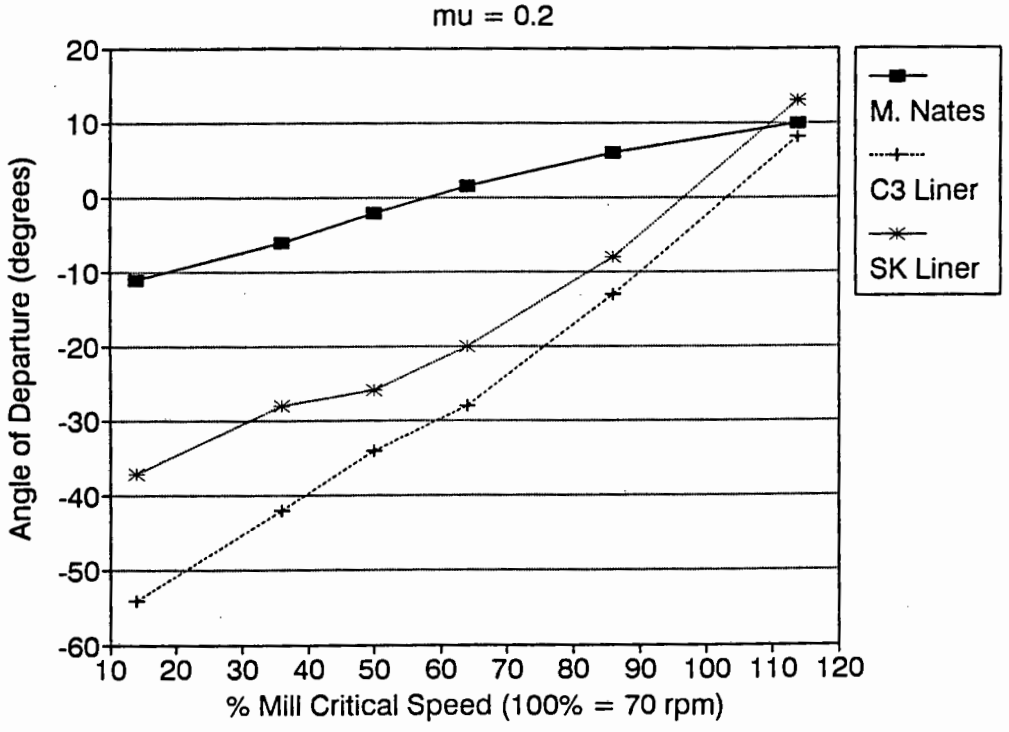

Figure 8.1: Comparison of Theoretical Results for Blocks on a Flat and Corrugated Liners (μ = 0.2)

The block travelling on a flat liner only oscillates at low coefficient of frictions and low speeds. If a comparison is made between the AOD's for a block on a flat and corrugated liner it can be seen (Figure 8.2) that there is no great difference in the AOD for the varying liner surfaces. This can be ascribed to the fact that at higher speeds the block on a flat liner has a lesser tendency to slip prior to departure from the flat liner.

The comparison of the AOD's for a block on a flat and corrugated liner, where the AOD is greater than 0° is also affected by the inclusion of the corrugated liner. The difference between the blocks initial point on the flat liner and the point of departure is approximately 35° whilst the distance between these points on the corrugated liner is never greater than 9°.

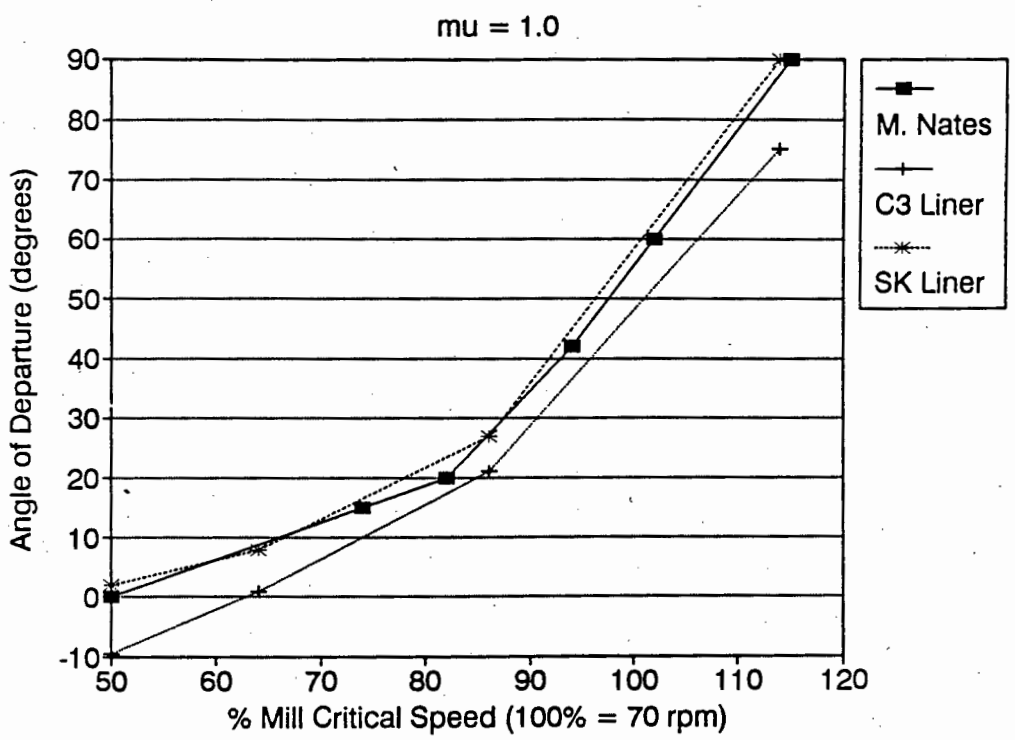

Figure 8.2: Comparison of Theoretical Results for Blocks on a Flat and Corrugated Liners (μ = 1.0)

The inclusion of the corrugated liner into the model for a block on a liner decreases the amount of slip that occurs between the block and the rotating liner of the tube mill.

8.3 Possible Extensions to Current Work

The models derived were for a block and a sphere on a corrugated liner. Of these two models only the model for a block was numerically solved. The next logical step would be to numerically solve the model for a sphere on a corrugated liner.

Once the motion of a single particle is fully understood it will be possible to extend the models to include more than one particle. The increase in the number of particles being modelled will also increase the complexity of the models. The governing equations of motion for the multiple particle model will have to be solved simultaneously because the particles interact with each other as well as with the liner. The numerical method used to solve the differential equations in this thesis is the Fourth-Order Runge-Kutta method. With the increase in the number of governing equations there will be a need to

improve the numerical method used to solve the governing equations. An improvement will be to use a Predictor-Corrector method to solve the governing equations.

As stated above, an increase in the number of particles being modelled increases the complexity of the model. A possible solution would be to investigate the motion of the mill charge as a whole and not by concentrating on one particle. One option is to investigate the charge motion using particle or fluid dynamics. The use of one of these methods would facilitate the inclusion of the effects of the interaction between the coal and grinding media.

CHAPTER 9

REFERENCES

1. Nates M.B., *An Investigation into the Parameters Affecting the Performance of Tube Mills*, M.Sc. Dissertation, University of Cape Town September 1989.

2. White H.A., *The Theory of the Tube Mill*, The Journal of the Chemical, Metallurgical and Mining Society of South Africa. May, 1905 pp. 290-305.

3. Davis E.W., *Fine Crushing in Ball Mills,* Trans. of the American Inst. of Mining and Metallurgical Engineers. 1919, Vol. 61, pp. 250-296.

4. Haultian H.E. & Dyer F.C., *Ball Paths in Tube Mills,* Canadian Institute of Mining and Metallurgy Transactions, 1922, Vol.25 pp. 276-291.

5. Gow A.M., Campbell A.B. & Coghill W.H., *A Laboratory Investigation of Ball Milling.,* AIME Trans., October 1029, pp. 51-81.

6. Fahrenwald A.W. & Lee H.E., *Ball Mill Studies.*, AIME Technical Publication No. 375., 1931.

7. Rose H.E. & Sullivan R.M., *Ball, Tube and Rod Mills.*, Constable, London, 1958.

8. McIvor R.E., *Effects of Speed and Liner Configuration on Ball Mill Performance.*, Mining Engineering, June 1983, pp. 617-622.

9. Vermeulen L.A., Ohlson De Fine M.J. & Schakowski F. *Physical information from the inside of a Rotary Mill.*, J. S. Afr. Inst. Min. Metall., Vol. 84, No 8, August 1984. pp. 247-253.

10. Vermeulen L.A., *The Lifting Action of Lifter Bars in Rotary Mills.*, J. S. Afr. Inst. Min. Metall., Vol 85, No 1, January 1985. pp. 51-63.

11. Powell M.S., *The Effect of Liner Design upon Charge Motion in a Rotary Mill.*, M.Sc. Dissertation, University of Cape Town, September 1988.

12. Gross J., *Crushing and Grinding.*, U.S.A Department of the Interior, Bureau of Mines.,1938

13. Hukki R.T., *Grinding at Supercritical Speeds in Rod and Ball Mills.*, Progress of Mineral Dressing, Trans. of 10th Int. Mining Dressing Congress, Stockholm, 1958. In: Svensta Gruvgöreningen and Jernkontoret. Almqvist and Wiksell, Stockholm, pp. 85-122.

14. Manz R., *Experimental investigation into slip of the charge of grinding medium in ball mills.*, Dechema Monographien Vol. 69, No. 1292-1326, 1072, pp 721-749. Mintek Translations from German, Tr 1174.

15. Henein H., Brimacombe J.K. & Watkinson A.P. *The Modelling of Transverse Solids Motion in a Rotary Kiln.*, Metallurgical Trans. B: Vol 14B, June 1983, pp. 207-220.

16. Vermeulen L.A., & Howat D.D., *Fluctuations in the slip of the Grinding Charge in Rotary Mills with Smooth Liners.*, Int. J. Miner. Process. 1986, Vol. 16, pp 153-168.

17. Henein H., Brimacombe J.K. & Watkinson A.P. *An Experimental Study of Segregation in Rotary Kilns.*, Metallurgical Trans. B: Vol 16B, December 1985, pp 763-774.

18. Nityanand N.B., Manley B. & Henien H, *An Analysis of Radial Segregation for Different sized Spherical Solids in Rotary Cylinders.*, Metallurgical Trans. Vol. 17B, June 1986, pp. 247-257.

19. Skorupa J.J., *Wear of Tube Mill Liners for South African Power Industry*, Phd. Dissertation, University of Cape Town, March 1989.

20. Gerald C. & Wheatley P., *Applied Numerical Analysis*, 1984, Addison-Wesley Publishing Co.

APPENDIX A

Derivation of the Fourier Series for Liner Shape taken from Skorupa's Thesis

This liner was chosen to be modelled because, in industrial trials, it was found to be the most wear resistant of the liners tested. The Fourier Series for the liner was derived using a mathematics package. The constants derived are substituted into Equation (2.1). The constants derived are listed below.

$$f(\beta) = \rho + \sum_{n=1}^{N} \left(c_n \mathrm{Cos}(\zeta_n \beta) + d_n \mathrm{Sin}(\zeta_n \beta) \right) \qquad (2.1)$$

	c_n	d_n	ζ_n
0	1.2261E-2	0.0	0
1	-7.1332E-3	-2.5126E-3	16
2	1.1469E-3	-4.0280E-4	32
3	1.7112E-4	1.0595E-3	48
4	-7.6730E-4	4.4830E-5	64
5	2.6712E-4	-1.6030E-4	80
6	4.1814E-5	1.4361E-4	96
7	5.9564E-5	1.4707E-4	112
8	-2.0695E-5	9.7892E-5	128
9	-4.2596E-5	-1.2739E-4	144
10	2.0695E-4	0.0	156
11	-4.2596E-5	1.2739E-4	172
12	-2.0695E-5	-9.7892E-5	188
13	5.9564E-5	-1.4707E-4	204

The first and second derivatives of equation (2.1) are given below.

$$f'(\beta) = \sum_{n=1}^{N} \left(-c_n \zeta_n \mathrm{Sin}(\zeta_n \beta) + d_n \zeta_n \mathrm{Cos}(\zeta_n \beta) \right) \qquad (A1)$$

$$f''(\beta) = \sum_{n=1}^{N} \left(-c_n \zeta_n^2 \mathrm{Cos}(\zeta_n \beta) - d_n \zeta_n^2 \mathrm{Sin}(\zeta_n \beta) \right) \qquad (A2)$$

APPENDIX B

Derivation of Tangent and Normal Vectors.

The vectors $\underset{\sim}{n}$ and $\underset{\sim}{t}$ are the normal and tangent unit vectors to the liner surface. The vector $\underset{\sim}{t}$ can be derived by taking the derivative of $r(\phi)$ with respect to s, where s is the distance measured along the surface.

$$\underset{\sim}{t} = \frac{d\underset{\sim}{r}}{ds} = \frac{d\underset{\sim}{r}}{d\phi}\frac{d\phi}{ds}$$

then

$$\underset{\sim}{t} = \alpha \left\{ f'(\beta)\, \underset{\sim}{e}_r + f(\beta)\, \underset{\sim}{e}_\phi \right\} \qquad \text{(B1)}$$

where $\alpha = \left(f(\beta)^2 + f'(\beta)^2 \right)^{-\frac{1}{2}}$

It is then possible to derive the equation for the vector $\underset{\sim}{n}$. This is possible because $\underset{\sim}{n}$ and $\underset{\sim}{t}$ are perpendicular to each other and $\underset{\sim}{n}.\underset{\sim}{t} = 0$. Thus

$$\underset{\sim}{n} = \alpha \left\{ f(\beta)\, \underset{\sim}{e}_r - f'(\beta)\, \underset{\sim}{e}_\phi \right\} \qquad \text{(B2)}$$

Appendix C

Derivation of the Equations of Motion for a Sphere, as used by Nates, from Equations in Section 2.3

One of the special conditions for the formulation of a block on a corrugated liner is that the liner could be flat. The formulation, used in Section 2.3 should simplify to the formulation derived by Nates.

When modeling a flat liner Equation (3.1) becomes

$$f(\beta) = \rho \tag{C1}$$

Where ρ = constant

Thus

$$f'(\beta) = f''(\beta) = 0$$

Substituting these values into Equations (3.19) and (3.20) the following equations are derived for the *Normal Reaction Force* and the *Tangential Friction Force.*

$$N_r = m\ \rho\ \dot{\phi}^2 - m\ g\ \mathrm{Sin}(\phi) \tag{C2}$$

$$N_t = m\ \rho\ \ddot{\phi} + m\ g\ \mathrm{Cos}(\phi) \tag{C3}$$

These are the same as the equations derived by Nates [1]. By substituting $f(\beta) = 0$ into Equation (3.25) then the equations of motion for a block on a flat liner can be derived.

$$B = \rho^2$$

$$C = 0$$

$$D = -\mu\ \rho^2$$

$$E = g\left(\rho\ \mathrm{Cos}(\beta) + \rho\ \mathrm{Sin}(\beta)\right)$$

Therefore Equation (3.25) becomes

$$- \mu \rho \dot{\phi}^2 + \rho \ddot{\phi} + g\Big(\mathrm{Cos}(\phi) + \mathrm{Sin}(\phi)\Big) = 0 \qquad \text{(C4)}$$

This is the same as the equation derived by Nates for a block sliding on a flat liner.

Appendix D

Solution of the Equations of Motion of a a Block on a Corrugated Liner using an Euler Forward Step Approximation.

The decomposition of the one Second Order Differential Equation [Equation (2.25)] into two first order equations can be done as follows:

$$B\ddot{\phi} + C\dot{\phi} + D\dot{\phi}^2 + E = 0 \qquad (2.25)$$

Let $$\dot{\phi} = \theta \qquad (D.1)$$

$$\therefore \quad \dot{\theta} = \ddot{\phi} \qquad (D.2)$$

Substituting Equation (D.2) into Equation (2.25) yields

$$\therefore \quad \dot{\theta} = -\frac{1}{B}\left\{C\dot{\phi} + D\dot{\phi}^2 + E\right\} \qquad (D.3)$$

Equations (D.1) and (D.3) make up a system of first order differential equations that can be solved simultaneously.

The general Runge-Kutta method is of the form

$$y_{j+1} = y_j + h\left(\sum_{l=1}^{t} \alpha_l k_l\right) \qquad (D.4)$$

where k_l are computed recursively according to

$$k_1 = f(x_j, y_j) \qquad (D.5)$$

and for $i = 2,\ldots,t$

$$k_i = f\left(x_j + h\mu_i,\ y_j + h\left(\sum_{m=1}^{i-1} \lambda_{im} k_m\right)\right) \qquad (D.6)$$

In (D.4), (D.5) and (D.6) α_l, μ_l and λ_{lm} are parameters to be chosaen to make the method as accurate as possible. The integer t in (D.4) is the number of stages in the method. For the Fourth-Order Runge-Kutta Method t = 4

$$k_1 = f(x_j, y_j) \tag{D.7a}$$

$$k_2 = f(x_j + \tfrac{1}{2} h,\ y_j + \tfrac{1}{2} h\ k_1) \tag{D.7b}$$

$$k_3 = f(x_j + \tfrac{1}{2} h,\ y_j + \tfrac{1}{2} h\ k_2) \tag{D.7c}$$

$$k_4 = f(x_j + h,\ y_j + h\ k_3) \tag{D.7d}$$

$$y_{j+1} = y_j + \frac{h}{6} (k_1 + 2\ k_2 + 2\ k_3 + k_4) \tag{D.7e}$$

Equations (D.7a)-(D.7e) are the governing equations for the Fourth-Order Runge-Kutta Method and applied to Equation 3.25 yields

$$\phi_{n+1} = \phi_n + h\ \dot{\phi}_{n+1} \tag{3.26}$$

$$\dot{\phi}_{n+1} = \dot{\phi}_n + h\ \ddot{\phi}_{n+1} \tag{3.27}$$

$$\ddot{\phi}_{n+1} = (k_1 + 2\ k_2 + 2\ k_3 + k_4)/6 \tag{3.28}$$

Where $k_1 = - h\ (C_n\ u_1 + D_n u_1^2 + E_n)/B_n \quad ; u_1 = \dot{\phi}_n$

$k_2 = - h\ (C_n\ u_2 + D_n u_2^2 + E_n)/B_n \quad ; u_2 = \dot{\phi}_n + 0.5 \cdot k_1$

$k_3 = - h\ (C_n\ u_3 + D_n u_3^2 + E_n)/B_n \quad ; u_3 = \dot{\phi}_n + 0.5\ k_2$

$k_4 = - h\ (C_n\ u_4 + D_n u_4^2 + E_n)/B_n \quad ; u_4 = \dot{\phi}_n + k_3$

h = Time Step

n = Present Increment

n+1 = Next Increment

B, C, D, E as stated in Equation (3.25)

APPENDIX E

LISTING OF EXPERIMENTAL AND THEORETICAL RESULTS FOR THE C3 LINER

List of Results of the Angle of Departure for a Large Steel Block

Theoretical Predictions			Experimental Results			
Ω_m (% N_c)	Uncertianty in μ		90% Confidence Level			
	μ = 0.270	μ = 0.406	N	Mean	Lower	Upper
36	-54.3°	-41.5°	10	-59.4°	-63.0°	-55.8°
50	-41.2°	-33.5°	8	-35.0°	-37.0°	-33.0°
64	-34.1°	-25.4°	10	-31.3°	-33.1°	-29.5°
86	-23.2°	-12.2°	10	-15.0°	-17.5°	-12.5°
114	-7.1°	9.0°	10	8.6°	7.5°	9.7°

List of Results of the Angle of Departure for a Small Steel Block

Theoretical Predictions			Experimental Results			
Ω_m (% N_c)	Uncertainty in μ		90% Confidence Level			
	μ = 0.290	μ = 0.446	N	Mean	Lower	Upper
36	-53.2°	-39.5°	9	-58.4°	-62.7°	-54.1°
50	-40.0°	-31.4°	9	-34.9°	-38.9°	-30.9°
64	-32.8°	-23.0°	10	-27.5°	-30.2°	-24.8°
86	-21.6°	-9.4°	10	-5.9°	-8.8°	-3.0°
114	-4.6°	13.8°	10	11.5°	9.5°	13.5°

List of Results of the Angle of Departure for a Large Cloth Covered Block

Theoretical Predictions			Experimental Results			
Ω_m (% N_c)	Uncertainty in μ		90% Confidence Level			
	μ = 0.512	μ = 0.613	N	Mean	Lower	Upper
36	-36.4°	-32.0°	10	-39.7°	-43.2°	-36.2°
50	-28.0°	-23.3°	10	-21.4°	-26.2°	-16.5°
64	-19.3°	-14.0°	10	-14.2°	-15.5°	-12.9°
86	-4.5°	2.0°	10	2.5°	0.5°	4.5°
114	21.0°	32.0°	10	34.0°	30.8°	37.2°

List of Results of the Angle of Departure for a Small Cloth Covered Block

Theoretical Predictions			Experimental Results			
Ω_m (% N_c)	Uncertainty in μ		90% Confidence Level			
	μ = 0.541	μ = 0.605	N	Mean	Lower	Upper
36	-35.1°	-32.3°	8	-35.3°	-37.9°	-32.6°
50	-26.7°	-23.7°	10	-22.4°	-27.1°	-17.7°
64	-17.7°	-14.5°	10	-12.0°	-14.4°	-9.6°
86	2.6°	1.6°	10	3.3°	0.8°	5.8°
114	24.3°	31.1°	10	36.7°	31.8°	41.6°

List of Results of the Angle of Slip for a Large Steel Block

Theoretical Predictions			Experimental Results			
Ω_m (% N_c)	Uncertainty in μ		90% Confidence Level			
	μ = 0.270	μ = 0.406	N	Lower	Mean	Upper
36	-73.0°	-65.1°	6	-69.9°	-67.8°	-65.9°
50	-71.1°	-62.4°	6	-61.9°	-58.7°	-55.5°
64	-68.6°	-58.8°	6	-60.0°	-56.5°	-53.0°
86	-63.7°	-51.6°	6	-61.5°	-55.7°	-49.9°
114	-54.7°	-38.0°	0			

List of Results of the Angle of Slip for a Large Cloth Covered Block

Theoretical Predictions			Experimental Results			
Ω_m (% N_c)	Uncertainty in μ		90% Confidence Level			
	μ = 0.512	μ = 0.613	N	Lower	Mean	Upper
36	-59.5°	-54.6°	6	-58.4°	-53.5°	-48.6°
50	-56.2°	-50.9°	5	-52.7°	-49.8°	-46.8°
64	-51.9°	-45.8°	6	-45.2°	-39.8°	-34.4°
86	-43.0°	-35.5°	6	-41.2°	-37.7°	-34.2°
114	-25.6°	-14.6°				

APPENDIX F

LISTING OF EXPERIMENTAL AND THEORETICAL RESULTS FOR THE SKORUPA LINER

List of Results of the Angle of Departure for the Large Steel Block

Theoretical Predictions			Experimental Results			
Ω_m (% N_c)	Uncertainty in μ		90% Confidence Level			
	μ = 0.273	μ = 0.469	N	Lower	Mean	Upper
14	——	-33.9°	10	-46.0°	-34.7°	-23.4°
36	-36.0°	-24.3°	9	-31.9°	-27.6°	-23.2°
50	-34.1°	-22.1°	8	-26.3°	-23.4°	-20.6°
64	-28.9°	-15.6°	6	-28.3°	-17.7°	-7.0°
86	-18.9°	-2.1°	6	-21.6°	-17.0°	-12.4°
114	-2.2°	19.6°	6	-0.2°	5.1°	10.6°

List of Results of the Angle of Departure for the Small Steel Block

Theoretical Predictions			Experimental Results			
Ω_m (% N_c)	Uncertainty in μ		90% Confidence Level			
	μ = 0.356	μ = 0.615	N	Lower	Mean	Upper
14	-39.3°	-27.5°	5	-40.4°	-27.2°	-14.0°
36	-30.8°	-16.5°	7	-26.3°	-22.7°	-19.1°
50	-28.8°	-14.3°	7	-23.1°	-19.0°	-14.9°
64	-23.0°	-7.0°	7	-20.5°	-13.4°	-6.4°
86	-11.4°	6.9°	7	-15.7°	-1.7°	12.5°
114	8.6°	36.6°	6	9.6°	15.1°	20.4°

List of Results of the Angle of Departure for a Large Block with a Cloth Lining

Theoretical Predictions			Experimental Results			
Ω_m (% N_c)	Uncertainty in μ		90% Confidence Level			
	μ = 0.523	μ = 0.645	N	Lower	Mean	Upper
14	-31.4°	-26.2°	6	-32.7°	-29.4°	-26.1°
36	-21.4°	-15.0°	7	-22.8°	-19.6°	-16.4°
50	-19.2°	-12.7°	11	-17.4°	-14.6°	-11.9°
64	-12.3°	-5.5°	6	-11.9°	-4.2°	3.5°
86	2.0°	8.2°	8	6.7°	8.9°	11.1°
114	26.4°	39.5°	8	26.4°	33.0°	39.5°

APPENDIX G

LISTING OF THE COMPUTER PROGRAM USED FOR THE SOLUTION OF GOVERNING EQUATIONS OF A BLOCK ON A CORRUGATED LINER

This appendix contains a listing of the computer program that was used to solve the governing equations of motion of block sliding on a corrugated liner. This program is a modified version of the PC based program developed by Nates[1] and is written in Fortran 77. The incorporation of the effect of the corrugated liner increased the computational time required to solve the governing equations. It was decided that the program developed by Nates would be transferred to the main frame computer at UCT. Minor modifications had to be made to the program to enable it to run on the main frame.

```
C*************************************************************************
c       program BALLS
C*************************************************************************
c     Purpose:      The Controlling Routine for the BALLS program
c     Developer:    M.Nates (September 1989)
c     Modified by:  K. von Bentheim (June 1991)
c     Language:     Fortran 77 (Vax Fortran)
c     Installation: UCT Main Frame with VMS ver.  5.5
C*************************************************************************
      include 'COMBALL.INC'
      character*1 dummy,dum
      equivalence(dummy,dum)
c        call curini
c
c---   Display program title page
       call BALLTITL
c
c---  Initialise
      markpr1=0
      markpr2=0
      markpr3=0
      anim=0
5     continue
c
c---  input of data output file names
      call BALLFILE(markpr1,markpr2,markpr3,anim)
c
      call BALLINPU
c
      call BALLVARA
c
      write(*,*)
      write(*,*)'    Program Running - Please Wait'
c
         call Ballincr
c
```

```
c---    Close all animation workstations if required
c         if(anim.eq.1)then
c        call finish()
c         endif
c
      write(*,*)
      write(*,*)'    Writing the Results to the required Output Files'
      write(*,*)'                        Please Wait'
c
      call balloutp
c
c---  Close all the files that where opened
      close(7)
      if(markpr1.eq.1)then
      close(8)
      end if
      if(markpr2.eq.1)then
      close(9)
      end if
c
c---   Possibilty of re-running program from within itself
        write(*,*)
        write(*,*)'    Do you wish to re-run the package?'
75      format(' Y or N ')
        write(*,75)
        call  YESNO(dum)
          if(dummy.eq.'Y'.or.dummy.eq.'y')then
          write(*,*)'    Note:'
          write(*,*)'    The new output files to be specified will'
          write(*,*)'    be written over those just created if their'
          write(*,*)'    names are not altered. '
          write(*,*)
          pause'-    Type "Continue" to Re-run Package'
          goto  5
          end if
c
```

```
stop
end
include 'BALLMISC.FOR'
```

```
C*******************************************************************************
      subroutine BALLTITL
C*******************************************************************************
c     Used to display a title page for the ball program
C*******************************************************************************
c
      IMPLICIT INTEGER*4  (A-Z)
      character*40  text(10)
      INCLUDE     '($SMGDEF)'
c
      text(1) = '**********************************'
      text(2) = ' A Program to Numerically Solve the '
      text(3) = '  Governing Differential Equation '
      text(4) = '  of a Single Block Sliding on the '
      text(5) = '    inside of a Corragated Cylinder.'
      text(6) = '**********************************'
      text(7) = '  Theory Developed by:  K. von Bentheim'
      text(8) = '                        G. Nurick'
      text(9) = '                        D. Reddy'
      text(10) = '          Please wait'
c
      status = SMG$CREATE_PASTEBOARD (NEW_PID,,,)
      IF (.NOT. status) CALL LIB$STOP(%VAL(status))
c
      status = SMG$CREATE_VIRTUAL_DISPLAY (124,180,DISPLAY_ID,,,)
      IF (.NOT. status) CALL LIB$STOP(%VAL(status))
c
      status = SMG$PASTE_VIRTUAL_DISPLAY (DISPLAY_ID,NEW_PID,2,20)
      IF (.NOT. status) CALL LIB$STOP(%VAL(status))
c
      status = SMG$PUT_LINE (DISPLAY_ID,text(1),2)
      IF (.NOT. status) CALL LIB$STOP(%VAL(status))
c
      status = SMG$PUT_LINE (DISPLAY_ID,text(2),2)
      IF (.NOT. status) CALL LIB$STOP(%VAL(status))
c
```

```
      status = SMG$PUT_LINE (DISPLAY_ID,text(3),2)
      IF (.NOT. status) CALL LIB$STOP(%VAL(status))
C
      status = SMG$PUT_LINE (DISPLAY_ID,text(4),2)
      IF (.NOT. status) CALL LIB$STOP(%VAL(status))
C
      status = SMG$PUT_LINE (DISPLAY_ID,text(5),2)
      IF (.NOT. status) CALL LIB$STOP(%VAL(status))
C
      status = SMG$PUT_LINE (DISPLAY_ID,text(6),2)
      IF (.NOT. status) CALL LIB$STOP(%VAL(status))
C
      status = SMG$PUT_LINE (DISPLAY_ID,text(7),2)
      IF (.NOT. status) CALL LIB$STOP(%VAL(status))
C
      status = SMG$PUT_LINE (DISPLAY_ID,text(8),2)
      IF (.NOT. status) CALL LIB$STOP(%VAL(status))
C
      status = SMG$PUT_LINE (DISPLAY_ID,text(9),2)
      IF (.NOT. status) CALL LIB$STOP(%VAL(status))
C
      status = SMG$PUT_LINE (DISPLAY_ID,text(10),2)
      IF (.NOT. status) CALL LIB$STOP(%VAL(status))
C
      return
      end
```

```
C*************************************************************************
      subroutine BALLFILE(MARKPR1,MARKPR2,MARKPR3,anim)
C*************************************************************************
      character*12 BALLIN, BALLOUT, CORDOUT, BALLSUM
      character*1 dummy,dum
      equivalence(dummy,dum)
      integer markpr1,markpr2,markpr3,anim
c
c---  initialise
      markpr1=0
      markpr2=0
      markpr3=0
      anim=0
c
c---  Default input data deck called BALL.DAT
      BALLIN='BALL.DAT'
c
c----  Create page for file handling
c      call cured
      write(*,*)'              File Specification for Output Files'
      write(*,*)'              ~~~~~~~~~~~~~~~~~~~~~~~~~~~~~~~~~~~~~~~'
      write(*,*)
c
c---  input of data output file name
c
15    format(a)
25    format(' Is a data output file required? Y or N -')
      write(*,25)
      call  YESNO(dum)
      if(dummy.eq.'Y'.or.dummy.eq.'y')then
c---  set print marker 1 to 1 ie markpr1=1 and read in name of output file
      markpr1=1
      write(*,*)
35    format( ' Enter name of output data file.-')
      write(6,35)
      read(*,15) BALLOUT
```

```
      end if
      write(*,*)
c
c---   open required files
      open(unit=7,status='old',file=BALLIN)
c
      open(unit=8,status='new',file=BALLOUT)
c
      return
      end
```

```
C*************************************************************************
      Subroutine BALLVARA
C*************************************************************************
c     This program is used to help with the altering and managment of
c     BALLCHAN routine, and the writing variables values to output files
C*************************************************************************
c
      include 'COMBALL.INC'
      character*1 dum,dummy
      equivalence (dummy,dum)

10    continue
C
C---- Check wether the initial default values need changing
      write(*,*)'Are the default values of the variables suitable ?'
75    format(' Y or N ')
      write(*,75)
      call  YESNO(dum)
      if(dummy.eq.'Y'.or.dummy.eq.'y')then
      goto  60
      end if
      call BALLCHAN
c       call cured
        write(*,*)
        write(*,*) '  Listing of the New Default Problem Variables.'
        write(*,*) '  ~~~~~~~~~~~~~~~~~~~~~~~~~~~~~~~~~~~~~~~~~~~~~~~~'
85      Format( 5x,' Size of time increments {s}    (H)   = ',F11.5,/,
     +          5X,' Mass of ball {kg}           (MASS)   = ',F11.5,/,
     +          5X,' Static Coeff. of Friction    (MUS)   = ',F11.4,/,
     +          5X,' Kinetic Coeff. of Friction   (MUK)   = ',F11.4,/,
     +          5X,' Mill Speed {rpm}           (OMEGAM)  = ',F11.2,/,
     +          5X,' Gravity {m/s2}                  (G)  = ',F11.2,/,
     +          5X,' Mill Radius {m}               (RHO)  = ',F11.4,/,
     +          5X,' Ball Dim. (Tangential) {m} (ATANG)   = ',F11.4,/,
     +          5X,' Ball Dim. (Normal) {m}      (ANORM)  = ',F11.4,/,
     +          5X,' Initial Ball Omega {rpm}  (OMEGAI)   = ',F11.2,/,
```

```
     +          5X,' Initial Theta (degrees)   (THETAI)  = ',F11.2,/,
     +          5x,' Time increments for flight (s)(HP)  = ',F11.5,/,
     +          5x,' Max. Number of Iterations(N)(IMAX)  = ',F11.0,/)
      write(6,85) H,MASS,MUS,MUK,OMEGAM,G,RHO,ATANG,ANORM,OMEGAI,
     &THETAI,hp,imax
      goto 10
60    continue
c
c---  write final values to output files,if required
      if(markpr1.eq.1)then
        write(8,*)
        write(8,*) '     Listing of the Problem Variables.'
        write(8,*) '     ~~~~~~~~~~~~~~~~~~~~~~~~~~~~~~~~~~~~'
      write(8,85) H,MASS,MUS,MUK,OMEGAM,G,RHO,ATANG,ANORM,OMEGAI,
     &THETAI,hp,imax
      end if
c
      if(markpr2.eq.1)then
        write(9,*)
        write(9,*) '     Listing of the Problem Variables.'
        write(9,*) '     ~~~~~~~~~~~~~~~~~~~~~~~~~~~~~~~~~~~~'
      write(9,85) H,MASS,MUS,MUK,OMEGAM,G,RHO,ATANG,ANORM,OMEGAI,
     &THETAI,hp,imax
      end if
c
      if(markpr3.eq.1)then
        write(10,*)
        write(10,*) '     Listing of the Problem Variables.'
        write(10,*) '     ~~~~~~~~~~~~~~~~~~~~~~~~~~~~~~~~~~~~'
      write(10,85) H,MASS,MUS,MUK,OMEGAM,G,RHO,ATANG,ANORM,OMEGAI,
     &THETAI,hp,imax
      end if
c
c---   Prepare screen for problem solution
c      call cured
       write(*,*) '            Problem Variables'
```

```
        write(*,*) '                ~~~~~~~~~~~~~~~~~'
      write(*,85) H,MASS,MUS,MUK,OMEGAM,G,RHO,ATANG,ANORM,OMEGAI,
     &THETAI,hp,imax
c
c---  Convert the input variables from degrees & rpm to rad & rad/s
c---   Convert thetai to radians
        thetai=thetai*pi/180
c---    convert omegam and omegai from rpm to radians
        omegai=omegai*pi/30
        omegam=omegam*pi/30
c----   Let the variable A=(tang/2) ie the radius of the block/ball
        A=0.5*sqrt(atang*atang+anorm*anorm)
c
      return
      end
```

```
C*************************************************************************
      subroutine BALLCHAN
C*************************************************************************
      character*12 BALLIN
      include 'COMBALL.INC'
      INTEGER MARKDEF,numval
      real num
c---  initialise
      MARKDEF=0
      numval=1
      num=0.0
c     Output the old input for display  and change
c.....................................................
*     write(*,*)
*     write(*,*)
*     write(*,*) '     Listing of the Problem Variables.'
*     write(*,*) '     ~~~~~~~~~~~~~~~~~~~~~~~~~~~~~~~~~~~~'
5     Format(a)
15    Format( 2x,' Size of time increments {s}     (H) [',F9.5,']= ')
25    Format( 2X,' Mass of ball {kg}             (MASS) [',F9.5,']= ')
35    Format( 2X,' Static Coeff. of Friction     (MUS) [',F9.4,']= ')
135   Format( 2X,' Kinetic Coeff. of Friction    (MUK) [',F9.4,']= ')
45    Format( 2X,' Mill Speed {rpm}            (OMEGAM) [',F9.2,']= ')
55    Format( 2X,' Gravity {m/s2}                 (G) [',F9.2,']= ')
65    Format( 2X,' Mill Radius {m}              (RHO) [',F9.4,']= ')
75    Format( 2X,' Ball Dim. (Tangential) {m} (ATANG) [',F9.4,']= ')
125   Format( 2X,' Ball Dim. (Normal)      {m} (ANORM) [',F9.4,']= ')
85    Format( 2X,' Initial Ball Omega {rpm}  (OMEGAI) [',F9.2,']= ')
95    Format( 2X,' Initial Theta {degrees}    (THETAI) [',F9.2,']= ')
105   Format( 2x,' Time increments for flight {s}(HP) [',F9.5,']= ')
145   Format( 2x,' Max. Number of Iterations{N}(IMAX) [',F9.0,']= ')
115   Format(f12.6)
c      call cured

      write(*,*)'*******************************************************
     &*****'
```

```
      write(*,*)'***  Input the new value at the equals sign,
     &  ***'
      write(*,*)'***  or press return for the bracketted default value
     &  ***'
      write(*,*)'*************************************************
     &*****'
c
      write(*,*)
      write(*,*)
      write(*,15) H
      call GETREAL(NUM,MARKDEF)
      IF(MARKDEF.NE.1)THEN
C---  MAKE H=NEW VALUE AND DO NOT USE DEFAULT
      H=NUM
      END IF
c
      write(*,25) mass
      call GETREAL(NUM,MARKDEF)
      IF(MARKDEF.NE.1)THEN
C---  MAKE mass=NEW VALUE AND DO NOT USE DEFAULT
      mass=NUM
      END IF
c
      write(*,35) mus
      call GETREAL(NUM,MARKDEF)
      IF(MARKDEF.NE.1)THEN
C---  MAKE mus=NEW VALUE AND DO NOT USE DEFAULT
      mus=NUM
      END IF
c
      write(*,135) muk
      call GETREAL(NUM,MARKDEF)
      IF(MARKDEF.NE.1)THEN
C---  MAKE muk=NEW VALUE AND DO NOT USE DEFAULT
      muk=NUM
      END IF
```

```
c
      write(*,45) omegam
      call GETREAL(NUM,MARKDEF)
      IF(MARKDEF.NE.1)THEN
C---  MAKE omegam=NEW VALUE AND DO NOT USE DEFAULT
      omegam=NUM
      END IF
c
      write(*,55) g
      call GETREAL(NUM,MARKDEF)
      IF(MARKDEF.NE.1)THEN
C---  MAKE g=NEW VALUE AND DO NOT USE DEFAULT
      g=NUM
      END IF
c
      write(*,65) rho
      call GETREAL(NUM,MARKDEF)
      IF(MARKDEF.NE.1)THEN
C---  MAKE rho=NEW VALUE AND DO NOT USE DEFAULT
      rho=NUM
      END IF
c
      write(*,75) atang
      call GETREAL(NUM,MARKDEF)
      IF(MARKDEF.NE.1)THEN
C---  MAKE a=NEW VALUE AND DO NOT USE DEFAULT
      atang=NUM
      END IF
c
      write(*,125) anorm
      call GETREAL(NUM,MARKDEF)
      IF(MARKDEF.NE.1)THEN
C---  MAKE a=NEW VALUE AND DO NOT USE DEFAULT
      anorm=NUM
      END IF
c
```

```
      write(*,85) omegai
      call GETREAL(NUM,MARKDEF)
      IF(MARKDEF.NE.1)THEN
C---  MAKE omegai=NEW VALUE AND DO NOT USE DEFAULT
      omegai=NUM
      END IF
c
      write(*,95) thetai
      call GETREAL(NUM,MARKDEF)
      IF(MARKDEF.NE.1)THEN
C---  MAKE thetai=NEW VALUE AND DO NOT USE DEFAULT
      thetai=NUM
      END IF
c
      write(*,105) Hp
      call GETREAL(NUM,MARKDEF)
      IF(MARKDEF.NE.1)THEN
C---  MAKE HP=NEW VALUE AND DO NOT USE DEFAULT
      HP=NUM
      END IF
C
      write(*,145) Imax
      call GETREAL(NUM,MARKDEF)
      IF(MARKDEF.NE.1)THEN
C---  MAKE HP=NEW VALUE AND DO NOT USE DEFAULT
      Imax=NUM
      END IF
C
C---  WRITE NEW VALUES TO DATA FILE,but first and then rewind file
      rewind(7)
      WRITE(7,* ) OMEGAM,MASS,MUS,MUK,RHO,G,H,OMEGAI,THETAI,HP,
     &ATANG,ANORM,imax
      rewind(7)

      RETURN
      END
```

```
c.....
c
c     File = GETREAL.FOR
c.....
c
c     Program..... GETREAL
c     Purpose ..... To get a real value, by first buffering the input
c                   using the CHRINI routines, from the keyboard.
c.....
c
      subroutine GETREAL(N,MARKDEF)
c
      real a(100),n
      integer iferr,numchr,maxchr,markdef
      parameter (maxchr=10)
      character*1 chrbuf(maxchr)
c
c---  initialize module
      call CHRINI
      markdef=0
c
10    continue
c
c---  get the real value to be read
      iofset = 48
      call CHRRED (iferr)
      if(iferr.ne.0)then
      write(*,*)'Error in reading input'
      goto 100
      end if
      call CHRSTR (chrbuf,maxchr,numchr,iferr)
      if(iferr.ne.0) then
         call CHRERR (iofset)
         write(*,1001) maxchr
1001     format(1h ,'=> Maximum number of characters in token = ',i2)
         goto 10
```

```
      else if(numchr.eq.0) then
         write(*,1003)
1003     format('=> Used Default Value ')
         write(*,*)
         markdef=1
         goto 100
      endif
      call CHRTOR (chrbuf,numchr,n,iferr)
      if(iferr.ne.0) then
         call CHRERR (iofset)
         write(*,1002)
1002     format(1h ,'=> Invalid real value specified, re-enter -  ')
         goto 10
      endif
c
100   continue
      return
      end
```

```
C*************************************************************************
      subroutine BALLINCR
C*************************************************************************
c
      include 'COMBALL.INC'
c---  Initialise required values
      real amp,mill
      integer i,marker,para,j
      marker=0
      Do 110 i = 1,10000
         Do 120 j = 1,3
          cord(i,j)=0
120      continue
110    continue
c
      Do 210 i = 1,10000
         Do 220 j = 1,6
          omega(i,j)=0
220      continue
210    continue
c
c---  Values of the variables at time t=0 or N=1
      finaln = 0
      npod = 0
      para = 0
      f = 0
      fd = 0
      fdd = 0
      i=1
      omega(1,1)=0
      omega(1,2)=omegai
      omega(1,3)=thetai
      omega(1,4)=mass*omegam*omegam*rho-mass*g*sin(omega(1,3))
      omega(1,5)=mass*g*cos(omega(1,3))
      cord(1,3)=thetai
```

```
        if(omegai .eq. omegam)then
          flag1 = 0
          motion(1) = 'st'
        else
          flag1 = 1
          motion(1) = 'sl'
        endif
c
        write(8,*) ' Skorupa Liner '
c
5       continue
c
        If(flag1 .eq. 0 ) then
c
c*************************************************************************
c       Implimentation of the Numerical Sol'n of the Non-Sliding Case
c*************************************************************************
c
c---   calculate the values for the liner functions as well as constants used
in
c     the analysis
c
         call FUNCTION(i)
c          f = 0.1825 + 0.008 * cos(16*(omega(i,3)-(i-1)*h*omegam))
c          fd = -0.128 * sin(16*(omega(i,3)-(i-1)*h*omegam))
c          fdd = -2.048 * cos(16*(omega(i,3)-(i-1)*h*omegam))
c
         an = 1/sqrt(f**2 + fd**2)
c
c---   calculate the values of the variables at time N+1
c
         omega(i+1,1)=i
c
         omega(i+1,2)=omegai
c
         omega(i+1,3)=omega(i,3)+h*omega(i+1,2)
```

```
c
          omega(i+1,6) = 0
c
          rr = omega(i+1,6)*fd+omega(i+1,2)**2*(fdd-f)-2*omegam*
     &    omega(i+1,2)*fdd+omegam**2*fdd
c
          rq = omega(i+1,6)*f+2*omega(i+1,2)**2*fd-2*omega(i+1,2)
     &    *omegam*fd
c
c---      Reaction Force
c
          omega(i+1,4) = mass*an*(fd*rq-f*rr)+mass*g*an*(fd
     &                   *cos(omega(i+1,3))-f*sin(omega(i+1,3)))
c
c---      Tangential Force
c
          omega(i+1,5) = mass*an*(fd*rr+f*rq)+mass*g*an*(f
     &                   *cos(omega(i+1,3))+fd*sin(omega(i+1,3)))
c
          motion(i+1) = 'st'
c
          if(abs(omega(i+1,5)).ge.abs(mus*omega(i+1,4)))then
            flag1 = 1
          endif
c
        else
c
c*************************************************************************
c       Implimentation of the Numerical Solution of the Sliding D.E.
c*************************************************************************
c       The kinetic Coefficient of Friction is used for sliding MUK
c
          call FUNCTION(i)
c
          an = 1/sqrt(f**2+fd**2)
          bn = 1/(an**2)
```

```
          cn = -2*omegam*(fd*fdd+muk*f*fdd-f*fd+muk*fd**2)
          dn = (fd+muk*f)*(fdd-f)+2*fd*(f-muk*fd)
          en = (omegam**2)*fdd*(fd+muk*f)+g*((f-muk*fd)*cos(omega(i,3))
     &         +(fd+muk*f)*sin(omega(i,3)))
c
c---    calculate the values of the variables at time N+1
c
          omega(i+1,1)=i
c
          call SOLVE(i)
c
c---      Angular Displacement of Block
c
          omega(i+1,3)=omega(i,3)+H*omega(i+1,2)
c
          rr = omega(i+1,6)*fd+omega(i+1,2)**2*(fdd-f)-2*omegam*
     &         omega(i+1,2)*fdd+omegam**2*fdd
c
          rq = omega(i+1,6)*f+2*omega(i+1,2)**2*fd-2*omega(i+1,2)
     &         *omegam*fd
c
c---     Reaction Force
c
          omega(i+1,4) = mass*an*(fd*rq-f*rr)+mass*g*an*(fd
     &                   *cos(omega(i+1,3))-f*sin(omega(i+1,3)))
c
c---     Tangential Force
c
          omega(i+1,5) = mass*an*(fd*rr+f*rq)+mass*g*an*(f
     &                   *cos(omega(i+1,3))+fd*sin(omega(i+1,3)))
c
          motion(i+1) = 'sl'
c
        endif
c
c---    calculate the cordinates of the ball centre
```

```
c          cord(i+1,1)=(rho-a)*cos(omega(i,3))
c          cord(i+1,2)=(rho-a)*sin(omega(i,3))
           cord(i+1,3)=cord(i,3)+h*omegam
           mill = cord(i+1,3)
c
c---     Check Number 1
c---     check if theta>89,9 and omega>=0
c---     then ball never leaves rim, but sticks to it
         If(omega(i+1,3).ge.1.569051.and.omega(i+1,2).gt.0)then
           write(*,*)'    !!!  Ball is centrifuged to liner    !!!'
           write(*,*)'    !!! before it has started to slide  !!!'
           write(*,*)'    !!! therefore the run is terminated !!!'
c
c---      End run because ball is centrifuged
           Npod=i+1
           Finaln=i+1
           goto 999
         End if
c
c---     Check Number 2
c---     check sign of reaction and see if required to 'kick-out'
         If(omega(i+1,4) .le. 0)then
c---   Normal P.O.D. has occured write it to screen and file
           write(*,*)'     Ball follows normal path and leaves liner.'
c
c--      mark that ball left liner "normally"
           Npod=i
c
c---     Call BALLPARA to calculate the ball parabolic path if the ball
c        leaves the liner
c
           call BALLPARA(mill)
           goto 999
         end if
c
c---     Increment N to N+1
```

```
      i=i+1
      goto 5
c
999   continue
c
      return
      end
```

```
C*************************************************************************
      subroutine FUNCTION(i)
C*************************************************************************
c
      include 'COMBALL.INC'
      real bdisp
c
      bdisp = (omega(i,3)-(i-1)*h*omegam)
c
c---- Function for liner No4 from Skorupa's Thesis
c
      if(bdisp.le.-1.570796.and.bdisp.gt.-1.588250)then
        f = 0.1925
        fd = 0
        fdd = 0
      else if (bdisp.le.-1.588250.and.bdisp.gt.-1.727876)then
        f = 0.09524 * bdisp + 0.343788
        fd = 0.09524
        fdd = 0
      else if (bdisp.le.-1.727876.and.bdisp.gt.-1.806416)then
        f = 0.1792
        fd = 0
        fdd = 0
      else if (bdisp.le.-1.806416.and.bdisp.gt.-1.867502)then
        f = -0.217726 * bdisp - 0.214103
        fd = -0.217722
        fdd = 0
      else if (bdisp.le.-1.867502)then
        f = 0.1925
        fd = 0
        fdd = 0
      endif
c
      return
      end
```

```
C*************************************************************************
      subroutine SOLVE(i)
C*************************************************************************
*
c     This subroutine solves the differential equations derived for the sphere
c     on the corrugated liner. The eqaution is solved using a 4th Order
c     Runge-Kutta method.
c*************************************************************************
*
      include 'COMBALL.INC'
c
c---  initialise variables
      integer i
      real u1,u2,k1,k2,k3,k4
c
      u1 = omega(i,2)
c
      u = u1
c
      k1 = -h*(cn*u+dn*u**2+en)/bn
c
      u = u1+0.5*k1
c
      k2 = -h*(cn*u+dn*u**2+en)/bn
c
      u = u1+0.5*k2
c
      k3 = -h*(cn*u+dn*u**2+en)/bn
c
      u = u1+k3
c
      k4 = -h*(cn*u+dn*u**2+en)/bn
c
      omega(i+1,2) = omega(i,2)+(k1+2*k2+2*k3+k4)/6
      omega(i+1,6) = (omega(i+1,2)-omega(i,2))/h
c
```

```
return
end
```

```
C*************************************************************************
      Subroutine BALLPARA(mill)
C*************************************************************************
c
      include 'COMBALL.INC'
      real SX,SY,UX,UY,VINI,POD,V,mill
      integer i
c---  Use the average of the last two iteration on the liner surface
      POD=(omega(NPOD+1,3)+omega(NPOD,3))/2
      Sx = cos(POD)*f
      Sy = sin(POD)*f
      Vini = ((omega(NPOD+1,2)+omega(NPOD,2))/2)
      Ux = Vini*(fd*cos(POD)-f*sin(POD))
      Uy = Vini*(fd*sin(POD)+f*cos(POD))
      vy = uy
      i = 0
c
c---  Output initial conditions to file, if required
      if(markpr1.eq.1)then
c
      write(8,*)
c
      write(8,*)'      Initial values at the start of Flight.'
      write(8,*)'      ~~~~~~~~~~~~~~~~~~~~~~~~~~~~~~~~~~~~~~~~~~~~~~~~~~~~~~~'
15    Format( 5x,' Point of Departure (degrees) (POD)  = ',F11.5,/,
     +        5X,' Initial Velocity (m/s)       (Vini)  = ',F11.5,/,
     +        5X,' Init. Horiz. displacement (m) (Sx)   = ',F11.5,/,
     +        5X,' Init. Vert. displacement (m)  (Sy)   = ',F11.5,/,
     +        5X,' Init. Horiz. velocity (m/s)   (Ux)   = ',F11.5,/,
     +        5X,' Init. Vert. velocity (m/s)    (Uy)   = ',F11.5,/,
     +        5X,' Mill Rotation at Departure (deg)     = ',F11.5,/)
      write(8,15)POD*180/3.14159,VINI,SX,SY,UX,UY,MILL*180/pi
      write(*,15)POD*180/3.14159,VINI,SX,SY,UX,UY,MILL*180/pi
c --  write heading
      write(8,*)
      write(8,*)'      Incremental Flight Path and Velocity Results'
```

```
        write(8,*)'            ~~~~~~~~~~~~~~~~~~~~~~~~~~~~~~~~~~~~~~~~~~~~~~~~~~'
       write(8,*)'       No          Sx           Sy              Vy          V
      &           Mill'
       write(8,*)'                   (m)          (m)           (m/s)       (m/s)
      &           (deg)'
c
        endif
10      continue
c
c---    Increment one time step using time increment of HP
        i=i+1
        sx=sx+ux*hp
        sy=sy+vy*h-g*hp*hp/2
        vy=vy-g*hp
        v=sqrt(vy*vy+ux*ux)
        mill = mill +hp *  omegam

c---    Check if against liner
        If(sx*sx+sy*sy.lt.rho*rho.or.i.lt.10)then
c--     print this steps values
11        format(4x,i4,4x,f8.4,4x,f8.4,4x,f8.4,4x,f8.4,4x,f8.4)
c         write results if required
          if(markpr1.eq.1)then
            write(8,11)i+Npod,sx,sy,vy,v,mill*180/pi
          endif
          goto 10
        endif
c
c---   Print final value and record Finaln
        if(markpr1.eq.1)then
        write(8,11)i+Npod,sx,sy,vy,v,mill*180/pi
        endif
        Finaln=1+I+NPOD
c
        return
        end
```

```
C*************************************************************************
      Subroutine BALLOUTP
C*************************************************************************
c     Used to process the output from the ballmill program
c.....................................................................
c
      include 'COMBALL.INC'
      integer j
c
c---  write array to output file
        write(8,*)
        write(8,*)'          Pre-Departure Incremental Results'
        write(8,*)'          ~~~~~~~~~~~~~~~~~~~~~~~~~~~~~~~~~'
        write(8,*)' Number   Theta dot   Theta    Reaction   Tangential
     &  Mill Rot.  Motion'
        write(8,*)'   N       (rad/s)   (degrees)    (N)         (N)
     &  Degrees)'
51    format(2x,f5.0,3x,f8.4,4x,f9.4,3x,f8.4,3x,f8.4,4x,f8.4,3x,a3)
        do 20 j=1,Npod+1
         write(8,51) omega(j,1),omega(j,2),omega(j,3)*180/pi,
     *  omega(j,4),omega(j,5),cord(j,3)*180/pi,motion(j)
20      continue
c
      return
      end
```

Appendix H

LIST OF COURSES COMPLETED

	Symbol Attained
END520Z Applied Mechanics I	3
END521Z Applied Mechanics II	2+
END522Z An Introduction to Finite Elements	2-
END523Z Finite Elements Analysis	3
AMA363F Numerical Analysis	3
AMA367F Continuum Mechanics	3
AMA368S Numerical Solutions of D.E.'s	2-